/
Article / Book Information

( )	
Title(English)	Robust control design with minor feedback and its applications to pneumatic control systems
( )	
Author(English)	Kimura Tetsuya
( )	: ( ), : , : 3104 , :1995 12 31 , : , :
Citation(English)	Degree:Doctor (Engineering), Conferring organization: Tokyo Institute of Technology, Report number: 3104 , Conferred date:1995/12/31, Degree Type:Course doctor, Examiner:
( )	
Type(English)	Doctoral Thesis

Robust Control Design with Minor Feedback

and

Its Applications

to Pneumatic Control Systems

Tetsuya Kimura

supervised by Professor Shinji Hara

August, 1995

Abstract

The finite dimensional linear time invariant (FDLTI) H_∞ control theory establishes one of the most powerful robust control. Though tractability of the FDLTI H_∞ is superior, its suitability with real modeling error is poor. Therefore, the resulting system performance is conservative if we directly apply the H_∞ control theory in practice. To reduce the conservativeness, FDLTI H_∞ control scheme with minor feedback have been examined in this thesis. The approach used here gains suitability of FDLTI H_∞ control without losing its tractability.

Since the minor feedback loop changes both the nominal plant and the uncertainty models, we cannot conclude immediately that it improves system performances even if the magnitude of uncertainty model is reduced. A disturbance rejection problem is introduced to investigate the effect of the minor feedback and a sufficient condition is derived on which the minor feedback improves system performance. Experimental results for a pressure control system will confirm the correctness of the sufficient condition.

Feedback linearization is a useful minor feedback control for nonlinear systems. However, the original formulation is not suitable for pneumatic control systems. In this thesis, its reformulation is proposed so that the linearized plant coincides with the linear approximated plant of the original nonlinear plant. According to this reformulation, it is easily concluded that feedback linearization improves system performance if nonlinearity of the real plant occupies dominant part of uncertainty model. In addition, a class of feedback linearizable plants is derived and linearization control with disturbance rejection is proposed. These results gain suitability of feedback linearization for pneumatic systems. Effectiveness of these results are verified experimentally for a pneumatic actuator systems with a rubber artificial muscle.

Under real parametric uncertainty, minor feedback should satisfy an H_∞ norm constraint to improve system performance subject to the uncertainty. A norm bound test for real parametric perturbed systems is given based on sign definite condition. Frequency restricted norm (FRN), a generalization of the H_∞ norm, is proposed and a special class of real parametric perturbed systems, such that their FRNs are bounded by the FRNs of fixed systems is derived. Based on these results, a design method of minor feedback controller against real parametric uncertainty is given by using parameter space design method.

要旨

多くの制御系設計法では、設計モデルと呼ばれる数学的モデルに基づいて補償器の設計が行なわれる。一般に高次の動特性やパラメータを厳密に同定することは困難であるため、モデル化誤差の存在を制御系設計時に考慮することが必要である。ロバスト制御では、モデル化誤差を包含するよう設計モデルを集合として取り扱いその影響を考慮する。ここで設計モデルは、一つの固定された基準プラントとプラントの集合である不確かさのモデルにより表現される。

ところで、補償器の設計法は次の2つの点で優れていることが求められる。1) 与えられた制御対象と設計仕様を自然に表現できる適合性、2) 補償器を求める手順が容易であるという可解性。この観点からすると、有限次元線形時不変 (FDLTI) H_∞ 制御はもっとも有効なロバスト制御の1つである。しかし、FDLTI-H_∞ 制御での不確かさのモデルはノルムの大きさにより特徴づけられているため、実際のモデル化誤差との不整合性が無視できない場合もある。したがって、直接 H_∞ 制御を適用すると、得られる性能が保守的になることが指摘されている。このため、非線形 H_∞ 制御や real-μ 設計等基準プラントや不確かさのモデルに対する仮定を見直し、保守性を減らそうという手法が存在するが、今までのところその可解性には問題がある。

本研究では、FDLTI-H_∞ 制御に対してマイナーフィードバックを併用することを考え、FDLTI-H_∞ 制御の可解性を損なうこと無しに適合性を高め、その結果保守性を減らすことを目的とする。また、空気の持つ非線形性やシール摩擦などの問題により、空気圧制御系に対してロバスト制御を体系的に適用した例は現在までのところほとんどない。ここでは、提案したロバスト制御を空気圧制御系に適用しその有効性を確認する。

以下に各章の概要を記す。

第1章 "Introduction" では、本研究の背景、概要及び論文の構成について述べる。

第2章 "Robust Control Synthesis with Minor Feedback" では、マイナーフィードバックを併用した FDLTI-H_∞ 制御の基本的な考え方を示す。マイナーフィードバックを併用した設計法自体は新しいものではないが、ロバスト制御の観点からの考察はない。そこでの問題点は、マイナーフィドバックにより基準モデルとモデル化誤差の両方が変化するため、たとえモデル化誤差がマイナーフィードバックにより減っても、性能が向上するとは必ずしも言えない点である。ここでは、外乱除去問題に基づいて考察を行い、マイナーフィードバックにより性能が向上するための十分条件として、基準モデルとモデル化誤差の両方の大きさが小さくなることが必要であることを示している。

第3章 "Minor Feedback Linearization" では、非線形な制御対象に対する代表的なマイナーフィードバックである厳密な線形化に関して、応用上適合性を増すためのいくつかの考察を行なう。これらの結果は、第6章で取り扱う空気圧駆動系への応用において特に有用である。現在提案されている線形化補償器の設計法では、得られる線形化された制御対象と元の非線形モデルの線形近似モデルとは必ずしも一致しない。したがってアウターループとして FDLTI-H_∞ 制御を適用した場合、非線形性がキャンセルされてモデル化誤差が小さくなったとしても性能が向上できるかどうかは直ちに結論づけられない。ここでは、元の非線形モデルの線形近似モデルと一致するような線形化制御則を与える。このことによ

り、線形化制御により制御特性が向上できることが直ちに結論づけられる。また、線形化可能であるかどうかの判定法はすでに知られているが、複雑な計算が必要であり、どのような制御対象が線形化可能であるかを明らかにすることは応用上重要である。ここでは、線形化可能な負荷を1次の非線形アクチュエータで駆動する系は線形化可能であることを証明している。最後にステップ状の外乱が加わった場合の線形化制御について考察を行なう。ここでは、状態に加えて外乱も測定可能とし、さらに外乱の加わり方と元の座標変換との間にある種のマッチング条件が満たされた場合、外乱除去を考慮した線形化制御則が計算可能であることを示している。

第4章"Minor Feedback Synthesis considering Real Parametric Uncertainty"では、実パラメータの不確かさを持つ系に対するマイナーフィードバックの設計法をパラメータ空間を用いて与える。モデル化誤差を線形とした場合、外乱除去の性能を向上させるためにはマイナーフィードバックはH_∞ノルム制約条件を満たさなければならない(詳しくは第2章で述べられている)。本章では、実パラメータの不確かさを持つ系に対するH_∞ノルム制約条件を満たすかどうかの判定法を定符合条件に基づいて与えている。さらに、H_∞ノルムの拡張である周波数帯域を制限したノルムに関する考察も行なう。これらの結果を利用することにより、パラメータ空間によりマイナーフィードバックが設計可能であることをPI補償器を例にとり示す。

第5章"Application to Pressure Control System"では、固定容器の圧力制御系に対して、第2章で提案された手法を適用する。周波数応答実験の結果、ここでの圧力制御系が提案手法の十分条件を満たしていることが確認された。また補償器を設計して外乱除去特性を実際に測定した結果、マイナーフィードバックにより性能が向上されることが確かめられた。

第6章"Application to Pneumatic Actuator System"では、第2章、第3章で提案された手法をゴム人工筋をアクチュエータとする空気圧駆動系に適用する。ここでは、動作気体の変化を等温的としたモデルを用い、空気圧駆動系が第3章で示された線形化可能なクラスに属することを示した。また、モデルに含まれない静止摩擦をステップ状の外乱と考え、第3章で提案された外乱除去を考慮した線形化制御を適用し、加速度補償を用いることによりその影響が除去できることを示した。最後に第2章で提案したマイナーフィドバックを併用したFDLTI-H_∞制御を行ない、空気圧駆動系でも外乱除去性能が向上されることが確認した。

第7章"Conclusion"では、本研究を通して得られた結果を総括している。

Acknowledgments

First, I would like to express my best appreciation to my supervisor Professor S. Hara for his helpful advice and support during my research. Without his guidance, I could not have completed this work.

I am also grateful to Professor T. Kagawa and Research Associate T. Fujita who offered me many useful comments from the viewpoint of practical application in pneumatic control. It is my pleasure to thank the following people: Professor M. Sampei for his useful comments on Proposition 3.3.1 in Section 3.3, Professor S. P. Bhattacharyya who gave me some valuable comments on the results in Chapter 4 and suggested the name "Sign Definite Condition", Dr. T. Iwasaki for his reviewing this manuscript in English, and Mr. Tomisaka for his cooperation in experiments.

Finally, I acknowledge to Professor T. Ono and Professor K. Osuka who introduced me the joy of research for the first time when I was an undergraduate student.

Contents

List of Figures

Chapter 1

Introduction

The purpose of controller design is to determine a controller for a given real plant to satisfy given control objectives. Most of the design methods are based on a mathematical model of a real plant, called *design model*, where a controller is determined by using mathematical manipulation based on the model. Design model had been assumed to be a *fixed* plant, called *nominal plant*. A controller designed based on a nominal plant might fail in practice if it does not consider the modeling error between the nominal plant and the real plant. The property to absorb the modeling error is an important design objective and it is called robustness.

We review the literature on robust control briefly: In so-called classical control, robustness has been considered implicitly. For example, gain and phase margins have been used as indices of robustness and controller has been designed guided by experience and rule of thumb.

On robustness for real parametric uncertainty, Kharitonov has investigated the Hurwitz-stability of plants for which the characteristic polynomials are interval polynomials. He has shown that only four fixed special extremal polynomials determine the stability of the interval plant[Kharitonov 1978]. Motivated by this result, some analogous results had been obtained for other design objectives, e.g., [Chapellat 1990][Kimura 1994]. These results are useful in analysis but not directly applicable to controller design.

Recently, finite dimensional linear time invariant (FDLTI) H_∞ control has been proposed[Doyle 1992] where design model is characterized as *nominal plant + model uncertainty*. Based on the FDLTI H_∞ control, some extensions have been proposed. For example, nonlinear H_∞ control[Imura 1994] for nonlinear plants and real μ-synthesis[Doyle 1982] for real parametric perturbed plants.

·We here recall two fundamental requirements for the controller design methods, namely, they should be

- *suitable* for treating given real plant and control objectives

- *tractable* in computing controller.

If an FDLTI H_∞ control design method meets these requirements, we claim that it is one of the most powerful design methods for robust control. This claim is due to its superiority of suitability and tractability. The former is based on the fact that we can treat the modeling error in higher frequency range naturally in the H_∞ control and the latter is on the fact that the H_∞ controller is determined by solving two Riccati equations.

The uncertainty model used in the H_∞ control is norm bounded, while real modeling error between the real plant and an FDLTI nominal plant is not. Therefore, the determination of the uncertainty model is conservative in particular applications. Fig. 1.0.1 illustrates the situation. Hence, by applying the H_∞ control to real applications directly, resulting system performance might be conservative.
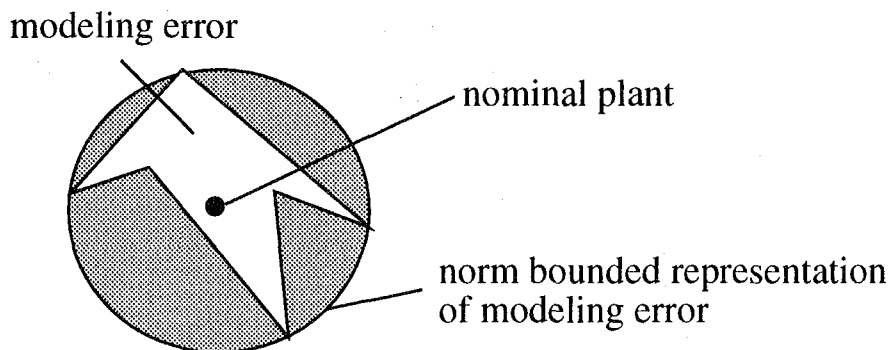
Figure 1.0.1: image of conservativeness of norm bounded representation

To reduce the conservativeness, nonlinear H_∞ control[Imura 1994] has been proposed to treat nonlinearity of the plant and real μ-synthesis[Doyle 1982] has been proposed to treat real parametric uncertainty. These approaches, however, do not fully succeeded so far because design scheme of the both theories are not tractable.

Throughout this thesis, we investigate a robust control design with minor feedback to reduce the conservativeness based on the FDLTI H_∞ control. The approach used here gains suitability of the FDLTI H_∞ control without losing its tractability. An image of reduction of conservativeness with minor feedback is depicted in Fig. 1.0.2.

We see examples of this idea in several areas of control engineering. Modification of the nominal plant with minor feedback is commonly used in practice. For position control system with pneumatic actuator, pressure control loop is used as a minor feedback to make the pressure control loop fast so that its dynamics can be neglected. In addition to the loop, position control loop is designed[Kawakami 1993]. For flexible structure systems, direct velocity feedback (DVFB) is applied

7

modified modeling error
with minor feedback

modified nominal plant
with minor feedback

norm bounded representation
of modified modeling error
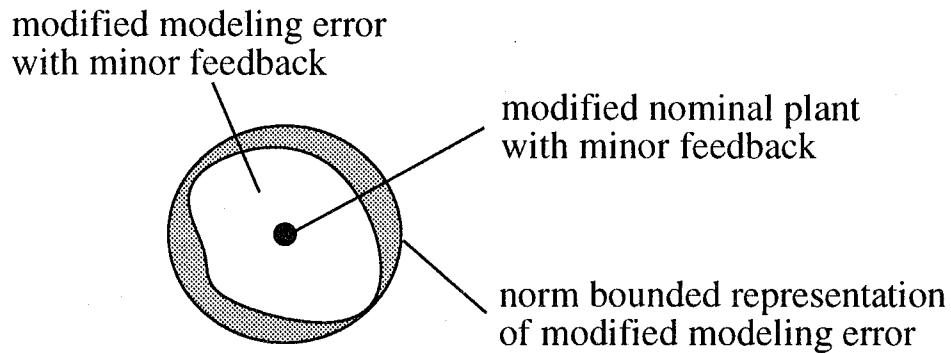
Figure 1.0.2: image of reduction of conservativeness with minor feedback

at first as a minor feedback to gain the stiffness of the systems and then, robust controller is design based on the modified plant. However, less attention is paid for modification of the uncertainty. Only a partial result for first and second order plants has been found in [Fukuda 1994].

A typical example of reducing the uncertainty model with minor feedback can be seen in feedback linearization[Su 1982]. The effectiveness of the feedback linearization has been confirmed by several applications, e.g., [Takagi 1993][Sugie 1993]. However, there had been few application of feedback linearization for pneumatic systems. We are aware of only one application in [Bouhal 1993]. Moreover, original linearization control is not compatible for pneumatic systems. For example, its linearizability has not been clarified yet. To deal with the problems, reformulation of linearizing control law, linearizability, and linearization with disturbance rejection are investigated in this thesis to gain the suitability of feedback linearization with pneumatic systems. We examine the effectiveness of the minor feedback linearization based on these results.

For real parametric uncertainty, the parameter space design method is tractable if the number of controller parameters is small. Since simple controller is preferable for the minor feedback, we here apply the method to design a minor feedback controller considering real parametric uncertainty.

This thesis is divided into seven chapters. A summary is given as follows:

Chapter 2: Robust Control Synthesis with Minor Feedback The basic idea of robust control with minor feedback is proposed to reduce the conservativeness of robust control. Disturbance rejection problem is introduced to investigate the effect of the minor feedback. A sufficient condition is derived under which the minor feedback improves a system performance.

Chapter 3: Minor Feedback Linearization First, a modified linearizing control is proposed to preserve the property of the first order approximated system. Next, a class of feedback lineariz-

able systems is derived. Last, linearization control with disturbance rejection is proposed. These are especially useful for pneumatic actuator systems.

Chapter 4: Minor Feedback Synthesis considering Real Parametric Uncertainty As described in Chapter 2, the minor feedback should satisfy a robust H_∞ norm constraint subject to the real parametric uncertainty in order to system performance. This chapter presents an H_∞ norm bounds test for plants with real parametric uncertainty. The test is based on Sign Definite Condition. In addition, bounds of frequency restricted norm, a generalization of H_∞ norm, is examined. A design example of PI-type controller for a parametric perturbed plant is illustrated based on parameter space design method.

Chapter 5: Application to Pressure Control System In this chapter, the proposed method is applied to a pressure control system, the most simple pneumatic system. Experimental results confirm the correctness of the method.

Chapter 6: Application to Pneumatic Actuator System In this chapter, the proposed methods are applied to a pneumatic actuator system with a rubber artificial muscle, which is more complex system than the pressure control system in the previous chapter. Experimental results shows that the proposed methods are also useful for the pneumatic actuator system.

Chapter 7: Conclusion We summarize the contribution of the thesis and point out some future research issues.

Chapter 2

Robust Control Synthesis with Minor Feedback

The basic idea for reducing of conservativeness of robust control with minor feedback is introduced in this chapter. Since the minor feedback changes both nominal plant and uncertainty model, we cannot conclude immediately that it improves system performance even if the magnitude of uncertainty model is reduced. A disturbance rejection problem is introduced to investigate the effect of the minor feedback and a sufficient condition is derived on which the minor feedback improves the attenuation level.

2.1 Conservativeness of Robust Control

We here review the conservativeness of robust control based on finite dimensional linear time invariant (FDLTI) H_∞ control theory. Since we cannot obtain an exact mathematical model of a real plant P_r, the design methods should take the modeling error of the mathematical representation into account. To deal with the modeling error, the design model used in the H_∞ control is a set of plants rather than a fixed one. The model is characterized by a FDLTI nominal plant combined with uncertainty model which is assumed to be a set of norm bounded systems. This design model $\mathcal{P}$ can be expressed as, e.g., in multiplicative perturbed form as

$$\mathcal{P} := \{P | P = P_0(1 + W_T \Delta), \ \|\Delta\|_\infty \leq 1\} \tag{2.1.1}$$

where W_T refers to the magnitude of the uncertainty model. Fig. 2.1.1 shows the design model in the multiplicative perturbed form. The magnitude of W_T is determined mainly in the frequency domain, and hence it is called the frequency weight corresponding to the uncertainty model.
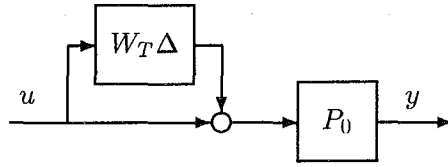
Figure 2.1.1: model expression in robust control : uncertainty model $W_T\Delta$ + nominal plant P_0

The determination of uncertainty model corresponding to real modeling error should be tight in order to achieve good system performance. However, the modeling error between the real plant and the FDLTI nominal plant is not coincident with the norm bounded uncertainty in practice. Therefore, the gap will make the magnitude of the uncertainty model large and this causes the conservativeness in robust control design.

Furthermore, suppose that the variation of the modeling error over the frequency domain is large as shown in Fig. 2.1.2-a. Then, the tighter evaluation requires the higher order weighting function, which is undesirable in practice. In other words, we usually use a low order weighting function to represent uncertainty model and thus the large variation of modeling error also leads to the conservativeness. Fig. 2.1.2-a illustrates the situation.

a) without minor feedback   b) with minor feedback
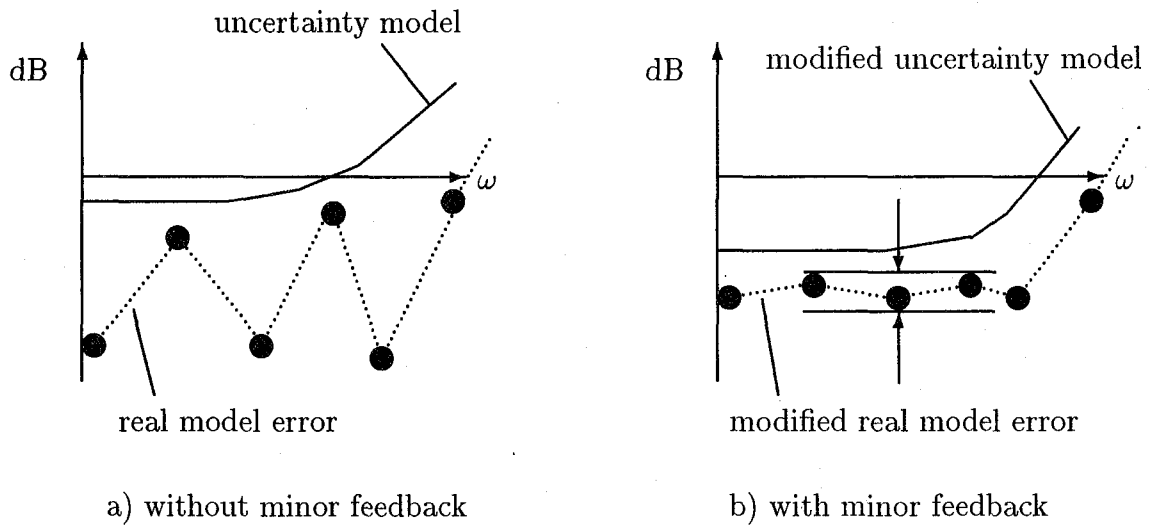
Figure 2.1.2: image of variation reduction with minor feedback

11

2.2 Reduction of Conservativeness with Minor Feedback

A design method with minor feedback is examined in order to reduce the conservativeness of robust control. We first focus on robust stability. By applying a minor feedback F for a given real plant P_r, we consider the modified plant P_r^F defined by[1]

$$P_r^F := P_r/(1 + P_r F) \tag{2.2.1}$$

instead of P_r itself (See Fig. 2.2.1.).
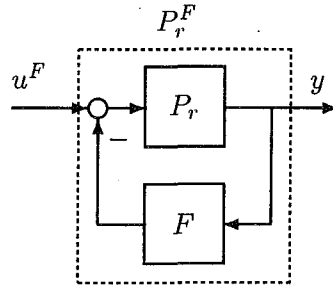
Figure 2.2.1: modified real plant P_r^F with minor feedback F

Here, we define a set of plants $\mathcal{P}^F$ in the multiplicative perturbed form defined as

$$\mathcal{P}^F := \{P^F | P^F = (1 + W_T^F \Delta)P_0^F, \ \|\Delta\|_\infty \le 1\} \tag{2.2.2}$$

where

$$P_0^F := (1 + P_0 F)^{-1} P_0. \tag{2.2.3}$$

Our aim is to determine $\mathcal{P}^F$, i.e., W_T^F so that

$$P_{ri}^F \in \mathcal{P}^F; \quad i = 1, \dots, N \tag{2.2.4}$$

hold, where P_{ri}^F; $i = 1, \dots, N$ are a series of plants experimentally identified for P_r^F. If such $\mathcal{P}^F$ is determined with a margin, we may believe that $P_r^F \in \mathcal{P}^F$. In other words, if an H_∞ controller robustly stabilizes $\mathcal{P}^F$, we can conclude that it also stabilizes P_r^F.

Therefore, if we can reduce the magnitude of W_T^F and/or the variation of the modeling error by the minor feedback F, we may claim that the conservativeness is reduced and the performance is improved. The reduction is illustrated in Figs. 2.1.2-b. and 2.2-b.

However, we cannot say whether the conjecture is true or false immediately, since the minor feedback changes the nominal plant P_0^F as well as the bound of model uncertainty W_T^F as already mentioned.

---

[1] The symbol with superscript $*^F$ means the corresponding $*$ modified by the minor feedback F from now on.
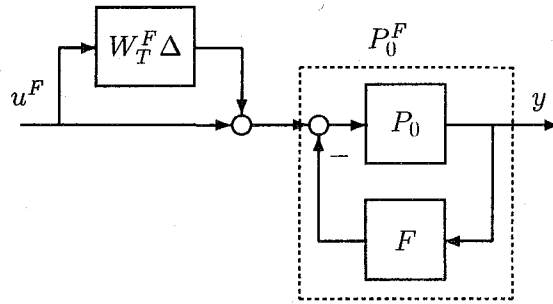
Figure 2.2.2: model expression in robust control : modified uncertainty $W_T^F \Delta$ + modified nominal plant P_0^F

a) without minor feedback

b) with minor feedback
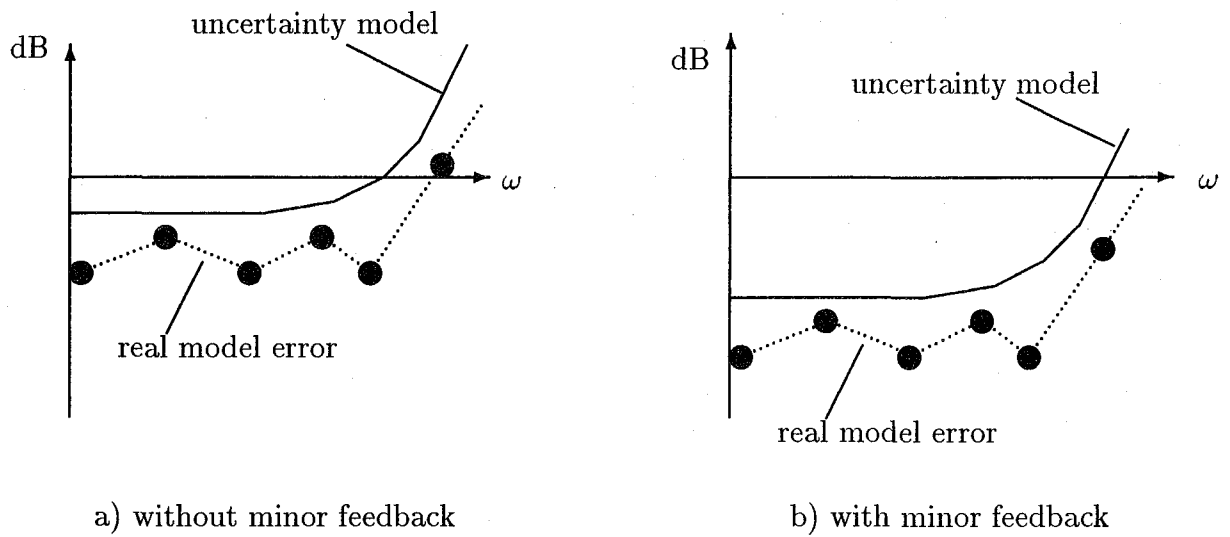
Figure 2.2.3: image of gain reduction with minor feedback

A disturbance attenuation problem is investigated to tackle the problem in the next section.

2.3 Disturbance Attenuation Problem

We consider a disturbance attenuation problem with a multiplicative perturbation defined as follows.

Disturbance Attenuation Problem *Find a stabilizing controller K which maximizes the disturbance attenuation level q subject to*

$$\|G_{zw}\|_\infty < 1 \tag{2.3.1}$$

where G_{zw} denotes the closed-loop transfer function from w to z in Fig. 2.3.1. The maximum value is denoted by $\bar{q}(F)$.
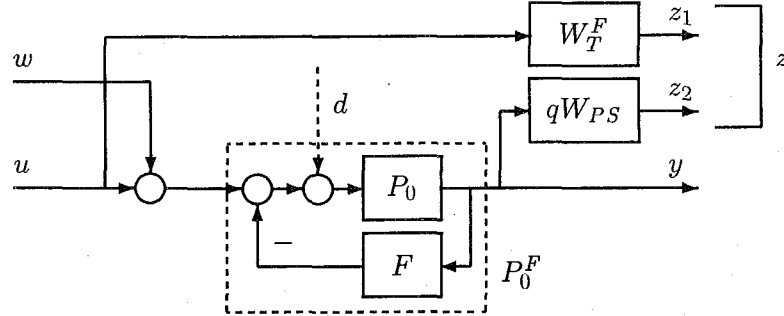
Figure 2.3.1: disturbance attenuation problem

Note that minimizing the gain of the closed-loop transfer function from w to z_2, denoted by G_{z_2w}, implies the disturbance attenuation from plant input to the plant output with frequency weight W_{PS} of level q. Although the actual disturbance at plant input channel is d, not w, in Fig. 2.3.1, the minimization of $\|G_{z_2w}\|_\infty$ instead of $\|G_{z_2d}\|_\infty$ seems to have less physical meaning, where G_{z_2d} refers to the closed-loop transfer function from d to z_2. However simple computation yields

$$G_{z_2w} = G_{z_2d} \tag{2.3.2}$$

and this identity makes the disturbance attenuation problem meaningful.

2.4 Reduction of Conservativeness in Disturbance Attenuation Problem with Minor Feedback

We show that the conjecture in the preceding section is true for the disturbance attenuation problem of maximizing the attenuation level $\bar{q}(F)$, which is described in the following proposition.

Proposition 2.4.1 *Consider the disturbance attenuation problem where the plant P_0 is single input multiple output system with size k expressed as*

$$P_0 = [p_1 \cdots p_k]^T \tag{2.4.1}$$

and the weighting function W_{PS} is a diagonal matrix.

14

Suppose two minor feedback controllers F_1 and F_2 satisfy the following three conditions:

$$C0 \quad : \quad ^\exists M : unimodular \ over \ RH_\infty \ \ s.t \ P_0^{F_1} = MP_0^{F_2}$$

$$C1 \quad : \quad |p_i^{F_1}(j\omega)| \quad > \quad |p_i^{F_2}(j\omega)| \ ; \quad ^\forall \omega \in \mathbf{R} \ and \ i = 1, \ldots, k. \qquad (2.4.2)$$

$$C2 \quad : \quad |W_T^{F_1}(j\omega)| \quad \geq \quad |W_T^{F_2}(j\omega)| \ ; \quad ^\forall \omega \in \mathbf{R}.$$

Then

$$\bar{q}(F_1) < \bar{q}(F_2) \qquad (2.4.3)$$

holds for any fixed weight W_{PS}.

The disturbance attenuation problem is equilibrate to the mixed sensitivity problem shown in Fig. 2.4.1 with $W_S^F := W_{PS}P_0^F$, and hence Proposition 2.4.1 is equilibrate to the following lemma:
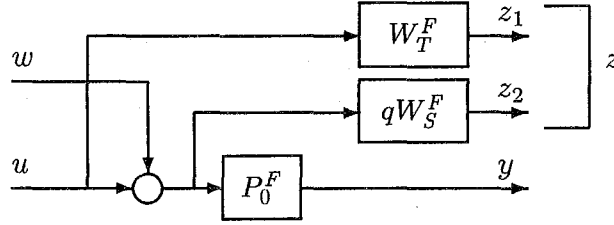
Figure 2.4.1: mixed sensitivity problem

Lemma 2.4.1 *Consider the disturbance attenuation problem where the plant P_0 is single input multiple output system with size k expressed as (2.4.1) and the weighting function W_S^F is a vector valued weighting function denoted as*

$$W_S^F = [w_1^F \cdots w_k^F]^T. \qquad (2.4.4)$$

Suppose two minor feedback controllers F_1 and F_2 satisfy the following three conditions:

$$C0 \quad : \quad ^\exists M : unimodular \ over \ RH_\infty \ \ s.t \ P_0^{F_1} = MP_0^{F_2}$$

$$C1 \quad : \quad |w_i^{F_1}(j\omega)| \quad > \quad |w_i^{F_2}(j\omega)| \ ; \quad ^\forall \omega \in \mathbf{R} \ and \ ^\forall i = 1, \ldots, k \qquad (2.4.5)$$

$$C2 \quad : \quad |W_T^{F_1}(j\omega)| \quad \geq \quad |W_T^{F_2}(j\omega)| \ ; \quad ^\forall \omega \in \mathbf{R}.$$

then

$$\bar{q}(F_1) < \bar{q}(F_2) \qquad (2.4.6)$$

holds.

Hence, we prove the above lemma instead of the proposition based on the following preliminary result:

15

Lemma 2.4.2 *Let G be a generalized plant of an H_∞ problem partitioned by*

$$G = \begin{bmatrix} G_{11} & G_{12} \\ G_{21} & G_{22} \end{bmatrix} \tag{2.4.7}$$

and γ_{opt} be the optimal attenuation level corresponding to G defined as

$$\gamma_{opt}(G) := \inf_{K \in \mathcal{K}} \|LFT(G, K)\|_\infty \tag{2.4.8}$$

where $\mathcal{K}$ is a set of stabilizing controllers and $LFT(G, K)$ is linear fractional transformation associated with G and K defined by

$$LFT(G, K) := G_{11} + G_{12}(I - KG_{22})^{-1}G_{21}. \tag{2.4.9}$$

Furthermore, let G_M be a generalized plant defined by

$$G_M := \begin{bmatrix} G_{11} & G_{12} \\ MG_{21} & MG_{22} \end{bmatrix} \tag{2.4.10}$$

where $M \in RH_\infty$ is a unimodular function. Then,

$$\gamma_{opt}(G) = \gamma_{opt}(G_M) \tag{2.4.11}$$

In other words, we can identify G with G_M in the sense of the H_∞ problem.

this result can be proven based on the fact that the unimodular part in the measurement channel can be cancelled out by the controller.

Proof of Lemma 2.4.2: First, we show that

$$\gamma_{opt}(G) \le \gamma_{opt}(G_M). \tag{2.4.12}$$

Let K_{opt} be a stabilizing controller for G which attains $\gamma_{opt}(G)$[2] Then, defining K_M as

$$K_M := KM^{-1} \tag{2.4.13}$$

yields

$$LFT(G_M, K_M) = LFT(G, K) \tag{2.4.14}$$

since stable pole-zero cancelation is allowed in the H_∞ problem. Therefore, we have (2.4.12).

The opposite of the inequality (2.4.12)

$$\gamma_{opt}(G) \ge \gamma_{opt}(G_M) \tag{2.4.15}$$

---

[2]if such K_{opt} dose not exist, we can carry out the proof in the same way by considering a series of controllers K_i, $i = 1, \ldots, n$ which satisfies $\|\text{LFT}(G, K_i)\|_\infty \to \gamma_{opt}(G)$ as $n \to \infty$.

can be shown in the same way so we conclude

$$\gamma_{opt}(G) = \gamma_{opt}(G_M) \qquad (2.4.16)$$

□

Proof of Lemma 2.4.1:

By viture of the condition C0), we identify $P_0^{F_1}$ with $P_0^{F_2}$ as a consequence of Lemma 2.4.2. Namely we replace $P_0^{F_2}$ as $P_0^{F_1}$. In addition, let $\overline{K}^{F_1}$ be an stabilizing controller which attains the maximum $\overline{q}(F_1)$. Then, we have

$$\begin{aligned} T^{F_1} &= T^{F_2} \\ S^{F_1} &= S^{F_2} \end{aligned} \qquad (2.4.17)$$

where T^F and S^F denote the complementary sensitivity function and the sensitivity function with a minor feedback F, respectively.

Furthermore, the relations

$$\begin{aligned} 1 &> \|G_{zw}^{F_1}\|_\infty \\ &= \sup_{w \in \mathbf{R}} \lambda_{\max}^{\frac{1}{2}}(G_{zw}(j\omega)^* G_{zw}(j\omega)) \\ &= \sup_{w \in \mathbf{R}} (|W_T^F(j\omega)T^F(j\omega)|^2 + q^2 \sum_{i=1}^{k} |w_i^F(j\omega)S^F(j\omega)|^2) \end{aligned} \qquad (2.4.18)$$

yield

$$\overline{q}^2(F_1) = \inf_{w \in R} \frac{1 - |W_T^{F_1}(j\omega)T^{F_1}(j\omega)|^2}{\sum_{i=1}^{k} |w_i^{F_1}(j\omega)S^{F_1}(j\omega)|^2}. \qquad (2.4.19)$$

Hence, knowing that the inequality

$$\|W_T^F T^F\|_\infty < 1 \qquad (2.4.20)$$

is satisfied for robust stability and taking account of the conditions C1 and C2, we have

$$\begin{aligned} \overline{q}^2(F_2) &= \inf_{w \in R} \frac{1 - |W_T^{F_2}(j\omega)T^{F_2}(j\omega)|^2}{\sum_{i=1}^{k} |w_i^{F_2}(j\omega)S^{F_2}(j\omega)|^2} \qquad &(2.4.21) \\ &= \inf_{w \in R} \frac{1 - |W_T^{F_2}(j\omega)T^{F_1}(j\omega)|^2}{\sum_{i=1}^{k} |w_i^{F_2}(j\omega)S^{F_1}(j\omega)|^2} \qquad &(2.4.22) \\ &> \frac{1 - |W_T^{F_1}(j\omega)T^{F_1}(j\omega)|^2}{\sum_{i=1}^{k} |w_i^{F_1}(j\omega)S^{F_1}(j\omega)|^2} \qquad &(2.4.23) \\ &= \overline{q}^2(F_1) \qquad &(2.4.24) \end{aligned}$$

17

and this concludes the lemma.

$\square$

We have the following more descriptive result based on the Proposition 2.4.1 if we restrict the class of the plant.

Corollary 2.4.1 *Consider the disturbance attenuation problem with an SIMO plant P_0 expressed as (2.4.1). Suppose two minor feedback controllers F_1 and F_2 satisfy the following three conditions:*

$$
\begin{aligned}
\text{C0} \quad & : \quad p_i^{F_1} \text{ and } p_i^{F_2} \text{ are stable} \\
& \quad \text{ and they have the same unstable zeros for } {}^{\forall} i = 1, \ldots, k \\
\text{C1} \quad & : \quad |p_i^{F_1}(j\omega)| \; > \; |p_i^{F_2}(j\omega)| \; ; \quad {}^{\forall}\omega \in \mathbf{R} \text{ and } {}^{\forall} i = 1, \ldots, k. \\
\text{C2} \quad & : \quad |W_T^{F_1}(j\omega)| \; \geq \; |W_T^{F_2}(j\omega)| \; ; \quad {}^{\forall}\omega \in \mathbf{R}.
\end{aligned}
\tag{2.4.25}
$$

Then

$$
\overline{q}(F_1) < \overline{q}(F_2) \tag{2.4.26}
$$

holds for any fixed weight W_{PS}.

Proof of Corollary 2.4.1:

First, assume that the components of $P_0^{F_1}$ and $P_0^{F_2}$ can be factorized as

$$
\begin{aligned}
p_i^{F_1} &= p_{Si}^{F_1} p_{USi} \\
p_i^{F_2} &= p_{Si}^{F_2} p_{USi}
\end{aligned}
\tag{2.4.27}
$$

for all $i = 1, \ldots, k$, where $p_{Si}^{F_1}, p_{Si}^{F_2} \in RH_\infty$ are unimodular functions and $p_{USi} \in RH_\infty$ is a factor corresponds to the common unstable zeros. In this case, C0) in Corollary 2.4.1 implies C0) in Proposition 2.4.1 by defining

$$
M = p_{Si}^{F_1} p_{Si}^{F_2{}^{-1}}. \tag{2.4.28}
$$

and hence the corollary is true in this case. These factorizations are possible if the plants satisfy the constraints of relative degree.

Next we confirm the generality of the assumption. Here we decompose the p_i^F over polynomials as

$$
p_i^F = \frac{n_{si}(s) n_{usi}(s)}{d_i(s)} \tag{2.4.29}
$$

where the polynomials $n_{si}(s)$ and $n_{usi}(s)$ are associated with stable and unstable zeros and $d_i(s)$ with the stable poles. To satisfy the assumption, here we augment the plant P^F as P_a^F defined by

$$
\begin{aligned}
P_a^F &:= [p_{a1}^F \cdots p_{ak}^F]^T \tag{2.4.30} \\
p_{ai}^F &:= \frac{n_{si}(s)(\delta_1 s + 1)^{n_{1i}}}{d_i(s)} \frac{n_{usi}(s)}{(\delta_2 s + 1)^{n_{2i}}} \tag{2.4.31} \\
&=: p_{Sai}^F p_{USai}, \quad i = 1, \ldots, k \tag{2.4.32}
\end{aligned}
$$

18

with sufficiently small $\delta_1 > 0$ and $\delta_2 > 0$, $\delta_1 \neq \delta_2$, where

$$
\begin{aligned}
n_{1i} &:= \text{ order of } d_i(s) - \text{order of } n_{si}(s) \\
n_{2i} &:= \text{ order of } n_{usi}(s)
\end{aligned}
\tag{2.4.33}
$$

Obviously p_{Sai}^F and p_{Uai} satisfy the condition C0) in Proposition 2.4.1. Furthermore, from the continuity of the H_∞ norm of a system with respect to its entries, the H_∞ norms of the closed-loop systems are almost equal to each other, that is, for any given $\epsilon > 0$, there exist δ_1 and δ_2 such that

$$
\left| \|G_{zw}^F\|_\infty - \|G_{zwa}^F\|_\infty \right| < \epsilon
\tag{2.4.34}
$$

for an arbitrary stabilizing controller, where G_{zwa}^F denotes the closed-loop transfer function form w to z with the augmented plant P_a^F in (2.4.31). Hence, the lemma is true for plants with any relative degree. $\qquad\square$

Remark : The conditions C1) and C2) in Proposition 2.4.1 mean that a minor feedback improves the disturbance attenuation level if it reduces the magnitude of nominal plant and uncertainty model. The former can be verified very easily from the nominal model. However, the latter cannot readily be checked out, because it is a constraint on the unknown part of the plant. One way to check the condition C2) is the experimental verification. We use this approach to the application of pneumatic systems in Chapter 5 and 6.

Another way is to use a priori information. Let U and U^F be the real modeling error and the modified modeling error with minor feedback F in multiplicative form. Then, simple computations lead to the following relation

$$
\begin{aligned}
U^F &= \frac{1}{1 + P_0(1+U)F} U \\
&= \frac{1}{1 + P_r F} U.
\end{aligned}
\tag{2.4.35}
$$

Therefore, knowing (2.2.3), C1) and C2) are satisfied if the minor feedback controller F satisfies the robust sensitivity constraint

$$
\left\| \frac{1}{1 + P_r F} \right\|_\infty < 1.
\tag{2.4.36}
$$

This is a clue to design the minor feedback controller and based on this fact, minor feedback synthesis for real parametric perturbed plants is investigated in Chapter 4.

Chapter 3

Minor Feedback Linearization

Minor feedback linearization is one of the useful techniques to deal with nonlinearity of plants. However, the original formulation summarized as Theorem 3.1.1 in the next section is not suitable for practical plants. In this chapter, some useful results are proposed to gain its suitability.

For notational convenience, the functions appearing this chapter are assumed to be sufficiently smooth, that is, we can differentiate the functions as many times as we need. In addition, arguments of functions are omitted if it is clear from the context, for example we denote $f(x)$ as f. The i-th component of a vector, say f, is represented with subscript i, e.g., f_i.

3.1 Preliminary

First, we summarize a well-known result on the feedback linearization to clarify the discussion.

Theorem 3.1.1 [Su 1982] *Consider a single input n-th order nonlinear plant expressed as*

$$\dot{x} = f(x) + g(x)\phi(x, u) \tag{3.1.1}$$

where the origin is an equilibrium point. Suppose this plant satisfies the following conditions:

p0) $\phi(0,0) = 0,\ \partial\phi/\partial u \neq 0$

p1) $\{ad_f^0 g, ad_f^1 g, \cdots, ad_f^{n-1} g\}$ *is linearly independent.*

p2) $\{ad_f^0 g, ad_f^1 g, \cdots, ad_f^{n-2} g\}$ *is involutive.*

Then there exists a non-singular coordinate transformation

$$\xi = T(x), \quad T(0) = 0 \tag{3.1.2}$$

which converts the plant (3.1.1) into

$$\frac{d}{dt}\begin{bmatrix} \xi_1 \\ \vdots \\ \xi_{n-1} \\ \xi_n \end{bmatrix} = \begin{bmatrix} \xi_2 \\ \vdots \\ \xi_n \\ \alpha(\boldsymbol{\xi}) \end{bmatrix} + \begin{bmatrix} 0 \\ \vdots \\ 0 \\ \beta(\boldsymbol{\xi}) \end{bmatrix} \phi(T^{-1}(\xi), u) \qquad (3.1.3)$$

Furthermore, the original nonlinear plant (3.1.1) becomes the following linear plant

$$\dot{\boldsymbol{\xi}} = \begin{bmatrix} 0 & 1 & 0 & \cdots & 0 \\ 0 & 0 & 1 & \cdots & \vdots \\ \vdots & \vdots & \vdots & \ldots & 0 \\ 0 & 0 & 0 & \cdots & 1 \\ 0 & 0 & 0 & \cdots & 0 \end{bmatrix} \boldsymbol{\xi} + \begin{bmatrix} 0 \\ 0 \\ \vdots \\ 0 \\ 1 \end{bmatrix} \nu \qquad (3.1.4)$$

by introducing a new input ν and defining u as

$$u = \phi^{-1}\left(x, \frac{\nu - \alpha(\boldsymbol{\xi})}{\beta(\boldsymbol{\xi})}\right) \qquad (3.1.5)$$

where $\phi^{-1}(\boldsymbol{x}, \cdot)$ denotes the inverse of ϕ with fixed x. $\qquad\qquad\Box$

3.2   Feedback Linearization Preserving Characteristics of the Original Plant

Feedback linearization controller is designed to cancel out the nonlinearity of a given real plant. Therefore, by using this as minor feedback, the model error between the modified linearized real plant and the modified nominal plant is smaller than that between the original real plant and a linear approximated nominal plant if nonlinearity is dominant in the original model error for FDLTI H_∞ control. That is, the magnitude of uncertainty model is reduced by the minor feedback linearization.

We here note that if we apply feedback linearization in [Su 1982] directly, the resulting linearized plant (3.1.4) is the plant of Brnouvsky's canonical form (3.1.4), which is not the linear approximated model of the original nonlinear model at an equilibrium point. Hence, we cannot conclude immediately that the resulting performance attained with the minor feedback linearization is better than that without the linearization even if the magnitude of uncertainty model is reduced. In addition, the linearized plant (3.1.4) does not reflect the structure of the original plant (3.1.1), in other words, it may lose the physical meaning. Hence, it is not easy to design the outer loop controller for the linearized plant.

In this section, linearizing control is reformulated so that the resulting linearized plant coincides with a linear approximated model of the original nonlinear model. By this reformulation, any existing linear controller designed based on the linear approximated model can be used for the outer loop controller without modification.

To do this, the input rearrangement given by

$$
\begin{aligned}
u &= \phi^{-1}(x, T_u \nu + F_{nl}) \\
T_u &:= \frac{b}{\beta(\xi)} \\
F_{nl} &:= \frac{\sum_{i=0}^{n-1} a_i \xi_i - \alpha(\xi)}{\beta(\xi)}
\end{aligned}
\tag{3.2.1}
$$

had been proposed to make the dynamics coincide with that of the linear approximated model in [Takagi 1993][Sugie 1993], where $a_i : i = 0, \ldots, n-1$ and b are constants determined by the following controllable canonical form of the linear approximated model (3.1.1):

$$
\dot{z} = \begin{bmatrix} 0 & 1 & \cdots & 0 \\ \vdots & \vdots & \ddots & \vdots \\ 0 & 0 & \cdots & 1 \\ a_0 & a_1 & \cdots & a_{n-1} \end{bmatrix} z + \begin{bmatrix} 0 \\ \vdots \\ 0 \\ b \end{bmatrix} u.
\tag{3.2.2}
$$

Here we propose an additional coordinate transformation from ξ to y defined by

$$
\begin{aligned}
y &= \left(\frac{dT(0)}{dx}\right)^{-1} \xi = \left(\frac{dT(0)}{dx}\right)^{-1} T(x) \\
&=: T_y(x)
\end{aligned}
\tag{3.2.3}
$$

which makes the measurement signals coincide with those of the linear approximated model.

Obviously $y = x$ holds in small neighborhood of the equilibrium point $x = 0$. In addition, relationship between ν and y is linear since this transformation is linear. Therefore, by using the reformulated linearizing control (3.2.1) and (3.2.3), the dynamics and the measurement signals of the resulting linearized plant coincide with those of the linear approximated plant. According to this, we can use controller design methods based on the linear approximated plant to determine the outer loop controller. In other words, by this reformulation, an existing controller which is designed based on the linear approximated plant can be used as an outer loop controller without any modification. Since the most common control for the pneumatic actuator plants is linear control designed based on the linear approximated model, this reformulation is useful in practice. The structure of the linearizing controller is illustrated in Fig. 3.2.1, where T_u, F_{nl} and T_y are input transformation, nonlinear feedback and output transformation defined in (3.2.1) and (3.2.3), respectively.
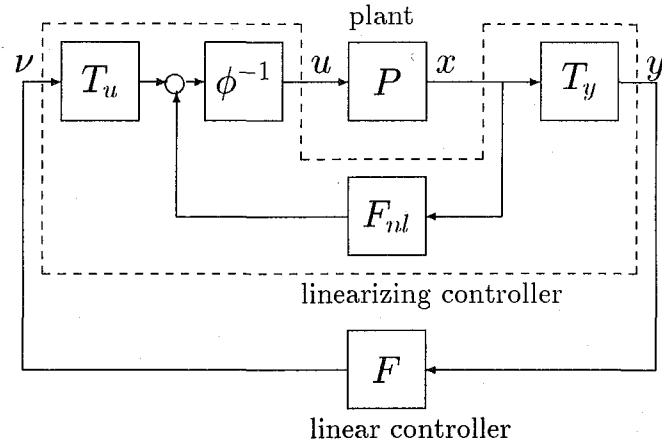
Figure 3.2.1: configuration of controller

In [Sampei 1993a][Sampei 1993b], a linearizing controller is designed such that the linear approximation of the overall controller involving the linearizing controller and a linear controller coincide with the linear controller designed based on the linear approximated model at an equilibrium point. The proposed reformulation of linearizing control gives an interpretation of the method used in [Sampei 1993a][Sampei 1993b] from the viewpoint of plants, which has been mainly considered from the viewpoint of controllers.

3.3 Feedback Linearizability

In general, nonlinear plants of order greater than or equal to three are not feedback linearizable. However, the following proposition shows that the plant composed of a single input linearizable load and a first order nonlinear actuator is linearizable even if the order of the entire plant is greater than or equal to three.

Proposition 3.3.1 *Consider a single input n-th order nonlinear load $\sum_p$ given by*

$$\sum_p \; : \; \dot{x}_p = f_p(x_p) + g_p(x_p)v \tag{3.3.1}$$

and a first order nonlinear actuator Σ_a whose dynamics depends on the state of the load $\sum_p$ expressed as

$$\sum_a : \begin{cases} \dot{x}_a &= f_a(x_{\mathrm{aug}}) + g_a(x_{\mathrm{aug}})\phi_a(x_{\mathrm{aug}}, u) \\ v &= h_a(x_{\mathrm{aug}}) \end{cases} \tag{3.3.2}$$

where $x_{\mathrm{aug}} := [x_p^T \; x_a]^T$. See Fig. 3.3.1

23
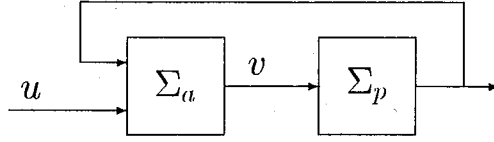
Figure 3.3.1: structure of model

If the load $\sum_p$ is input-state feedback linearizable, then the $n+1$-st order augmented plant involving $\sum_p$ and $\sum_a$ defined by

$$\sum_{\text{aug}} \; : \; \dot{x}_{\text{aug}} = \begin{bmatrix} f_p(x_p) + g_p(x_p)h_a(x_{\text{aug}}) \\ f_a(x_{\text{aug}}) \end{bmatrix} + \begin{bmatrix} 0 \\ g_a(x_{\text{aug}}) \end{bmatrix} \phi_a(x_{\text{aug}}, u) \tag{3.3.3}$$

is also input-state feedback linearizable.

Proof: Since $\sum_p$ is linearizable, there exists a non-singular coordinate transformation $\xi = T(x_p)$ such that

$$\frac{d}{dt} \begin{bmatrix} \xi_1 \\ \vdots \\ \xi_{n-1} \\ \xi_n \end{bmatrix} = \begin{bmatrix} \xi_2 \\ \vdots \\ \xi_n \\ \alpha_p(\xi) \end{bmatrix} + \begin{bmatrix} 0 \\ \vdots \\ 0 \\ \beta_p(\xi) \end{bmatrix} v =: f_\xi(\xi) + g_\xi(\xi)v \tag{3.3.4}$$

holds. For the augmented plant, let us define a new state variable ξ_{n+1} as

$$\xi_{n+1} := \dot{\xi}_n = \alpha_p(\xi) + \beta_p(\xi)h_a(x_{\text{aug}}). \tag{3.3.5}$$

Then, noting that $T(x_p)$ is independent of x_a, we see that the coordinate transformation T_{aug} from x_{aug} into $[\xi^T \; \xi_{n+1}]^T$ defined by

$$T_{\text{aug}} := \begin{bmatrix} T(x_p) \\ \alpha_p(T^{-1}(x_p)) + \beta_p(T^{-1}(x_p))h_a(x_{\text{aug}}) \end{bmatrix} \tag{3.3.6}$$

is non-singular.

In addition, knowing that the derivative of ξ_{n+1} can be expressed as

$$\dot{\xi}_{n+1} = \alpha_{\text{aug}}(\xi, x_a) + \beta_{\text{aug}}(\xi, x_a)\phi_a(x_{\text{aug}}, u) \tag{3.3.7}$$

$$\alpha_{\text{aug}}(\xi, x_a) \; := \; \left(\frac{d\alpha_p}{d\xi} + \frac{d\beta_p}{d\xi}h_a\right)\left(f_\xi + g_\xi h_a\right) + \beta_p\left(\frac{\partial h_a}{\partial x_p}(f_p + g_p h_a) + \frac{\partial h_a}{\partial x_a}f_a\right),$$

$$\beta_{\text{aug}}(\xi, x_a) \; := \; \beta_p\frac{\partial h_a}{\partial x_p}g_a,$$

24

we introduce a new input ν and define u as

$$u = \phi_a^{-1}\left(x_{\text{aug}}, \frac{\nu - \alpha_{\text{aug}}}{\beta_{\text{aug}}}\right). \tag{3.3.8}$$

Then, by applying the coordinate transformation (3.3.6) and the input transformation (3.3.8), the augmented plant $\sum_{\text{aug}}$ can be converted into the following linear form:

$$\frac{d}{dt}\begin{bmatrix} \xi_1 \\ \vdots \\ \xi_n \\ \xi_{n+1} \end{bmatrix} = \begin{bmatrix} \xi_2 \\ \vdots \\ \xi_{n+1} \\ 0 \end{bmatrix} + \begin{bmatrix} 0 \\ \vdots \\ 0 \\ 1 \end{bmatrix}\nu. \tag{3.3.9}$$

This completes the proof. $\qquad\qquad\qquad\qquad\qquad\qquad\qquad\qquad\qquad\qquad\qquad\qquad\square$

3.4 Feedback Linearization with Disturbance Rejection

Consider a single-input nonlinear plant affine in control signal u and disturbances $d_i(t)$, $i = 1, \ldots, m$ represented by

$$\dot{x} = f(x) + g(x)\phi(x, u) + \sum_{i=1}^{m} h_i(x)d_i(t). \tag{3.4.1}$$

Suppose that we can measure not only the state variable x but also the disturbances d_i, $i = 1, \ldots, m$, i.e., we consider the full information case. In addition, the disturbances are assumed to be step-type, that is, $\frac{d}{dt}d_i(t) \equiv 0$, $i = 1, \ldots, m$.

Though we postulate that the order of the plant is three for simplicity from now on, the result described in this section can be extended to plants with any order. Moreover, we assume that the nominal plant of (3.4.1) is feedback linearizable. Namely, there exists a nonsingular coordinate transformation

$$\xi = T(x) \tag{3.4.2}$$

such that

$$L_g T_1 = L_g L_f T_1 \equiv 0, \quad L_g L_f^2 T_1 \neq 0. \tag{3.4.3}$$

Our aim is to find out a linearizing control law by using information of d_i, $i = 1, \ldots, m$. By following the nominal coordinate transformation in (3.4.2) and knowing that the disturbances are step-type, i.e., $\dot{d}_i(t) = 0$, $i = 1, \ldots, m$, let us define a new coordinate ξ^d by

$$\begin{aligned} \xi_1^d &:= \xi_1 = T_1(x), \\ \xi_2^d &:= \dot{\xi}_1^d = L_{f+\sum h_i d_i} T_1, \\ \xi_3^d &:= \dot{\xi}_2^d = L_{f+\sum h_i d_i}^2 T_1 + \phi L_g L_{\sum h_i d_i} T_1. \end{aligned} \tag{3.4.4}$$

Note that we can compute the value of $\boldsymbol{\xi}^d$, since $T_1(x)$ is a known function and x and d_i, $i = 1, \ldots, m$ are measurable.

Under this coordinate transformation, the plant (3.4.1) can be expressed as

$$
\begin{aligned}
\dot{\xi}_1^d &= \xi_2^d \\
\dot{\xi}_2^d &= \xi_3^d \\
\dot{\xi}_3^d &= L_{f+\sum h_i d_i}^3 T_1 + \phi L_g L_{f+\sum h_i d_i}^2 T_1 + L_{f+g\phi+\sum h_i d_i}(\phi L_g L_{\sum h_i d_i} T_1)
\end{aligned}
\tag{3.4.5}
$$

Here we assume

$$
L_g L_{\sum h_i d_i} T_1 \equiv 0 \tag{3.4.6}
$$

which leads to

$$
\dot{\xi}_3^d = L_{f+\sum h_i d_i}^3 T_1 + \phi L_g L_{f+\sum h_i d_i}^2 T_1. \tag{3.4.7}
$$

Then, introducing a new input ν and defining u as

$$
u = \phi^{-1}\left(x, \frac{\nu - L_{f+\sum h_i d_i}^3 T_1}{L_g L_{f+\sum h_i d_i}^2 T_1}\right), \tag{3.4.8}
$$

the original plant (3.4.1) can be converted into a linear plant

$$
\begin{aligned}
\dot{\xi}_1^d &= \xi_2^d \\
\dot{\xi}_2^d &= \xi_3^d \\
\dot{\xi}_3^d &= \nu
\end{aligned}
\tag{3.4.9}
$$

under the new coordinate $\boldsymbol{\xi}^d$ defined in (3.4.4). A sufficient condition for (3.4.6) is given by

$$
\frac{dT_1(x)}{dx} h_i(x) \equiv 0, i = 1, \ldots, m \tag{3.4.10}
$$

By summarizing the discussion, we have the following proposition.

Proposition 3.4.1 *Consider a disturbed nonlinear plant (3.4.1) and assume that the disturbances are measurable and step-type. Then, if the matching condition (3.4.10) is satisfied, we can reject the disturbances d_i, $i = 1, \ldots, m$ by using the coordinate transformation (3.4.4) and the input modification (3.4.8).*

Chapter 4

Minor Feedback Synthesis considering Real Parametric Uncertainty

In this chapter, we consider linear time-invariant models having transfer function coefficients subject to perturbations, where we can not exactly determine the parameters of the models. These parametric perturbed descriptions are more suitable to real application than transfer function descriptions with fixed coefficients.

A minor feedback synthesis method considering such real parametric uncertainty is proposed based on a parameter space design method.

4.1 Introduction

In this chapter, we consider real parametric perturbed plants whose transfer function description has coefficients varying independently in a prescribed range. Such plants are called *interval plants*.

As stated in Section 2.4, minor feedback controller should be designed to satisfy a robust H_∞ norm bound constraint (2.4.36) in the disturbance attenuation problem to improve the attenuation level with minor feedback.

It has been shown that the worst case H_∞-norm bounds of such interval plants can be determined by H_∞-norm bounds for a finite number of segment plants[Chapellat 1990], where a segment plant is a one-parameter plant. The treatment of one-parameter plants is not so easy in general. In fact, if we allow continuous variations of the parameter, the perturbed plant may be characterized as infinite sets. Therefore, applying a simple-minded direct strategy, the determination of the H_∞ norm bounds could only be carried out by checking an uncountably many systems and this is obviously infeasible. In Section 4.2.4, a feasible and useful test based on Sign Definite Condition is proposed to determine

the H_∞ norm bounds of interval plants.

For interval plants, Kharitonov has investigated the Hurwitz-stability and shown that only four fixed special extremal polynomials determine the stability of the interval polynomial [Kharitonov 1978]. Similar results have been obtained for the H_∞-norm bounds of the interval plants, i.e., the bounds can be determined by the H_∞-norm bounds of a finite number of fixed systems if the interval plant has a special structure. Therefore, the H_∞-norm bounds of interval systems can be checked by tests for fixed plants [Boyd 1989] [Hara 1991] in this case.

Motivated by these results, we consider the frequency restricted norm (FRN) bounds for SISO interval plants, where the FRN is defined as a generalization of the H_∞-norm in [Boyd 1989] [Hara 1991]. In spite of the fact that the worst case H_∞-norm of interval plants is bounded by those of some fixed plants for the special class of the plant, the counter example shows that this does not happen in general if we use the FRN instead of the H_∞-norm. A special class of interval plants such that the FRNs are bounded by those of the fixed plants is derived. The entries of this class are expressed as a reciprocal of an interval polynomial with a first order weight. Given that FRN constraints for fixed plants can be easily checked, the FRN bounds of the interval plants in this class are computed in a finite number of steps, even if these interval plants are characterized as infinite sets.

A minor feedback synthesis method considering such real parametric uncertainty is proposed based on a parameter space design method.

Based on these results, a design example of minor feedback against parametric uncertainty is presented in Section 4.4.

4.2 H_∞ Norm Bounds Test based on Sign Definite Condition

4.2.1 Preliminaries

Definition 4.2.1 (Sign Definite Condition) : *A function $f(x) : \mathbf{R}_{+c} \mapsto \mathbf{R}$ is sign definite in the interval $x \in [a,b], a < b$ (denoted by $f(x) \in \mathbf{N}_0[a,b]$ from now on), if $f(x)$ preserves its sign in the interval, or it does not cross zero in the interval (see Fig. 4.2.1).*

If $f(x)$ is a polynomial in x, then the SDC, $f(x) \in \mathbf{N}_0[a,b]$, can be checked by Strum's Theorem[Takagi 193 In particular, if the interval is $[0,\infty]$, the criterion for the SDC is simplified to a Routh-Hurwitz type criterion on the basis of the following lemma.

Lemma 4.2.1 [Siljak 1971] : *An n-th order polynomial $f(x)$ with real coefficients is sign definite in $x \in [0,\infty]$, if and only if the following equality holds:*

$$V[f(x)] = n \tag{4.2.1}$$

28
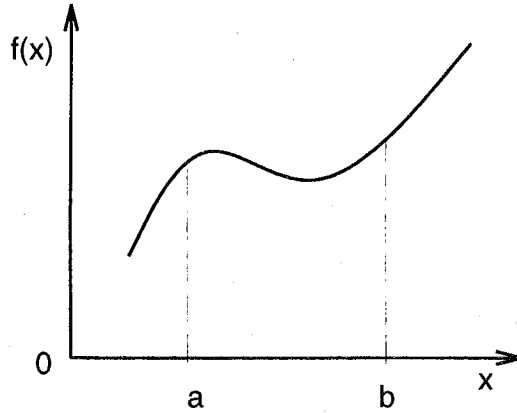
Figure 4.2.1: an image of SDC, $f(x) \in \mathbf{N}_0[a, b]$

where V is the number of the sign changes in the most left column of the Modified Routh Table defined as

$$
\begin{array}{cccc}
(-1)^n f_n & (-1)^{n-1} f_{n-1} & \cdots & -f_1 \quad f_0 \\
(-1)^n n f_n & (-1)^{n-1}(n-1) f_{n-1} & \cdots & -f_1 \\
\cdot & \cdot & \cdot & \\
\vdots & & & \\
f_0 & & &
\end{array}
\tag{4.2.2}
$$

Note that an equivalent Hurwitz type criterion can also be stated [Siljak 1971].

Since the sign definite condition defined over a general interval, say $f(x) \in \mathbf{N}_0[a, b]$, can be transformed to an equivalent condition on $f(z) \in \mathbf{N}_0[0, \infty]$ by the bilinear transformation

$$
\begin{cases}
z = -(x-a)/(x-b) & \text{if } |a|, |b| < \infty \\
z = x - a & \text{if } |a| < \infty, b = \infty \quad , \\
z = -(x-b) & \text{if } a = -\infty, |b| < \infty
\end{cases}
\tag{4.2.3}
$$

we can check the SDC over a general interval $[a, b]$ by the Routh-Hurwitz type criterion represented by Lemma 4.2.1.

4.2.2 Problem Formulation

Consider a unity feedback system composed of a fixed SISO controller $C(s)$ and a parametric perturbed plant $\mathcal{P}$ defined by

$$
\mathcal{P} := n(s)/d(s)
$$

$$n(s) := \sum_{i=0}^{m} n_i s^i, \quad n_i \in [\underline{n}_i, \overline{n}_i] \; ; \; i = 0, \ldots, m$$

$$d(s) := \sum_{i=0}^{n} d_i s^i, \quad d_i \in [\underline{d}_i, \overline{d}_i] \; ; \; i = 0, \ldots, n$$

$$m \leq n.$$

We denote the four Kharitonov polynomials associated with $n(s)$ as

$$\begin{cases} k_n^1(s) := \overline{n}_0 + \overline{n}_1 s + \underline{n}_2 s^2 + \underline{n}_3 s^3 + \cdots \\ k_n^2(s) := \overline{n}_0 + \underline{n}_1 s + \underline{n}_2 s^2 + \overline{n}_3 s^3 + \cdots \\ k_n^3(s) := \underline{n}_0 + \overline{n}_1 s + \overline{n}_2 s^2 + \underline{n}_3 s^3 + \cdots \\ k_n^4(s) := \underline{n}_0 + \underline{n}_1 s + \overline{n}_2 s^2 + \overline{n}_3 s^3 + \cdots \end{cases} \tag{4.2.4}$$

Let $\mathcal{K}_n$ be the set of four Kharitonov polynomials associated with $n(s)$ defined by

$$\mathcal{K}_n := \{k_n^1(s), \; k_n^2(s), \; k_n^3(s), \; k_n^4(s)\}. \tag{4.2.5}$$

Also we denote the four Kharitonov segment polynomials associated with $n(s)$ as

$$\begin{cases} s_n^1(s) := (1 - t)k_n^1(s) + t k_n^2(s) \\ s_n^2(s) := (1 - t)k_n^1(s) + t k_n^3(s) \\ s_n^3(s) := (1 - t)k_n^2(s) + t k_n^4(s) \\ s_n^4(s) := (1 - t)k_n^3(s) + t k_n^4(s) \end{cases} \tag{4.2.6}$$

where $t \in [0, 1]$. Let $\mathcal{S}_n$ be the set of four Kharitonov segment polynomials associated with $n(s)$ defined by

$$\mathcal{S}_n := \{s_n^1(s), \; s_n^2(s), \; s_n^3(s), \; s_n^4(s)\} \tag{4.2.7}$$

Similarly, associated with $d(s)$, we refer to the Kharitonov polynomials, the set of Kharitonov polynomials, the Kharitonov segments and the set of Kharitonov segments as $k_d^i(s)$; $i = 1, \ldots, 4$, $\mathcal{K}_d$, $s_d^i(s)$; $i = 1, \ldots, 4$ and $\mathcal{S}_d$, respectively. Finally, following [Keel 1991], let $\mathcal{P}_{CB}$ be the CB-system of $\mathcal{P}$ defined by

$$\begin{aligned} \mathcal{P}_{CB} := \quad & \{n(s)/d(s) \mid \\ & (n(s) \in \mathcal{K}_n \text{ and } d(s) \in \mathcal{S}_d) \\ & \text{or } (n(s) \in \mathcal{S}_n \text{ and } d(s) \in \mathcal{K}_d)\}. \end{aligned} \tag{4.2.8}$$

Theorem 4.2.1 (Theorem 4.1 in [Chapellat 1990]) *Given an interval family $\mathcal{P}$ of strictly proper plants and a fixed stabilizing controller $c(s)$, the inequality*

$$\max_{p(s) \in \mathcal{P}} \left\| \frac{W(s)}{1 + p(s)c(s)} \right\|_\infty < \gamma \tag{4.2.9}$$

holds if and only if

$$\max_{p(s) \in \mathcal{P}_{CB}} \left\| \frac{W(s)}{1 + p(s)c(s)} \right\|_\infty < \gamma \tag{4.2.10}$$

holds, where $W(s)$ is a fixed proper weighting function.

Therefore, determination of H_∞-norm bounds of these parametric perturbed systems can be carried out by checking the H_∞-norm bounds of the corresponding CB-systems.

Since a CB-system $p(s)$ is characterized by one varying parameter, for example,

$$p(s) = \frac{k_n^1(s)}{(1-t)k_d^1(s) + tk_d^2(s)} \tag{4.2.11}$$

the stable closed-loop segment system associated with $\mathcal{P}_{CB}$

$$g(s) := \frac{c(s)}{1 + p(s)c(s)}, \quad p(s) \in \mathcal{P}_{CB} \tag{4.2.12}$$

may be written in the form $g(s) = \beta(s,t)/\alpha(s,t)$; $t \in [0,1]$, where $\alpha(s,t)$ and $\beta(s,t)$ are both first order polynomials with respect to t. Hence, from Theorem 4.2.1 and the next lemma, we obtain the following proposition:

Lemma 4.2.2 *A stable system $g(s) = n(s)/d(s)$ satisfies H_∞-norm constraint with level γ if and only if*

$$|G(\infty)| < \gamma \tag{4.2.13}$$

and

$$\begin{aligned} f(\omega) &:= n(j\omega)n(-j\omega) - \gamma^2 d(j\omega)d(-j\omega) \\ &\in \mathbf{N}_0[-\infty, \infty]. \end{aligned} \tag{4.2.14}$$

Proposition 4.2.1 *A segment system $g(s)$ defined by (4.2.12) satisfies H_∞-norm constraint with the level γ if and only if*

$$f_t(\omega, t) \neq 0 \quad \text{for all } \omega \in \mathbf{R}, \ t \in [0,1] \tag{4.2.15}$$

where

$$\begin{aligned} f_t(\omega, t) &:= \beta(j\omega, t)\beta(-j\omega, t) \\ &\quad -\gamma^2 \alpha(j\omega, t)\alpha(-j\omega, t). \end{aligned} \tag{4.2.16}$$

In general, it is very hard to check the SDC with two variables. However, considering the fact that the order of $f_t(\omega, t)$ with respect to t is 2, we have the following theorem.

4.2.3 SDC test

Theorem 4.2.2 *Consider a double variate polynomial $f(w,u)$, where the order with respect to u is 2 and express it as*

$$f(w, u) =: a(\omega)u^2 + b(\omega)u + c(\omega). \tag{4.2.17}$$

Here we assume that $a(\omega)$ and $b(\omega)$ are not simultaneously equal to 0. Then,

$$P1: \quad f(w,u) \neq 0 \quad \text{for all } w \in \mathbf{R}, \ u \in [0, \infty]$$

31

holds, if and only if the following three conditions are satisfied:

$$C1) \quad f(0, u) \in \mathbf{N}_0[0, \infty]$$

$$C2) \quad c(\omega) \in \mathbf{N}_0[-\infty, \infty]$$

$$C3\text{-}1) \quad b^2(\omega) - 4a(\omega)c(\omega) \in \mathbf{N}_0[-\infty, \infty]$$

$$or$$

$$C3\text{-}2) \quad {}^{\exists}\omega_0 \in \mathbf{R} \ s.t. \ b^2(\omega_0) - 4a(\omega_0)c(\omega_0) = 0$$

$$\Longrightarrow b(\omega_0) < 0.$$

Proof:

For simplicity, we assume $a(\omega) \neq 0 \ {}^{\forall}w \in \mathbf{R}$. (This will be removed in later.)
Then, the constraint P1 is equivalent to

$$P2: \ f_2(w, u) = \ u^2 + p(\omega)u + q(\omega) \neq 0$$
$$\text{for all } w \in \mathbf{R}, \ u \in [0, \infty]$$

where

$$p(\omega) := b(\omega)/a(\omega), \quad q(\omega) := c(\omega)/a(\omega).$$

(We omit w from $p(\omega)$ and $q(\omega)$ for convenience from now on.)

We readily see that the constraint P2 is satisfied if and only if

$$q > 0 \text{ and } (p > 0 \text{ or } p^2 - q < 0) \tag{4.2.18}$$

hold. In p-q plane, (4.2.18) means that the point $(p(\omega), q(\omega))$ is in the doted area II. (See Fig. 4.2.2.) The condition C1) implies that the point $(p(0), q(0))$ is in the admissible area II. Varying w from 0 to $\pm\infty$, C2) and C3-1,2) imply that $(p(\omega), q(\omega))$ does not touch the boundary ∂II. Therefore we can conclude that the conditions C1),C2) and C3-1,2) are sufficient for P2, or equivalently for P1.

From these discussions, the proof of necessity is almost obvious and omitted here.
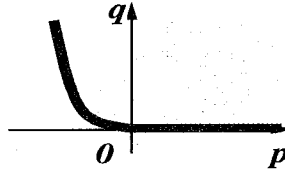
Figure 4.2.2: Admissible region in p-q plane

Next, we investigate the singular case: Suppose $\exists \omega_0$ s.t. $a(\omega_0) = 0$. Then, at this ω_0, the parabola $f_2(\omega, u)$ changes its shape into a line $b(\omega_0)u + c(\omega_0)$. We confirm the validity of the theorem by investigating the following two cases:

case 1) If the multiplicity of zeros associated with $a(\omega)$ is odd, $a(\omega)$ changes its sign when w passes through ω_0. Then, from the continuity, the parabola changes its concavity and we verify that there exists ω_* so that the constraint P1 is violated. (See Fig. 4.2.3.)
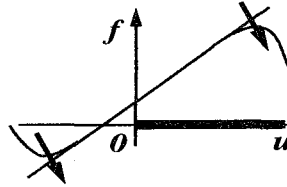
Figure 4.2.3: Change of the concavity (case 1)

case 2) If the multiplicity of zeros associated with $a(\omega)$ is even, $a(\omega)$ preserves its sign (although it becomes zero) when w passes through ω_0. Then, from the continuity, the parabola does not change its concavity. Therefore we verify that the the theorem is valid in the singular case. (See Fig. 4.2.4.)

$\square$
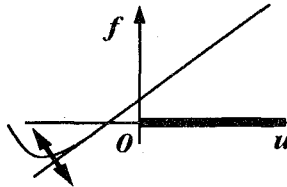
Figure 4.2.4: Change of the concavity (case 2)

4.2.4 Numerical Example

Example 1[Chapellat 1990]

Consider a segment system defined by

$$r_t(s) := \frac{3(1 - s + \lambda_1 s^2 + s^3)}{1 + 3s + \lambda_2 s^2 + \lambda_3 s^3 + s^4} \tag{4.2.19}$$

$$\begin{aligned} \lambda_1 &:= (1 - t)3.4 + t5 \\ \lambda_2 &:= (1 - t)2.4 + t4 \\ \lambda_3 &:= (1 - t)4.4 + t6 \end{aligned} \tag{4.2.20}$$

33

and check whether $r_t(s)$ satisfies the norm constraint $\|r_t(s)\|_\infty < 35$ for all $t \in [0,1]$. We have

$$f_t(\omega, t) =$$
$$(-3112.96w^4 - 3136.w^6)t^2 +$$
$$(3891.2w^2 + 2449.92w^4 - 13328.w^6)t +$$
$$(-1216. - 5197.2w^2 + 22956.w^4$$
$$-17827.w^6 - 1225w^8), \tag{4.2.21}$$

and by transforming the interval $t \in [0,1]$ to $u \in [0,\infty]$ by $u := t/(1-t)$, we obtain

$$f(\omega, u) = a(\omega)u^2 + b(\omega)u + c \tag{4.2.22}$$

$$\begin{aligned}
a(\omega) &:= -1216. - 1306.w^2 + 22293.w^4 \\
&\quad -34291.w^6 - 1225w^8 \\
b(\omega) &:= -2432. - 6503.2w^2 + 48362.w^4 \\
&\quad -48982.w^6 - 2450w^8 \\
c(\omega) &:= -1216. - 5197.2w^2 + 22956.w^4 \\
&\quad -17827.w^6 - 1225w^8.
\end{aligned}$$

The Modified Routh Array associated with $f_u(0,u)$ is given as

$$-1216, \ -2432, \ 2432, \ -1824, \ -1216. \tag{4.2.23}$$

Thus we conclude $f_u(0,u) \in \mathbf{N}_0[0,\infty]$ from SDC test (Lemma 4.2.1).

Also we know that

$$c(\omega) \in \mathbf{N}_0[-\infty,\infty] \tag{4.2.24}$$

by the SDC test. This can also be verified by seeing that the zeros of $c(\omega)$ are

$$\begin{aligned}
&-0.820145 \pm 0.00604397j, \\
&6.19972 \ 10^{-22} \pm 0.373107j, \\
&7.66034 \ 10^{-15} \pm 3.96972j, \\
&0.820145 \pm 0.00604397j.
\end{aligned} \tag{4.2.25}$$

Furthermore, we know that

$$D(\omega) := b^2(\omega) - 4a(\omega)c(\omega) \notin \mathbf{N}_0[-\infty,\infty] \tag{4.2.26}$$

from its SDC test. Then, the zeros of $D(\omega)$ are

$$\begin{aligned}
&\pm 0.899129, \ \pm 0.812302, \\
&-1.99765 \ 10^{-15} \pm 1.62865j, \\
&0, \ 0, \ 0, \ 0, \ 0, \\
&1.94206 \ 10^{-15} \pm 1.67364j,
\end{aligned} \tag{4.2.27}$$

and we have

$$b(\pm 0.899129) \;=\; 3008.5$$
$$b(\pm 0.812302) \;=\; 203.069 \tag{4.2.28}$$
$$b(0) \;=\; 2432.$$

Hence, from Theorem 4.2.2, we can conclude that this segment system satisfies the H_∞-norm constraint with level $\gamma = 35$.

Example 2

Again consider the parametric perturbed system (4.2.19) with H_∞-norm constraint level $\gamma = 34$. Then, we see that the corresponding $c(\omega)$ is such that

$$c(\omega) \notin \mathbf{N}_0[-\infty, \infty] \tag{4.2.29}$$

since its zeros are

$$\pm 0.822801, \quad \pm 0.817622,$$
$$-5.57062\ 10^{-17} \pm 3.96971j, \tag{4.2.30}$$
$$6.18731\ 10^{-22} \pm 0.372989j.$$

Hence, from Theorem 4.2.2, we can conclude that this CB-system does not satisfy the H_∞-norm constraint with level $\gamma = 34$. Note that the exact upper bound of the H_∞-norm is 34.14.

4.3 Frequency Restricted Norm Bounds for Real Parametric Perturbed Plants

First, we introduce the frequency restricted norm (FRN) [Boyd 1989][Hara 1991], a generalization of the H_∞-norm, for a stable rational transfer matrix $G(s)$. The FRN of $G(s)$ is defined as

$$\|G(s)\|_{[\omega_L, \omega_H]} := \sup_{0 \le \omega_L \le \omega \le \omega_H} \bar{\sigma}(G(j\omega)). \tag{4.3.1}$$

The FRN constraint results in alternative ways to shape the gain characteristics of feedback systems by specifying the gains in several frequency domain intervals. Hence, the FRN is one of the useful performance criteria for control system design.

Consider an SISO interval rational function $G(s)$ expressed as

$$G(s) = b(s)/a(s) \tag{4.3.2}$$

where $a(s)$ and $b(s)$ are interval polynomials with coefficients varying independently in a prescribed

range, i.e., $a(s)$ and $b(s)$ are given by

$$a(s) = \sum_{i=0}^{n} a_i s^i \quad ; \ a_i \in [\underline{a}_i, \bar{a}_i] \quad (i = 0, 1, \ldots, n)$$
$$b(s) = \sum_{j=0}^{m} b_j s^j \quad ; \ b_j \in [\underline{b}_j, \bar{b}_j] \quad (j = 0, 1, \ldots, m) \qquad m \leq n \qquad (4.3.3)$$

According to [Chapellat 1990], we can also define sixteen Kharitonov systems associated with the interval system (4.3.2) as

$$K_{i,j}(s) = b_j^k(s)/a_i^k(s) \ ; \quad i, j = 1, 2, 3, 4 \qquad (4.3.4)$$

where $a_i^k(s) \ ; \ i = 1, \ldots, 4$ and $b_j^k(s) \ ; \ j = 1, \ldots, 4$ are the Kharitonov polynomials associated with $a(s)$ and $b(s)$, respectively.

It has been shown in [Chapellat 1990] that the H_∞-norm bounds of the interval system defined in (4.3.2) are determined by the H_∞-norm of the associated sixteen Kharitonov systems. Unfortunately, if we restrict the frequency bound, the norm bounds cannot be determined by the Kharitonov systems as shown by the following counter example:

Example 1: Consider a stable interval system $G(s)$ given by

$$G(s) = \frac{0.98 + 3.69 \times 10^{-3}s + 2.02s^2 + 4 \times 10^{-3}s^3 + s^4}{\alpha + 4s + 101s^2 + s^3 + s^4} \ ; \quad \alpha \in [90, 110]. \qquad (4.3.5)$$

We see from Fig. 4.3.1 that the following inequality holds in this case.

$$\max_{\alpha = 90, 110} \|G(s)\|_{[0.98, 1.02]} < |G(1.005j)| \ ; \quad \alpha = 101 \qquad (4.3.6)$$

This indeed implies that the maximum of the FRNs corresponding to the Kharitonov systems $\|K_{i,j}\|_{[\omega_L, \omega_H]}$ does not determine the FRN bound for interval systems $\|G(s)\|_{[\omega_L, \omega_H]}$ in general.

Note that similar to the other frequency domain specifications investigated in [Bhattacharyya 1991] and [Bhattacharyya 1992], a weighted FRNs of a closed-loop system with an interval plant and a fixed controller can be determined by checking the corresponding FRNs of the CB-systems defined in [Bhattacharyya 1991] and [Bhattacharyya 1992], where the CB-systems are segment systems. This can be easily justified on the basis of the fact that by fixing the frequency, the sum of weighted interval polynomials is contained in the polygon whose edges are corresponding to the CB-systems.

Hence, we now investigate some special cases where the Kharitonov systems determine the FRN bound for the class of plants subject to parametric perturbations. We consider two types of interval systems given by

$$G(s) = q(s)/a(s) \qquad (4.3.7)$$

and

$$\hat{G}(s) = 1/a(s)q(s) \qquad (4.3.8)$$

36
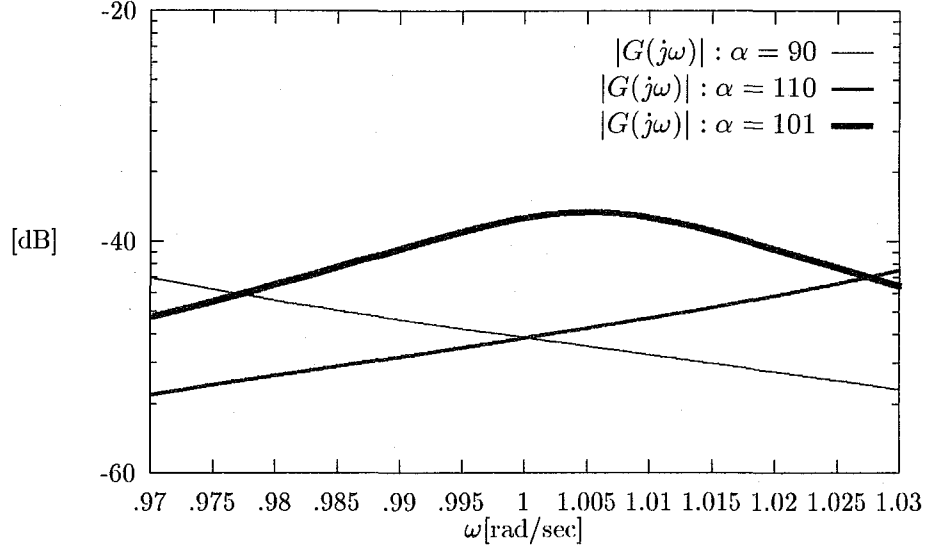
Figure 4.3.1: Example 1 (a counter example)

where $a(s)$ and $q(s)$ are interval polynomials expressed as

$$
\begin{aligned}
a(s) &= \sum_{i=0}^{n} a_i s^i \ ; \quad a_i \in [\underline{a}_i, \overline{a}_i] \quad (i = 0, 1, \ldots, n) \\
q(s) &= q_1 s + q_0; \quad q_j \in [\underline{q}_j, \overline{q}_j] \quad (j = 0, 1).
\end{aligned}
\tag{4.3.9}
$$

In other words, $a(s)$ is an interval polynomial of any order, while $q(s)$ is a first order interval polynomial or just an interval.

Let us now define the four Kharitonov polynomials $k_i(s)$; $i = 1, \ldots, 4$ and the four segment polynomials $S_i(s)$; $i = 1, \ldots, 4$ of the Kharitonov rectangle associated with $a(s)$ as

$$
\left\{
\begin{aligned}
k_1(s) &:= \overline{a}_0 + \overline{a}_1 s + \underline{a}_2 s^2 + \underline{a}_3 s^3 + \cdots \\
k_2(s) &:= \overline{a}_0 + \underline{a}_1 s + \underline{a}_2 s^2 + \overline{a}_3 s^3 + \cdots \\
k_3(s) &:= \underline{a}_0 + \overline{a}_1 s + \overline{a}_2 s^2 + \underline{a}_3 s^3 + \cdots \\
k_4(s) &:= \underline{a}_0 + \underline{a}_1 s + \overline{a}_2 s^2 + \overline{a}_3 s^3 + \cdots
\end{aligned}
\right.
\tag{4.3.10}
$$

$$
\left\{
\begin{aligned}
S_1(s) &:= (1 - \lambda) k_1(s) + \lambda k_2(s) \\
S_2(s) &:= (1 - \lambda) k_1(s) + \lambda k_3(s) \\
S_3(s) &:= (1 - \lambda) k_2(s) + \lambda k_4(s) \\
S_4(s) &:= (1 - \lambda) k_3(s) + \lambda k_4(s)
\end{aligned}
\right.
\tag{4.3.11}
$$

respectively, where $\lambda \in [0, 1]$. We also define $\underline{q}(s)$ and $\overline{q}(s)$ as

$$
\overline{q}(s) = \overline{Q}_1 s + \overline{Q}_0 \ , \quad \underline{q}(s) = \underline{Q}_1 s + \underline{Q}_0
\tag{4.3.12}
$$

37

where

$$\overline{Q}_i := \begin{cases} \overline{q}_i; & |\overline{q}_i| \geq |\underline{q}_i| \\ \underline{q}_i; & |\overline{q}_i| < |\underline{q}_i| \end{cases}, \qquad \underline{Q}_i := \begin{cases} 0; & 0 \in [\underline{q}_i, \overline{q}_i] \\ \overline{q}_i; & |\overline{q}_i| < |\underline{q}_i| \quad ; \quad i = 0,1. \\ \underline{q}_i; & |\overline{q}_i| \geq |\underline{q}_i| \end{cases} \tag{4.3.13}$$

Under these definitions, we enunciate the following theorems.

Theorem 4.3.1 *The frequency restricted norm bounds of the stable interval systems $G(s)$ defined by (4.3.7) are given as follows:*

$$\begin{aligned} \min_{i=1\sim4} \left\| \underline{q}(s)/k_i(s) \right\|_{[\omega_L,\omega_H]} &\leq \|G(s)\|_{[\omega_L,\omega_H]} \\ &\leq \max\left[\max_{j=1\sim4} \|\overline{q}(s)/k_i(s)\|_{[\omega_L,\omega_H]}, M(\omega_L), M(\omega_H) \right] \end{aligned} \tag{4.3.14}$$

where

$$M(\omega) := |\overline{q}(j\omega)| / \min_{i=1\sim4} S_i^m(\omega) \tag{4.3.15}$$

$$S_i^m(\omega) := \min_{\lambda \in [0,1]} |S_i(j\omega)|. \tag{4.3.16}$$

Theorem 4.3.2 *The frequency restricted norm bounds of the stable interval systems $\hat{G}(s)$ defined by (4.3.8) are given as follows:*

$$\begin{aligned} \min_{i=1\sim4} \left\| \frac{1}{\overline{q}(s)k_i(s)} \right\|_{[\omega_L,\omega_H]} &\leq \|\hat{G}((s)\|_{[\omega_L,\omega_H]} \\ &\leq \max\left[\max_{j=1\sim4} \left\| 1/\underline{q}(s)k_i(s) \right\|_{[\omega_L,\omega_H]}, \hat{M}(\omega_L), \hat{M}(\omega_H) \right] \end{aligned} \tag{4.3.17}$$

where

$$\hat{M}(\omega) := |1/\underline{q}(j\omega)| / \min_{i=1\sim4} S_i^m(\omega) \tag{4.3.18}$$

where $S_i^m(\omega)$; $i = 1, \ldots, 4$ are defined in (4.3.16).

Proof) Since the proofs of Theorems 4.3.1 and 4.3.2 are carried out in the same manner, we here prove Theorem 4.3.1 only.

1) Proof for the lower bound: We first notice that

$$|\underline{Q}_0 + \underline{Q}_1 j\omega| \leq |q_0 + q_1 j\omega| \leq |\overline{Q}_0 + \overline{Q}_1 j\omega| \tag{4.3.19}$$

holds for any $\omega \in \mathbf{R}$. Defining $R(\omega)$ and $I(\omega)$ as

$$\begin{aligned} R(\omega) &:= (a_0 + a_4\omega^4 + \cdots) - (a_2\omega^2 + a_6\omega^6 + \cdots) \\ I(\omega) &:= (a_1\omega + a_5\omega^5 + \cdots) - (a_3\omega^3 + a_7\omega^7 + \cdots) \end{aligned} \tag{4.3.20}$$

then we have

$$a(j\omega) = R(\omega) + jI(\omega). \tag{4.3.21}$$

Observing the structures of $R(\omega)$ and $I(\omega)$, we can readily verify that

$$|a(j\omega)| \leq \max_{i=1\sim4} |k_i(j\omega)| ; \quad {}^\forall\omega \in \mathbf{R}. \tag{4.3.22}$$

Inequalities (4.3.19) and (4.3.22) lead to the lower bound of (4.3.14).

2) Proof for the upper bound: First we restrict our attention to the numerator $q(s)$ in (4.3.7). Inequality (4.3.19) leads to the fact that $\overline{q}(s)$ maximizes the value of $\|G(s)\|_{[\omega_L,\omega_H]}$ for any $a(s)$. Hence, we can fix the numerator $q(s)$ as $\overline{q}(s)$ from now on.

Next we focus our attention on the denominator. Since the interval system $G(s)$ is assumed to be stable, $|G(j\omega)|$ is bounded for all parameter variations and $\omega \in [\omega_L, \omega_H]$. In other words there exist parameters $a_k^\#(k = 0, 1, \ldots, n)$ and $\omega^\# \in [\omega_L, \omega_H]$ which achieve the maximum of $|G(j\omega)|$ in $\omega \in [\omega_L, \omega_H]$, i.e.,

$$|G^\#(j\omega^\#)| \geq \|G(s)\|_{[\omega_L,\omega_H]} ; \quad {}^\forall G(s) \in \mathcal{G} \tag{4.3.23}$$

holds, where

$$G^\#(s) := \frac{\overline{q}(s)}{a^\#(s)} ; \quad a^\#(s) := a_0^\# + a_1^\# s + \cdots a_n^\# s^n. \tag{4.3.24}$$

$\mathcal{G}$ refers to the set of all systems defined by (4.3.7), i.e.,

$$\mathcal{G} := \{G(s) = q(s)/a(s) \mid a(s) \in \mathcal{A}\} \tag{4.3.25}$$

where $\mathcal{A}$ denotes the set of all polynomial defined by (4.3.9), i.e.,

$$\mathcal{A} := \{a(s) \mid a_i \in [\underline{a}_i, \overline{a}_i] ; \ i = 0, 1, \ldots, n\} \tag{4.3.26}$$

Note that the script $^\#$ indicates the values associated with the maximum. In addition, we define $\mathcal{V}$ and $\mathcal{K}$ as the set of the vertex polynomials associated with $a(s)$ and the set of the Kharitonov polynomials associated with $a(s)$ respectively, i.e.,

$$\begin{aligned}
\mathcal{V} &:= \{a(s) \mid a_i = \underline{a}_i \text{ or } \overline{a}_i ; \ i = 0, 1, \ldots, n\} \\
\mathcal{K} &:= \{k_1(s), \ k_2(s), \ k_3(s), \ k_4(s)\}
\end{aligned} \tag{4.3.27}$$

In view of these definitions, the proof will be completed by using the following two claims:

Claim 1) Suppose that $G^\#(s) = \overline{q}(s)/a^\#(s)$ attains the maximum of the FRN at a frequency $\omega^\#$ in the open interval (ω_L, ω_H) over all parameter variations. Then the denominator, $a^\#(s)$, is a vertex polynomial, i.e., if there exist $a^\#(s) \in \mathcal{A}$ and $\omega^\# \in (\omega_L, \omega_H)$ such that $|G^\#(j\omega^\#)| \geq \|G(s)\|_{[\omega_L,\omega_H]}$ holds for all $G(s) \in \mathcal{G}$, then $a^\#(s) \in \mathcal{V}$.

39

Claim 2) Consider $G^{\#}(s) = \bar{q}(s)/a^{\#}(s)$ whose the denominator is a vertex polynomial, i.e., $a^{\#}(s) \in \mathcal{V}$. If $G^{\#}(s)$ attains the maximum of the FRN at a frequency $\omega^{\#}$ in the open interval (ω_L, ω_H) over all parameter variations, then the denominator $a^{\#}(s)$ is a Kharitonov polynomial. In other words, if there exist $a^{\#}(s) \in \mathcal{V}$ and $\omega^{\#} \in (\omega_L, \omega_H)$ such that $|G^{\#}(j\omega^{\#})| \geq \|G(s)\|_{[\omega_L, \omega_H]}$ holds for all $G(s) \in \mathcal{G}$, then $a^{\#}(s) \in \mathcal{K}$.

The proofs of the claims are shown in Appendix A.

We conclude from Claims 1) and 2) that if the maximum of the FRN is achieved at $\omega^{\#} \in (\omega_L, \omega_H)$, the upper bound is given by

$$\max_{i=1\sim4} \left\| \frac{\bar{q}(s)}{k_i(s)} \right\|_{[\omega_L, \omega_H]} \geq \|G(s)\|_{[\omega_L, \omega_H]} \; ; \; {}^{\forall}a(s) \in \mathcal{A} \tag{4.3.28}$$

Other possibilities for attaining the upper bound of $\|G(s)\|_{[\omega_L, \omega_H]}$ are $|G(j\omega_L)|$ and $|G(j\omega_H)|$. Let us remember that the interval polynomial $a(j\omega)$ is contained in the Kharitonov rectangle for any fixed $\omega \in \mathbf{R}$. This readily yields

$$\left| \frac{1}{G(j\omega)} \right| \geq \max_{i=1\sim4} \left| \frac{S_i(j\omega)}{\bar{q}(j\omega)} \right| \; ; \; {}^{\forall}\omega \in \mathbf{R} \tag{4.3.29}$$

and hence we have

$$|G(j\omega)| \leq \max_{i=1\sim4} \left| \frac{\bar{q}(j\omega)}{S_i(j\omega)} \right| \; ; \; {}^{\forall}\omega \in \mathbf{R} \tag{4.3.30}$$

where $S_i(s)$; $i = 1, \ldots, 4$ are the segment polynomials defined in (4.3.11). Therefore, from (4.3.28) and (4.3.30), the upper bound (4.3.14) can be proved.

$\square$

According to Example 1, the FRNs of interval systems are not bounded by the extremal systems in general. In other words, we need to compute all FRNs corresponding to the whole systems subject to all parameter variations to determine the bounds of the FRN associated with the general interval systems defined by (4.3.2). Namely, we need to search over all the corresponding parameter space expressed as a hypercube in $\mathbf{R}^{m+n}$, where m and n refer to the order of the numerator and that of the denominator associated with the interval systems, respectively. Therefore, there is no direct efficient method to compute FRN bounds for interval systems in general.

In contrast, the FRN bounds for the class of the systems given by (4.3.7) and (4.3.8) can be computed by four FRNs corresponding to the four Kharitonov systems and the norms of the systems for all parametric perturbations at two boundary frequencies ω_L and ω_H. Therefore, since the computation of both FRN of a fixed system and the norm of the system for all parametric perturbations at a fixed frequency can be computed by considering only one parameter variation, several analytical/numerical methods (e.g., bisection method) can be applied to compute the FRN bounds for these systems [Hara 1991].

We will show two simple examples to illustrate the theorems:

Example 2: Consider an interval system defined by

$$G(s) = \frac{1}{s^2 + 0.15s + \alpha} \; ; \quad \alpha \in [0.2, 1.3]$$

and investigate the upper bound of the FRN of this system with frequency interval $\omega \in [0.1, 1]$. In this case, we have two Kharitonov systems

$$G_1(s) = \frac{1}{s^2 + 0.15s + 0.2}$$
$$G_2(s) = \frac{1}{s^2 + 0.15s + 1.3}$$

and two functions subject to the perturbation $\lambda \in [0, 1]$ at the boundary frequencies $\omega = 1.0$, 1.1, namely,

$$G_l(\lambda) = \frac{1}{s^2 + 0.15s + 0.2(1 - \lambda) + 1.3\lambda} \; ; \quad s = 1.0j$$
$$G_h(\lambda) = \frac{1}{s^2 + 0.15s + 0.2(1 - \lambda) + 1.3\lambda} \; ; \quad s = 1.1j.$$

Our aim here is to determine the maximum of $|G(j\omega)|$ over all $(\omega, \alpha) \in [0.1, 1] \times [0.2, 1.3]$ in $\mathbf{R}^2$. Applying Theorem 4.3.1, we can compute the upper bound of the FRN of this parametric perturbed system by searching not over all the rectangular $[0.1, 1] \times [0.2, 1.3]$ in $\mathbf{R}^2$ but over two frequency edges, i.e., $\omega \in [0.1, 1]$ and $\lambda = 0, 1$ and two edges associated with the parameter perturbation, i.e., $\omega = 0.1, 1$ and $\lambda \in [0, 1]$.

With simple algebra, the upper bound can be computed as follows:

$$\max_{\alpha \in [0.2, 1.3]} \|G(s)\|_{[0.1,1]} = \max\{\|G_1(s)\|_{[0.1,1]} \, , \, \|G_2(s)\|_{[0.1,1]} \, , \, \max_{\lambda \in [0,1]} |G_l(\lambda)| \, , \, \max_{\lambda \in [0,1]} |G_h(\lambda)|\}$$
$$= \max\{23.6[\mathrm{dB}] \, , \, 9.49[\mathrm{dB}] \, , \, 14.4[\mathrm{dB}] \, , \, 16.5[\mathrm{dB}]\}$$
$$= 23.6[\mathrm{dB}].$$

We see from these computations that the maximum is attained on the frequency edge.

Example 3: Consider an interval system defined by

$$G(s) = \frac{1}{s^2 + 2s + \alpha} \; ; \quad \alpha \in [0.1, 6]$$

and investigate the upper bound of the FRN of this system with frequency interval $\omega \in [1, 2.5]$. In this case, we also have two Kharitonov systems

$$G_1(s) = \frac{1}{s^2 + 2s + 0.1}$$
$$G_2(s) = \frac{1}{s^2 + 2s + 6}$$

and two systems at boundary frequencies $\omega = 1.0$ and 2.5 given by

$$G_l(\lambda) = \frac{1}{s^2 + 2s + 0.1(1 - \lambda) + 6\lambda} \; ; \quad s = 1.0j$$

$$G_h(\lambda) = \frac{1}{s^2 + 2s + 0.1(1 - \lambda) + 6\lambda} \; ; \quad s = 2.5j$$

where $\lambda \in [0, 1]$. In the same way as in Example 2, by applying Theorem 4.3.1, we can compute the upper bound of the FRN of this parametric perturbed system by searching over two frequency edges, i.e., $\omega \in [1, 2.5]$ and $\lambda = 0, 1$ and two edges associated with the parameter perturbation, i.e., $\omega = 1, 2.5$ and $\lambda \in [0, 1]$ as follows:

$$\max_{\alpha \in [0.1, 6]} \|G(s)\|_{[1,2.5]} = \max\{\|G_1(s)\|_{[1,2.5]} \, , \, \|G_2(s)\|_{[1,2.5]} \, , \, \max_{\lambda \in [0,1]} |G_l(\lambda)| \, , \, \max_{\lambda \in [0,1]} |G_h(\lambda)|\}$$

$$= \max\{-6.82[\text{dB}] \, , \, -13.0[\text{dB}] \, , \, -6.02[\text{dB}] \, , \, -14.0[\text{dB}]\}$$

$$= -6.02[\text{dB}].$$

We can see from these computations that the maximum is attained on the parameter edge.

4.4 Design Example by a Parameter Space Approach

Consider a PI-type feedback control system shown in Fig. 4.4.1.
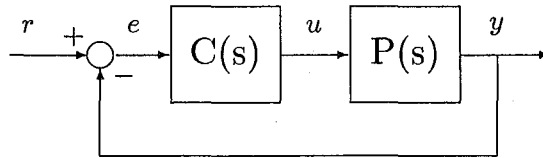
Figure 4.4.1: PI type unity feedback system

By using the results in the previous section, we can design a robust PI type controller

$$K(s) = \frac{K_I + K_P s}{s} \tag{4.4.1}$$

for a parametric perturbed plant with constant numerator

$$P(s) = \frac{b}{a(s)} \tag{4.4.2}$$

if we apply a method of parameter space design in [Hara 1991], where $a(s)$ is an interval polynomial. Our objective here is to obtain the parameters K_I and K_P which satisfy a robust stability property under both parametric and unstructured perturbations. In other words the complementary sensitivity function

$$T(s) \quad := \quad \frac{P(s)K(s)}{1 + P(s)K(s)}$$

$$= \quad \frac{K_I + K_P s}{a_n s^{n+1} + \cdots + a_1 s^2 + (a_0 + bK_p)s + bK_I} \tag{4.4.3}$$

must satisfy the FRN constraints

$$\|T(s)\|_{[\omega_{Li}, \omega_{Hi}]} < \gamma_i \quad (i = 1 \sim k). \tag{4.4.4}$$

Note that the PD type controller can be designed in a similar way.

We will show an illustrative design example. Consider a first order unstable plant given by

$$P(s) = \frac{1}{s - \alpha} \; ; \quad \alpha \in [\underline{\alpha}, \overline{\alpha}] \; , \quad \underline{\alpha} = 1 \; , \quad \overline{\alpha} = 4.5 \tag{4.4.5}$$

where α denotes the parametric perturbation. We consider two FRN constraints

$$\|T(s)\|_{[\omega_t, \infty]} < \gamma_1 \quad , \quad \|T(s)\|_{[0, \omega_t]} < \gamma_2 \tag{4.4.6}$$

where $\omega_t = 20, \gamma_1 = -10[\text{dB}]$ and $\gamma_2 = 15[\text{dB}]$ and $T(s)$ is given by

$$T(s) = \frac{K_I + K_P s}{s^2 + (K_P - \alpha)s + K_I}. \tag{4.4.7}$$

From Theorem 4.3.1, the two FRN constraints in (4.4.6) are satisfied under the parametric perturbations if and only if the following nine conditions hold.

(c0) the close loop system is stable for all $\alpha \in [\underline{\alpha}, \overline{\alpha}]$

(c1) $\|T(s)\|_{[\omega_t, \infty]} < \gamma_1 \; ; \quad \alpha = \overline{\alpha}$

(c2) $\|T(s)\|_{[\omega_t, \infty]} < \gamma_1 \; ; \quad \alpha = \underline{\alpha}$

(c3) $M_1(j\omega_t) < \gamma_1$

(c4) $M_1(j\infty) < \gamma_1$

(c5) $\|T(s)\|_{[0, \omega_t]} < \gamma_2 \; ; \quad \alpha = \overline{\alpha}$

(c6) $\|T(s)\|_{[0, \omega_t]} < \gamma_2 \; ; \quad \alpha = \underline{\alpha}$

(c7) $M(j0) < \gamma_2$

(c8) $M(j\omega_t) < \gamma_2$

From the Kharitonov's theorem, (c0) is satisfied if and only if $K_P > \overline{\alpha}$. In addition, since $M(j\infty) = 0$, $M(j0) = 1$, $T(s)$ is strictly proper and $\gamma_2 > 1$, the conditions (c4) and (c7) are automatically satisfied. Also note that (c3) leads to (c8) since $\gamma_1 < \gamma_2$. Hence, we can remove the conditions (c4), (c7) and (c8). Though the details of the calculation are omitted here, we can obtain the admissible
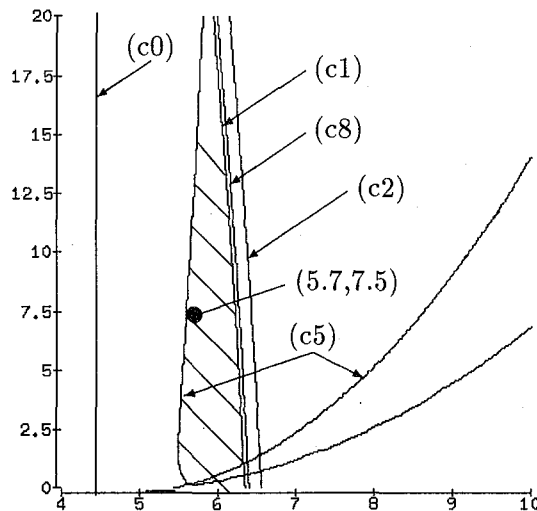
Figure 4.4.2: Admissible parameter regions. ($\gamma_1 = -10[\text{dB}]$, $\gamma_2 = 15[\text{dB}]$)

region in the K_P-K_I space as shown in Fig. 4.4.2 by using a computational module in a CAD system *CtrlNet* [Hara 1992]. Taking the parameters K_P and K_I in the intersection, e.g., $K_P = 5.7$ and $K_I = 7.5$, we can satisfy all the constraints (see Fig. 4.4.3).

Next, in order to attenuate the peak at $\omega \simeq 3$, we reduce the constraint level of $\gamma_2 = 15[\text{dB}]$ in the lower frequency to $\gamma_2 = 7[\text{dB}]$. Unfortunately, there is no intersection through the original FRN constraint in the higher frequency band with $\gamma_1 = -10[\text{dB}]$. Therefore, loosing the FRN constraint in the higher frequency band as $\gamma_1 = -10[\text{dB}] \rightarrow \gamma_1 = -7[\text{dB}]$, we can obtain a new admissible region as shown in Fig. 4.4.4. Taking the parameters in the intersection, e.g., $K_p = 8.7$ and $K_i = 5$, we can satisfy the new constraints (see Fig. 4.4.5).

Note that the constraint in (c6) is satisfied in the whole plane with $K_p \in [4,10]$ and $K_i \in [0,20]$ in Fig. 4.4.2 and Fig. 4.4.4.

4.5 Concluding Remarks

We have proposed an algebraic criterion for H_∞-norm constraint of plants with one varying parameter(Theorem 4.2.2). Since it has been shown that the norm bounds for the plant determine the norm bounds for parametric perturbed plants [Chapellat 1990], we can check H_∞-norm constraints for the parametric perturbed plant by the proposed method in a finite number of steps.

We have investigated the frequency restricted norm (FRN) bounds of interval plants. It has been shown that the FRN for an interval plant is not bounded by FRNs of extremal plants in general. We have also shown that the FRN of any reciprocal of an interval polynomial with a first order weight is

44
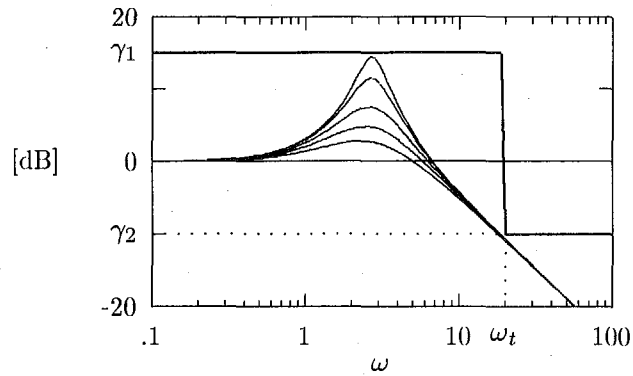
Figure 4.4.3: Gain plots of $T(j\omega)$ for $\alpha = 1, 2, 3, 4, 4.5$. ($\gamma_1 = -10[\text{dB}]$, $\gamma_2 = 15[\text{dB}]$)

bounded by the FRNs of the four extremal plants (Theorems 4.3.1 and 4.3.2). This implies that the determination of the FRN bounds is feasible, since we are not required to compute the FRNs of the whole plants to determine the bound.

Furthermore, an example of minor feedback synthesis considering such real parametric uncertainty is proposed based on a parameter space design method.

One of the interesting topics to be investigated in the future is to show the relationship between our result and a recent independent work on weighted H_∞-norm bounds for interval plants [Hollot 1992].
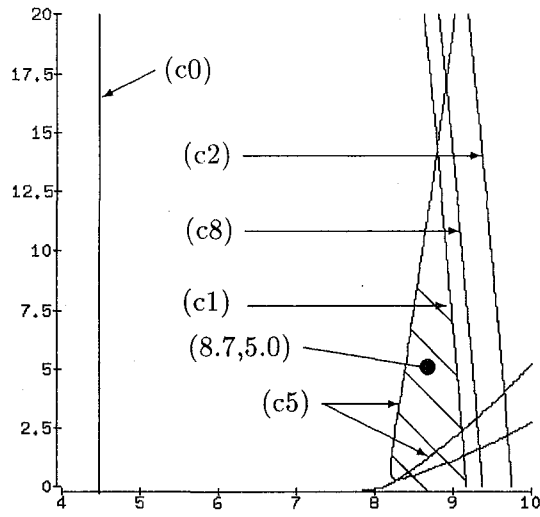
Figure 4.4.4: Admissible parameter regions. ($\gamma_1 = -7[\text{dB}]$, $\gamma_2 = 7[\text{dB}]$)
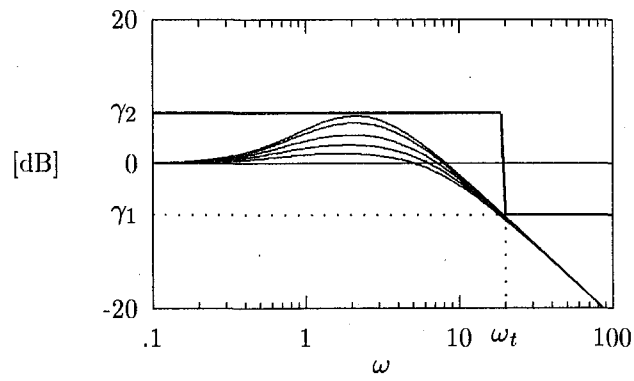
Figure 4.4.5: Gain plots of $T(j\omega)$ for $\alpha = 1, 2, 3, 4, 4.5$. ($\gamma_1 = -7[\text{dB}]$, $\gamma_2 = 7[\text{dB}]$)

46

Chapter 5

Application to Pressure Control System

In the disturbance attenuation problem, minor feedback improves the attenuation level if it reduces the magnitude of nominal plant and uncertainty model (Corollary 2.4.1). It is shown that a pressure control system, the most simple pneumatic system, satisfies the both conditions and experimental results verify that a minor pressure feedback improves the attenuation level.

<div align="center">

— Notation —

</div>

R : gas constant

V_0 : volume of chamber

Θ_0 : air temperature

p_a : air pressure

S_e : the effective area whose inverse exists

f_G : nonlinear function due to air

5.1 Modeling

Fig. 5.1.1 shows the experimental apparatus: The valve is driven by the command voltage v so that the inside pressure of the chamber is changed. The supply pressure p_s and the inside pressure of the chamber p are measured. The chamber is an isothermal chamber proposed in [Kawashima 1993], so that we can neglect temperature change during experiment. Then, the dynamics is described as a nonlinear differential equation

$$\dot{p} = \frac{R\Theta_0}{V_0} f_G(p_s, p) \sqrt{\frac{273}{\Theta_a}} S_e(v) \qquad (5.1.1)$$

where

$$\text{if } u \geq 0$$

$$f_G(p, u) = \begin{cases} 22.2\sqrt{p(p_s - p)} & (p/p_s > 0.5) \\ 11.1p_s & (p/p_s \leq 0.5) \end{cases}$$

$$\text{if } u < 0$$

$$f_G(p, u) = \begin{cases} 22.2\sqrt{p_a(p - p_a)} & (p_a/p > 0.5) \\ 11.1p_s & (p_a/p \leq 0.5) \end{cases} \tag{5.1.2}$$

and

$$Se(u) = \begin{cases} d_2 u^2 + d_1 u & \text{if } u \geq 0 \\ d_3 u^3 & \text{if } u < 0. \end{cases} \tag{5.1.3}$$

Note that the product

$$G(p_s, p, u) = f(p_s, p)\sqrt{\frac{273}{\Theta_a}} S_e(v) \tag{5.1.4}$$

gives the flow rate. We obtain a feedback linearizing controller by introducing a new input u and defining the control voltage v as

$$v = S_e^{-1}(Au/f(p_s, p)). \tag{5.1.5}$$

It yields the following linear relation between u and p

$$\dot{p} = \frac{R\Theta_0}{V_0}f(p_s, p)\frac{Au}{f(p_s, p)} = \frac{R\Theta_0}{V_0}Au \tag{5.1.6}$$

where A is a constant determined by the linear approximation of the flow rate at an equilibrium point p_{eq}. We consider this linearized model (5.1.6) as a nominal plant, denoted as P_0.
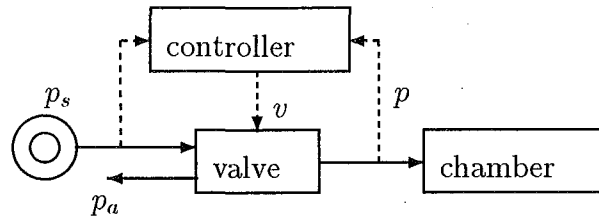
Figure 5.1.1: experimental apparatus of pressure control system

5.2 Minor Feedback Controller Design

Comparison is made with the following two constant minor feedback controllers

$$F_1 = \epsilon \text{ and } F_2 = 40$$

with sufficiently small $\epsilon > 0$. Note that

$$\bar{q}(\epsilon) \sim \bar{q}(0) \qquad (5.2.1)$$

holds in the disturbance attenuation problem for sufficiently small $\epsilon > 0$. Thus, we can consider $\bar{q}(\epsilon)$ as the performance level attained by directly applying H_∞ control method without minor feedback.

Note that the nominal model P_0 of the pressure control system (5.1.6) satisfies conditions C0 and C1 of Corollary 2.4.1 for constant minor feedback controllers with $0 < F_1 < F_2$. Gain plots of the nominal plant P_0^F with/without minor feedback are shown in Fig. 5.2.1; we see that condition C1 is satisfied.
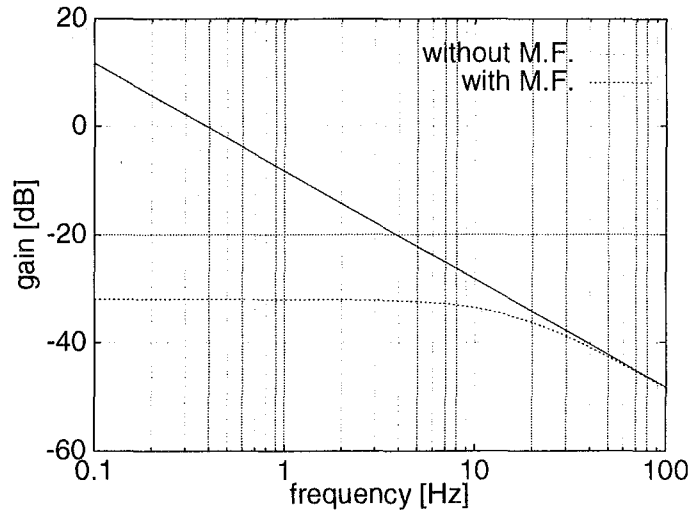
Figure 5.2.1: gain plots of nominal plants with/without minor feedback

Condition C2 will be examined experimentally in the next section. If this is the case, we can improve the performance by minor feedback.

5.3 Experimental Results

The numerical values used here are

$$p_s = 6 \ [\mathrm{kgf/cm^2}], \quad V_0 = 170 \ [\mathrm{cm^3}], \quad p_{eq} = 3.5 \ [\mathrm{kgf/cm^2}].$$

Frequency responses of various amplitudes at each frequency are measured to estimate the model uncertainties. The weighting functions with/without minor feedback are determined based on these data as shown in Fig. 5.3.1. Thanks to the minor feedback F_2, the magnitude of the model error is reduced and its variation over frequency is also reduced. This means that C2 of Corollary 2.4.1 is satisfied.
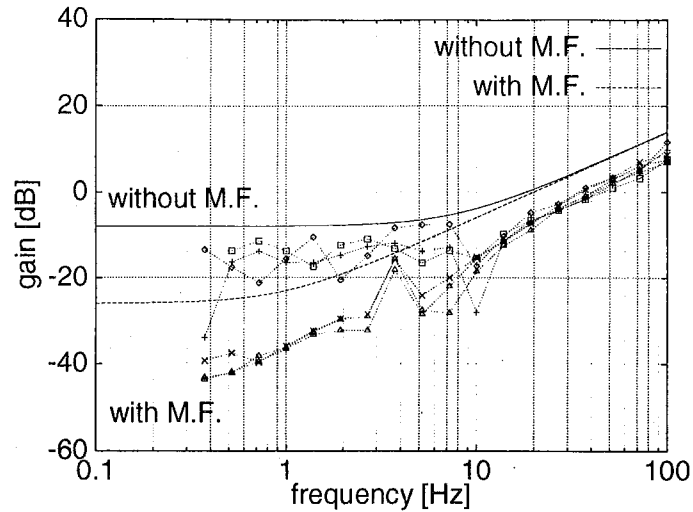
Figure 5.3.1: model errors and corresponding weighting functions

Therefore, from Corollary 2.4.1, we conclude that disturbance attenuation level is improved by using the minor feedback. Actually, we have

$$\bar{q}(\epsilon) = 4.0 < \bar{q}(40) = 7.3, \tag{5.3.1}$$

namely, the attenuation level is improved with approximately 5 [dB] according to the minor feedback. This is verified experimentally: Fig. 5.3.2 shows the gain plots of frequency responses from the disturbance to the output, where curves and points refer to simulation and experimental results, respectively. In both case, gains are reduced in approximately 5[dB] over lower frequency range.

The pressure responses in time domain with the disturbance $d = 8\sin 2.5 \cdot 2\pi$ are plotted in Fig. 5.3.3.

The disturbances of the above experiments are applied before the feedback linearizing control law. That is, these disturbances are not applied in particular situation. Thus, we apply disturbances before the feedback linearizing control law in order to investigate properness of the design method in practice. The experimental results are shown in Fig. 5.3.4 and we see that effects of the disturbance is reduced with the minor feedback. This result confirms the properness of the proposed design method in practice.

5.4 Concluding Remarks

Experimental results for a pressure control system with an isothermal chamber have shown that a minor feedback reduces the magnitude and the variation of the modified modeling error. over the
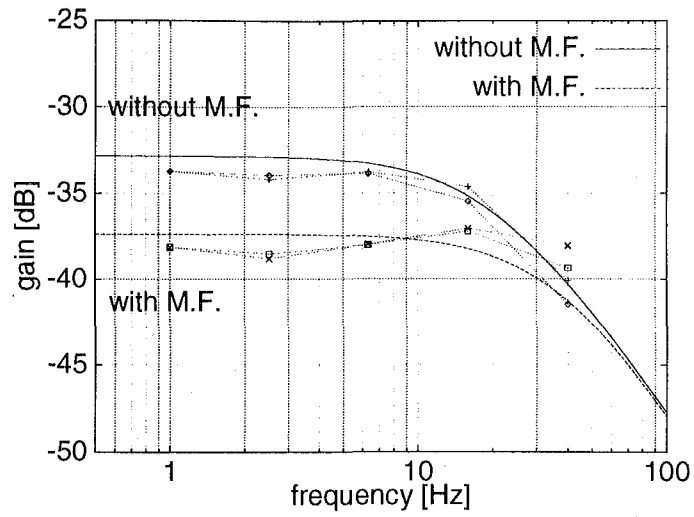
Figure 5.3.2: gain plots from disturbance w to output y : experimental and simulation results

frequency domain. From the sufficient condition in Corollary 2.4.1, we conclude that the minor feedback improves the disturbance attenuation level and this has been confirmed experimentally.
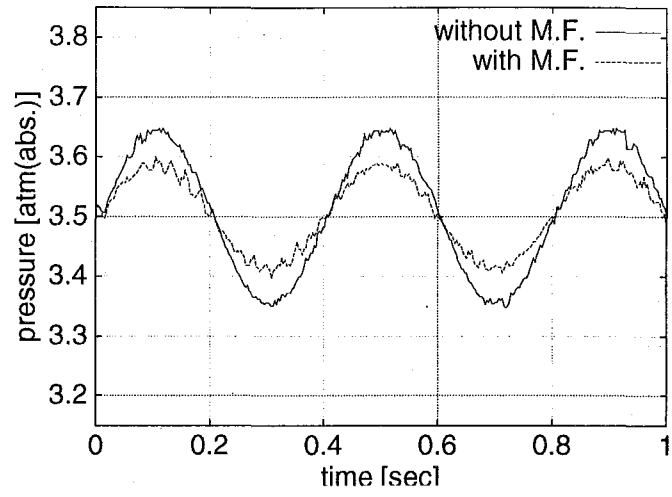
Figure 5.3.3: disturbance responses at control input (experimental)
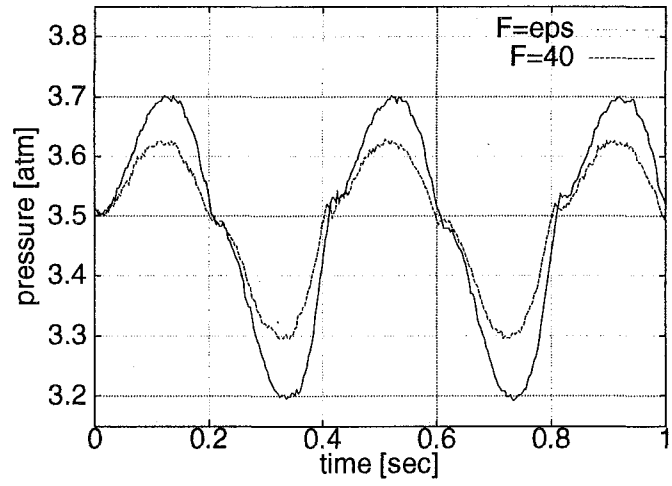
Figure 5.3.4: disturbance responses at control input (experimental) applied before linearization

52

Chapter 6

Application to Pneumatic Actuator System

In this chapter, the design methods proposed in Chapters 2 and 3 are applied to a pneumatic actuator system with a rubber artificial muscle. First, the effectiveness of the minor feedback linearization is verified experimentally. Next, it is shown that the pneumatic actuator system satisfies the conditions of Proposition 2.4.1 with a minor pressure loop and the attenuation level reduction is confirmed experimentally.

6.1 Introduction

Though a pneumatic actuator is widely used in industrial applications, it is not easy to control it due to several nonlinearities; n1) the nonlinearity in the valve, n2) compliance variation and n3) generating force. In practice, most common control for the pneumatic actuator systems is linear control designed based on the linear approximated model at an equilibrium point, e.g., [Matsushita 1993][Osuka 1990]. Using the linear control, when the state of the system is far from the equilibrium point, the nonlinearities deteriorate the control performance. Gain scheduling controls for the compliance variation have been proposed for air cylinder actuator system in [Miyata 1990] and [Pu 1993], which cancel out the nonlinearity n2). However, effects of the other nonlinearities n1) and n3) have not been investigated yet.

The method of feedback linearization is one of the useful techniques to cooperate with nonlinearity[Su 198? and its validity has been verified experimentally in mechanical systems and electrical systems[Sampei 1993a][? In contrast, there is a few applications of the feedback linearization in pneumatic systems. It has been applied to an air tank system for pressure regulation in [Bouhal 1993]. However, there exists no application for pneumatic actuator systems. This is due to the difficulty in constructing considerably

accurate mathematical models for the pneumatic systems, which are really required in the feedback linearization.

Recently, there have been progress in analysis of pneumatic systems and some mathematical models have been proposed for pneumatic actuator systems[Kagawa 1993]. In this chapter, we investigate feedback linearizaton for pneumatic actuator systems based on the proposed model with a rubber artificial muscle[Kagawa 1993]. Section 6.2 describes the model of the pneumatic actuator system. Following [Kagawa 1993], we show that the model can be described as a third order nonlinear system composed of a second order linear load driven by a first order nonlinear actuator whose dynamics depends on the state of the load. According to Proposition 3.3.1, we show that these systems are feedback linearizable.

Sections 6.3 and 6.4 are devoted to the experimental results. We verify that the proposed feedback linearization method with disturbance rejection is useful in pneumatic systems. Furthermore, it is shown that disturbance attenuation level of the pneumatic actuator system can be improved using constant pressure feedback as minor loop as well as a pressure control system in Chapter 5.

— Notation —

$L_0[\text{m}]$: initial length of R.A.M.

$x[\text{m}]$: displacement of R.A.M.

ϵ : relative displacement of R.A.M.(x/L_0)

$p[\text{Pa}]$: inside pressure of R.A.M.(abs.)

$F[\text{N}]$: generating force of R.A.M.

$V[\text{m}^3]$: volume of R.A.M.

$u[\text{V}]$: control voltage for valve

$Se[\text{mm}^2]$: effective area of valve

$m[\text{kg}]$: mass of load

$c[\text{N} \cdot \text{s/m}]$: friction coefficient

$g[\text{m/s}^2]$: gravity constant

$R[\text{J/(kg} \cdot \text{K)}]$: gas constant

$p_a[\text{Pa}]$: air pressure

$\Theta_a[K]$: temperature of the air

$\epsilon_0, \dot{\epsilon}_0, P_0$: values of $\epsilon, \dot{\epsilon}, P$ at equilibrium point

$\alpha[\text{N/Pa}], \beta[\text{N/Pa}], \gamma[\text{N}]$: coeff. of equation between ϵ, P and F

$v_2[\text{m}^3], v_1[\text{m}^3], v_0[\text{m}^3]$: coeff. of equation between V and ϵ

$d_1[\text{m}^2/\text{V}], d_2[\text{m}^2/\text{V}^2], d_3[\text{m}^2/\text{V}^3]$: coeff. of equation between u and Se
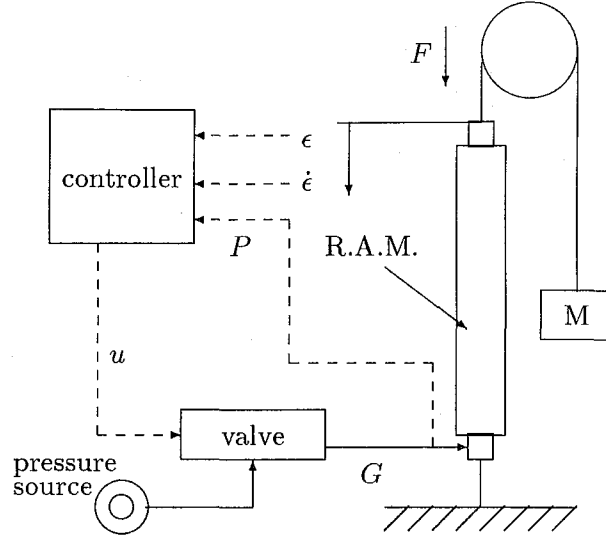
Figure 6.2.1: experimental apparatus

6.2 Modeling

We use a rubber artificial muscle (R.A.M.), as an actuator. An R.A.M. consists of a rubber tube and a sleeve of interwoven fiber cord covering. When the pressure inside the R.A.M., p, is increased, it contracts in a longitudinal direction and generates force F. Fig. 6.2.1 shows the experimental apparatus: The valve is driven by the command voltage u so that the air flows into or flows out of the R.A.M. Then, due to the flow rate G, the inside pressure of the R.A.M. P is changed and the R.A.M. generates the force F. The mass attached to the R.A.M. by a wire through a pulley moves up or down associated with the generating force F so that the displacement of the R.A.M., ϵ, is determined. Here we assume that the displacement ϵ, the velocity $\dot{\epsilon}$ and the pressure P of the R.A.M. can be measured.

In order to derive a mathematical model, the following three assumptions A1)–A3) are made:

A1 The air is ideal gas.

A2 Change of the air is isothermal.

A3 The friction is linear.

Then, taking the state variables as deviation from an equilibrium point as

$$\delta\epsilon := \epsilon - \epsilon_0, \quad \delta\dot{\epsilon} := \dot{\epsilon} - \dot{\epsilon}_0, \quad \delta p := p - p_0$$

leads to the following nonlinear model[Kagawa 1993]:

$$\Sigma_p \ : \ \frac{d}{dt}\begin{bmatrix} \delta\epsilon \\ \delta\dot{\epsilon} \end{bmatrix} = \begin{bmatrix} 0 & 1 \\ 0 & -\dfrac{c}{m} \end{bmatrix}\begin{bmatrix} \delta\epsilon \\ \delta\dot{\epsilon} \end{bmatrix} + \begin{bmatrix} 0 \\ 1 \end{bmatrix} v$$

$$\Sigma_a \ : \ \begin{cases} \dot{\delta p} = -(\delta p + p_0)\dfrac{V(\delta\epsilon)}{V(\delta\epsilon)} + \dfrac{R\Theta_a}{V(\delta\epsilon)}G(\delta p, u) \\[2mm] v = \dfrac{F(\delta\epsilon, \delta p) - mg - cL_0\dot{\epsilon}_0}{mL_0} \end{cases} \tag{6.2.1}$$

where

$$p = \delta p + p_0$$
$$F(\delta\epsilon, \delta p) = (p - p_a)(\alpha(1 - (\delta\epsilon + \epsilon_0))^2 + \beta) + \gamma$$
$$V(\delta\epsilon) = v_2(\delta\epsilon + \epsilon_0)^2 + v_1(\delta\epsilon + \epsilon_0) + v_0$$

and $G()$ is defined in (5.1.4). Note that the origin is an equilibrium point of the system. The first order approximated model of the nonlinear model (6.2.1) at the origin is expressed as

$$\dot{x} = Ax + Bu, \quad x = [\delta\epsilon \ \delta\dot{\epsilon} \ \delta p]^T$$

$$A = \begin{bmatrix} 0 & 1 & 0 \\ A_{21} & A_{22} & A_{23} \\ 0 & A_{32} & 0 \end{bmatrix}, \quad B = \begin{bmatrix} 0 \\ 0 \\ B_3 \end{bmatrix} \tag{6.2.2}$$

Note that the system (6.2.1) is characterized as the nonlinear system composed of a single input linear load Σ_p actuated by a first order nonlinear actuator Σ_a whose dynamics depends on the state variables of Σ_p (See Fig. 3.3.1).

In practice, there is static friction between the covering code and the rubber tube of the R.A.M. This causes hysteresis characteristics among the generating force F, the inside pressure p and the displacement ϵ. Fig. 6.2.2 shows force—displacement hysteresis characteristics of the rubber artificial muscle.

Thus, the inference of the hysteresis can be considered by the replacement

$$F(\delta\epsilon, \delta p) \rightarrow F(\delta\epsilon, \delta p) + d \tag{6.2.3}$$

in (6.2.1), where d refers to the disturbance corresponding to the hysteresis characteristics. Note that since the hysteresis of the R.A.M. is due to the static friction, this can be considered as a step-type disturbance for the position control.

6.3 Minor Feedback Linearization with Disturbance Rejection

6.3.1 Controller Design

We see that the pneumatic actuator system (6.2.1) is in the class defined by (3.3.1) and (3.3.2) in Proposition 3.3.1 by setting
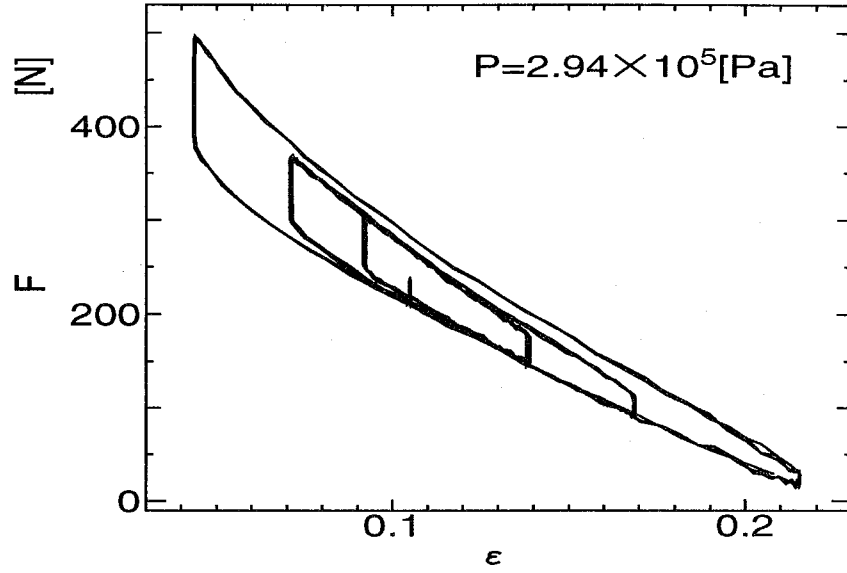
Figure 6.2.2: Force−Displacement Hysteresis Characteristics

$$x_p = \begin{bmatrix} \delta\epsilon \\ \delta\dot\epsilon \end{bmatrix}, \quad f_p = \begin{bmatrix} 0 & 1 \\ 0 & -\dfrac{c}{m} \end{bmatrix} \begin{bmatrix} \delta\epsilon \\ \delta\dot\epsilon \end{bmatrix},$$

$$g_p = \begin{bmatrix} 0 \\ 1 \end{bmatrix}, \quad x_a = \delta P,$$

$$f_a = -\delta\dot\epsilon \frac{\dot V(\delta\epsilon)}{V(\delta\epsilon)}, \quad g_a = \frac{R\Theta_a}{V(\delta\epsilon)},$$

$$h_a = \frac{F(\delta\epsilon, \delta P) - mg - cL_0\dot\epsilon_0}{mL_0}, \quad \phi_a = G.$$

(6.3.1)

This implies that the plant (6.2.1) is feedback linearizable.

Pneumatic actuators satisfying the assumptions A1) and A2) can be modeled in the form of (3.3.2). Therefore, Proposition 3.3.1 concludes that the system involving a linearizable load driven by a pneumatic actuator is linearizable.

Comparison is carried out by implementing the linear controller F in the following three forms:

●E1 : No linearizing compensation

The configuration of the overall controller is depicted in Fig. 3.2.1, where

$$\phi^{-1} = I, \ T_u = I, \ T_y = I, \ F_{nl} = 0.$$

●E2 : Feedback linearization

According to (3.3.6), let the coordinate transformation $T^{\text{exp}}(x)$ be

$$T^{\text{exp}}(x) = \begin{bmatrix} \delta\epsilon \\ \delta\dot{\epsilon} \\ \dfrac{F(\delta\epsilon, \delta P) - mg - cL_0(\delta\dot{\epsilon} + \dot{\epsilon}_0)}{mL_0} \end{bmatrix} \tag{6.3.2}$$

and by following (3.2.1), let the input u be

$$u = G^{-1}\left(\delta P, T_u^{\text{exp}}\nu + F_{nl}^{\text{exp}}\right)$$

where

$$\begin{aligned} T_u^{\text{exp}} &= \frac{b}{\beta(\delta\epsilon)} \\ F_{nl}^{\text{exp}} &= \frac{\sum_{i=0}^{2} a_i\xi_i - \alpha(\delta\epsilon, \delta\dot{\epsilon}, \delta P)}{\beta(\delta\epsilon)}. \end{aligned}$$

Then, the relation between the new input ν and the new coordinate $y = T_y^{\text{exp}}(x)$ is linear, where

$$\begin{aligned} T_y^{\text{exp}}(x) &:= \left(\frac{dT^{\text{exp}}(0)}{dx}\right)^{-1} T^{\text{exp}}(x) \\ \alpha(\delta\epsilon, \delta\dot{\epsilon}, \delta P) &:= -\frac{c}{m}\left(\frac{F(\delta\epsilon, \delta P) - mg - cL_0(\delta\dot{\epsilon} + \dot{\epsilon}_0)}{mL_0}\right) \\ &\quad + \frac{1}{mL_0}\left(\frac{\partial F(\delta\epsilon, \delta P)}{\partial \delta\epsilon}\delta\dot{\epsilon} - \frac{\partial F(\delta\epsilon, \delta p)}{\partial \delta p}(\delta p + p_0)\frac{\dot{V}(\delta\epsilon)}{V(\delta\epsilon)}\right) \\ \beta(\delta\epsilon) &:= \frac{1}{mL_0}\frac{\partial F(\delta\epsilon, \delta P)}{\partial \delta P}\frac{R\Theta_a}{V(\delta\epsilon)}. \end{aligned} \tag{6.3.3}$$

The configuration of the overall controller is depicted in Fig. 3.2.1 where

$$\phi^{-1} = G^{-1}, \ T_u = T_u^{\text{exp}}, \ T_y = T_y^{\text{exp}}, \ F_{nl} = F_{nl}^{\text{exp}}.$$

The linear controller F does not use the output $\delta\epsilon$, $\delta\dot{\epsilon}$ and δP of the plant P directly, but it uses the modified values for $\delta\epsilon$, $\delta\dot{\epsilon}$ and δP_{eq} by the coordinate transformation T_y, which corresponds to the values evaluated at the equilibrium point. The output of the linear controller F is modulated by the input transformation T_u and nonlinear feedback F_{nl} is added to cancel the nonlinearity of the plant P.

●E3 : Feedback linearization with disturbance rejection

From the correspondence (6.3.1), the plant with hysteresis (6.2.3) is expressed as

$$\dot{x}_{\text{aug}} = \begin{bmatrix} f_p(x_p) + g_p(x_p)h_a(x_{\text{aug}}) \\ f_a(x_{\text{aug}}) \end{bmatrix} + \begin{bmatrix} 0 \\ g_a(x_{\text{aug}}) \end{bmatrix} \phi_a(x_{aug}, u) + \begin{bmatrix} 0 \\ 1 \\ \overline{mL_0} \\ 0 \end{bmatrix} d \qquad (6.3.4)$$

Thus, the inference of the disturbance d to the system does not depend on the state. Moreover, the first entry of the nominal coordinate transformation defined in (6.3.2) is linear in the state of the plant. Therefore, we see that the plant satisfies a sufficient condition (3.4.10). Hence we can reject the disturbance associated with the hysteresis of the R.A.M. if the disturbance d can be measured. Though the disturbance d can not be measured directly, we can compute the value of d by measuring the acceleration $\ddot{\epsilon}$ and the state $\delta\epsilon$, $\dot{\delta\epsilon}$ and δP as follows:

$$d = mL_0\ddot{\epsilon} - F(\delta\epsilon, \delta P) - mg - cL_0(\dot{\delta\epsilon} + \dot{\epsilon}_0) \qquad (6.3.5)$$

From (3.4.4) and (3.4.8), the configuration of the overall controller is shown in Fig. 3.2.1 where

$$\phi^{-1} = G^{-1}, \ T_u = T_u^{\text{exp}}, \ T_y = T_{y,a}^{\text{exp}} \ F_{nl} = F_{nl,a}^{\text{exp}}$$

and

$$T_{y,a}^{\text{exp}} = \left(\frac{dT^{\text{exp}}(0)}{dx} \right)^{-1} \boldsymbol{\xi}_a$$

$$\boldsymbol{\xi}_a = \begin{bmatrix} \xi_{1,a} \\ \xi_{2,a} \\ \xi_{3,a} \end{bmatrix} := \begin{bmatrix} \delta\epsilon \\ \delta\dot{\epsilon} \\ \ddot{\epsilon} \end{bmatrix}$$

$$F_{nl,a}^{\text{exp}} = \frac{\sum_{i=0}^{2} a_i \xi_{i,a} - \alpha_a}{\beta(\delta\epsilon)}$$

$$\alpha_a = -\frac{c}{m}\ddot{\epsilon} + \frac{1}{mL_0} \left(\frac{\partial F(\delta\epsilon, \delta P)}{\partial \delta\epsilon}\delta\dot{\epsilon} - \frac{\partial F(\delta\epsilon, \delta p)}{\partial \delta p}(\delta p + p_0)\frac{\dot{V}(\delta\epsilon)}{V(\delta\epsilon)} \right).$$

Since $\ddot{\epsilon}$ can not be measured directly in our experimental setup, we use an estimated value $\ddot{\epsilon}_f$ from the position ϵ through a second order filter.

6.3.2 Experimental Results

Since the maximum relative displacement of the rubber artificial muscle is 0.3, we determine the equilibrium point as

$$\epsilon_0 = 0.15, \ \dot{\epsilon}_0 = 0, \ p_0 = 3.4 \times 10^5 [\text{Pa}].$$

The displacement and the pressure are measured and the velocity is calculated from the displacement by numerical differentiation. The numerical values used in the experiment are as follows:

$$m = 11.3[\text{kg}], \quad c = 35.0[\text{N} \cdot \text{s/m}], \quad L_0 = 0.3[\text{m}],$$
$$\alpha = 4.92 \times 10^{-3}[\text{N/Pa}], \quad \beta = -1.87 \times 10^{-3}[\text{N/Pa}],$$
$$\gamma = -291.4[\text{N}], \quad v_2 = -1.70 \times 10^{-3}[\text{m}^3],$$
$$v_1 = 1.04 \times 10^{-3}[\text{m}^3], \quad v_0 = 28.1 \times 10^{-6}[\text{m}^3],$$
$$d_1 = 1.50 \times 10^{-1}[\text{m}^2/\text{V}], \quad d_2 = 1.66 \times 10^{-1}[\text{m}^2/\text{V}^2],$$
$$d_3 = 8.84 \times 10^{-3}[\text{m}^2/\text{V}^3], \quad a_0 = 0[1/\text{s}^3],$$
$$a_1 = -1247[1/\text{s}^2], \quad a_2 = -3.10[\text{Pa/s}^3],$$
$$b = 65.1[1/\text{V} \cdot \text{s}^3].$$

The simulation is carried out based on the linear approximated model (6.2.2) with the following values:

$$A_{21} = -468[1/\text{s}^2], \quad A_{22} = -3.10[1/\text{s}]A_{23} = 5.00 \times 10^{-4}[1/\text{Pa} \cdot \text{s}^2],$$
$$A_{32} = -1.57 \times 10^6[\text{Pa}], \quad B_3 = 1.31 \times 10^5[\text{Pa/V}].$$

In order to verify the validity of the minor feedback linearization with disturbance rejection, a simple linear controller is used in the outer loop. Here we use constant state feedback controller as for the linear controller F, which is designed by pole placement technique with closed-loop poles -2.5, $-2.6 + 33j$, $-2.6 - 33j$.

This is implemented as

$$u = -(F_\epsilon \delta\epsilon + F_{\dot{\epsilon}} \delta\dot{\epsilon} + F_P \delta p) + G_r \delta\epsilon_r \tag{6.3.6}$$

with values

$$F_\epsilon = 9.35[\text{V}], \quad F_{\dot{\epsilon}} = -2.26[\text{V} \cdot \text{s}], \quad F_P = 3.54 \times 10^{-5}[\text{V/Pa}], \quad G_r = 42.7[\text{V}]$$

where $\delta\epsilon_r$ denotes the reference signal and G_r is a constant selected so that the steady gain of the closed loop system from $\delta\epsilon_r$ to $\delta\epsilon$ is 1 for convenience of the comparison.

The following four step width in normalized displacement are used in the experiment:

2%   (0.14——→0.16)
5%   (0.125——→0.175)
10%   (0.1——→0.2)
20%   (0.05——→0.25)

The results are normalized by step width in Fig. 6.3.1–6.3.4, i.e., the reference signal is 1 in the figures. Note that the responses for the 10% case are not plotted in Fig. 6.3.1–6.3.4, since they resemble those for the 20% case.
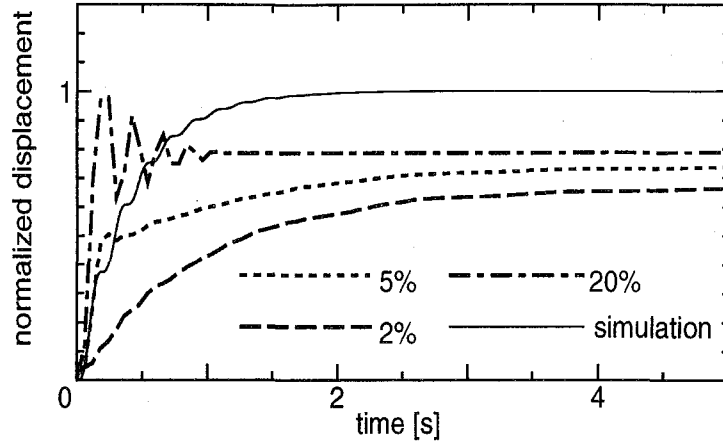
Figure 6.3.1: step responses (no linearizing compensation)

E1 : No linearizing compensation (Fig. 6.3.1)

In the 2% case, the difference between the simulation result and experimental one is large regardless of the small effect of the nonlinearities. This can be caused by hysteresis of the rubber artificial muscle. Increasing step width as 5%, 10% and 20%, the effect of the hysteresis becomes small against the step width. However, the difference between the simulation result and experimental one are still large because of the nonlinearity.

E2 : Feedback linearization (Fig. 6.3.2)

In the 2% case, the response is similar to that of the no linearization case, because the proposed linearizing controller is less active in the neighborhood of the equilibrium point due to the modification (3.2.1) and (3.2.3). Increasing step width as 5%, 10% and 20%, the effect of the hysteresis becomes small against the step width and the nonlinearity is canceled out by the linearizing controller, so that the linearity is improved and hence the experiment results tend to match the simulation results.

However, the steady state error is large. This can be explained by considering the hysteresis described as follows: By applying the nominal linearizing control law to the disturbed system (6.3.4), we obtain

$$\dot{y} = Ay + B\nu + \begin{bmatrix} 0 \\ \frac{1}{mL_0} \\ 0 \end{bmatrix} d, \quad y = T_y^{\mathrm{exp}}(x) \tag{6.3.7}$$

where A and B are constant matrices defined by the linear approximated model (6.2.2) and T_y^{exp} is defined in (6.3.4). Hence, combining the outer loop linear control defined in (6.3.6) yields the resultant

closed loop system

$$\dot{y} = \begin{bmatrix} 0 & 1 & 0 \\ A_{21} & A_{22} & A_{23} \\ -B_3 F_\epsilon & A_{32} - B_3 F_\epsilon & -B_3 F_P \end{bmatrix} y + \begin{bmatrix} 0 \\ 0 \\ B_3 G_r \end{bmatrix} \delta\epsilon_r + \begin{bmatrix} 0 \\ 1/mL_0 \\ 0 \end{bmatrix} d. \qquad (6.3.8)$$

The steady state can be determined by equating right hand side of (6.3.8) to 0. Thus, we see that the displacement at steady state, denoted $\delta\epsilon_\infty$, is given by

$$\delta\epsilon_\infty = -4.92 \times 10^{-4} d + \delta\epsilon_r. \qquad (6.3.9)$$

Comparison of theoretical values determined by (6.3.9) and experimental values are illustrated in Fig. 6.3.3, where the steady displacement is normalized by the step width, that is, $\delta\epsilon_\infty/\delta\epsilon_r$ is plotted, where d is determined by considering the size of the force-displacement hysteresis loop in [Kimura 1993]. This figure shows that the steady state error is mainly caused by the hysteresis.
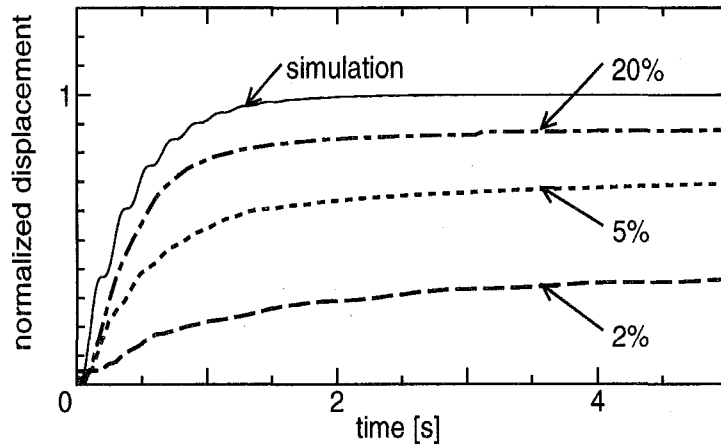
Figure 6.3.2: step responses (linearizing compensation)
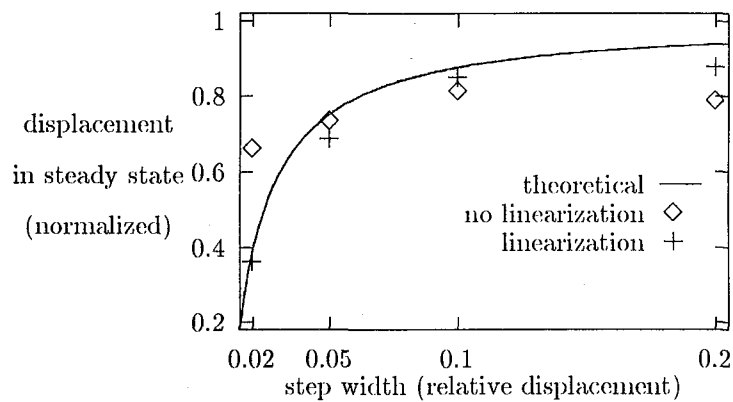
Figure 6.3.3: steady displacement vs. step width

E3 : Feedback linearization with disturbance rejection (Fig. 6.3.4)

When compared with the nominal feedback linearization case E2, all responses are improved by the feedback linearization with disturbance rejection. Especially, steady state error caused by the hysteresis described in the previous experiment E2 is reduced. Hence, we see that the proposed linearizing control with disturbance rejection is carried out effectively.
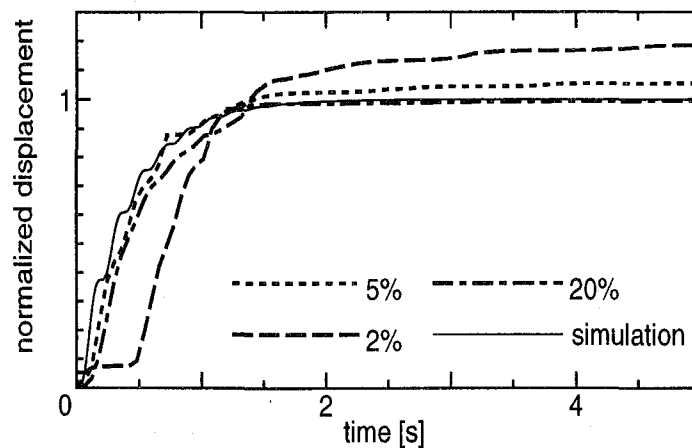
Figure 6.3.4: step responses (linearizing compensation with disturbance rejection)

The pressure responses for 10% step width is shown in Fig. 6.3.5. The linearizing control used here compensates the pressure in such a way that the corresponding value of p evaluated at the equilibrium point, denoted p_{eq}, varies linearly. We see from Fig. 6.3.5 that the linearizing control works well. Fur-

thermore, in comparison with the nominal feedback linearization control, proposed linearizing control with disturbance rejection can suppress the hysteresis characteristics so that linearity is improved.
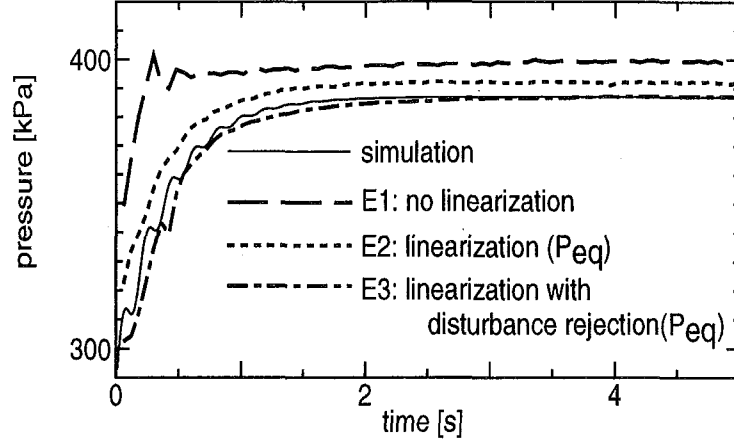
Figure 6.3.5: pressure responses for 10% step width

6.4 Disturbance Attenuation Level Reduction with Minor Feedback

6.4.1 Controller Design

In the previous section, it have been shown that minor feedback linearization with disturbance rejection is effective for the pneumatic actuator system, that is, it greatly improves the linearity of the pneumatic actuator system. In this section, we design a linear controller based on the disturbance attenuation problem in Chapter 2 with minor feedback. Namely, linear H_∞ controller is designed based on the linearized system (6.2.2) with a minor feedback loop.

Comparison is carried out with the following two constant minor feedback controllers

$$F_1 = [0 \ 0 \ F_{p1}]^T \text{ and } F_2 = [0 \ 0 \ F_{p2}]^T$$

where

$$F_{p1} = \epsilon \text{ and } F_{p2} = 5$$

with sufficiently small $\epsilon > 0$. As well as in Chapter 5, the case with F_1 refers to the case without minor feedback. Here we note that the minor feedback controllers satisfies the conditions C0 of Corollary

2.4.1. From the gain plots of nominal plant modified by the minor feedback in Figs. 6.4.1 and 6.4.2, we see that C1 of Corollary 2.4.1 is satisfied.
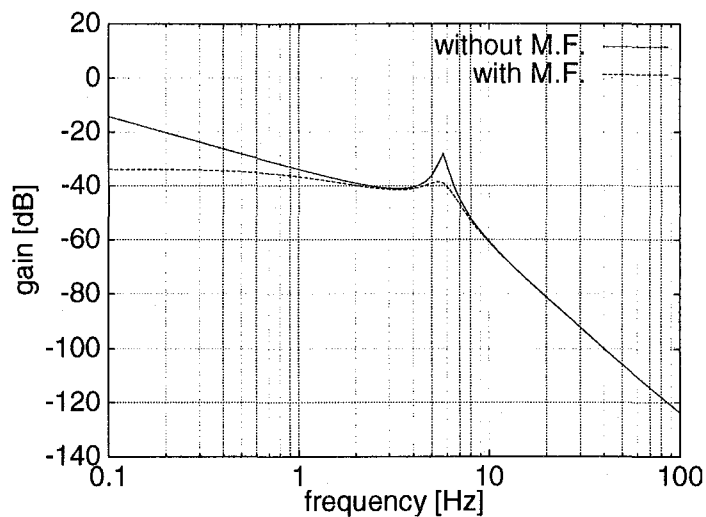
Figure 6.4.1: gain plots of nominal plants : from input u to displacement ϵ
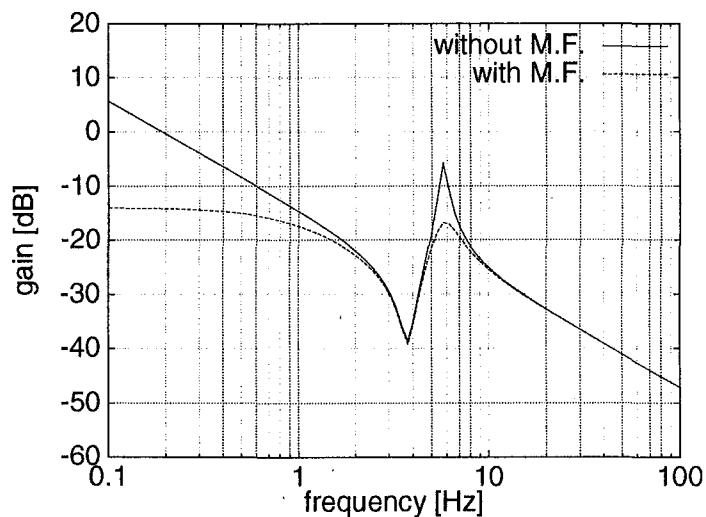
Figure 6.4.2: gain plots of nominal plants : from input u to pressure p

Therefore, if the minor feedback reduces the magnitude of uncertainty model, we can improve the disturbance attenuation level. This is examined experimentally in the next section. If this is the case, we can improve the performance by minor feedback same as the pressure control systems in Chapter 5.

6.4.2 Experimental Results

Since this pneumatic actuator system is too fragile to measure the frequency responses, we here verify the magnitude reduction of uncertainty model in the following way: Fist we design an H_∞ controller with a weighting function of uncertainty model. If the resulting closed-loop system is unstable in experiment, it implies that the real model error is not bounded by the uncertainty model. If not, it bounds the model error. Therefore, we can estimate the magnitude of uncertainty model by changing weighting function by iterating the procedure.

An H_∞ controller is design based on the disturbance rejection problem shown in Fig. 2.3.1 with the following weighting functions

$$W_T(s) = k_T W_{T0}(s) \tag{6.4.1}$$

$$W_{PS}(s) = \text{diag}\{W_R(s), 0, k_q W_R(s)\} \tag{6.4.2}$$

where

$$W_{T0}(s) = \frac{(s/2\pi + 1)^2}{(s/2\pi \times 10^3 + 1)^2} \tag{6.4.3}$$

$$W_R(s) = 10^{\frac{35}{20}} \frac{s/2\pi \times 5 + 1}{s/2\pi \times 10^3 + 1} \tag{6.4.4}$$

$$k_q = 0.1 \tag{6.4.5}$$

and k_T refers to the magnitude of the uncertainty model. The profiles of the weighting functions W_T and W_{PS} are determined according to the corresponding closed loop transfer function with the constant state feedback in the previous section. Step responses of displacement with $k_T = -8[\text{dB}]$ and $k_T = -20[\text{dB}]$ are shown in Figs. 6.4.3 and 6.4.4, where 0 refers to the equilibrium point.
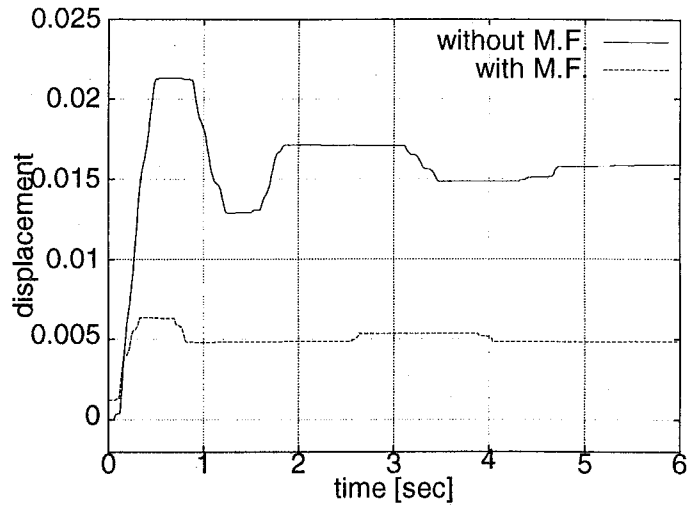
Figure 6.4.3: step responses with $k_T = -8[dB]$
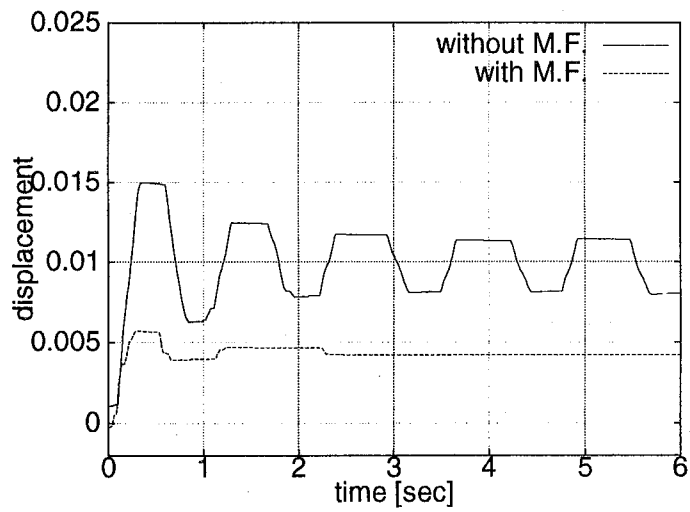
Figure 6.4.4: step responses with $k_T = -20[dB]$

67

In Fig. 6.4.3, both cases are stable and hence we see that the uncertainty is bounded by the weighting function $k_T W_{T0}(s)$ with $k_T = -8[\text{dB}]$. In Fig. 6.4.4, step response without minor feedback is unstable. This implies that the corresponding modeling error is not bounded by the weighting function $k_T W_{T0}(s)$ with $k_T = -20[\text{dB}]$. In contrast, step response with minor feedback is stable and this implies the modified modeling error with minor feedback is bounded by the weighting function. Hence, we can conclude that the magnitude of uncertainty is reduced with the minor feedback. According to Proposition 2.4.1, we see that disturbance attenuation level is reduced with the minor feedback.

H_∞ controllers with/without minor feedback are designed with the same uncertainty magnitude of

$$k_T = -8[dB] \tag{6.4.6}$$

Actually, we have

$$0.18 = \bar{q}(F_1) < \bar{q}(F_2) = 0.63 \tag{6.4.7}$$

namely, the attenuation level is improved with approximately 10[dB] according to the minor feedback.

This improvement is verified experimentally: Fig. 6.4.5 shows the gain plots of frequency responses from the disturbance to the displacement where curves and points refer to simulation and experimental results, respectively. In both case, gains are reduced in approximately 10[dB] over lower frequency range.
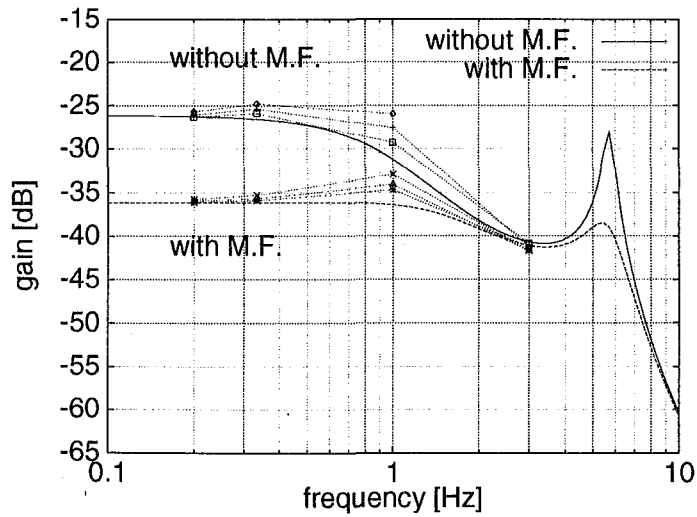
Figure 6.4.5: gain plots of closed-loop transfer function from disturbance to displacement

Fig. 6.4.6 shows the experimental result of disturbance response in time domain with sinusoidal disturbance input of $d = \sin 2\pi$.
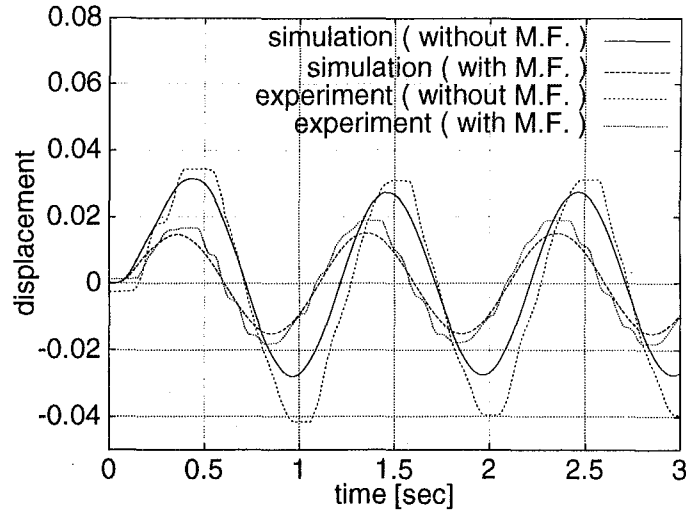
Figure 6.4.6: disturbance responses with $d = 1 \sin 2\pi$

Gain profiles of the resulting closed-loop functions are depicted in Figs. 6.4.7 through 6.4.9. From these figures, we see that the resulting closed-loop system satisfies given design specifications.

6.5 Concluding Remarks

We have applied a method of feedback linearization for a pneumatic actuator system to handle the nonlinearity based on a nonlinear model in [Kagawa 1993], where a rubber artificial muscle is used as an actuator. While conventional linear control can not treat the nonlinearities n1)–n3) in Section 6.1 directly, the feedback linearization allows us to design a controller by taking account of the nonlinearities.

Experimental results have led the following results: 1) It is verified that the linearizing control is effective for pneumatic systems. 2) The model used here is appropriate for the linearizing control. 3) The proposed feedback linearization with disturbance rejection reduces a disturbance due to the hysteresis of the R.A.M. effectively. 4) It has been confirmed that minor pressure feedback improves the disturbance attenuation level as well as for the pressure control system in Chapter 5.

Finally, we wish to thank Mr. S. Ohno for his cooperation in the experiment and Bridgestone Co. who provided the rubber artificial muscle used in the experiment.
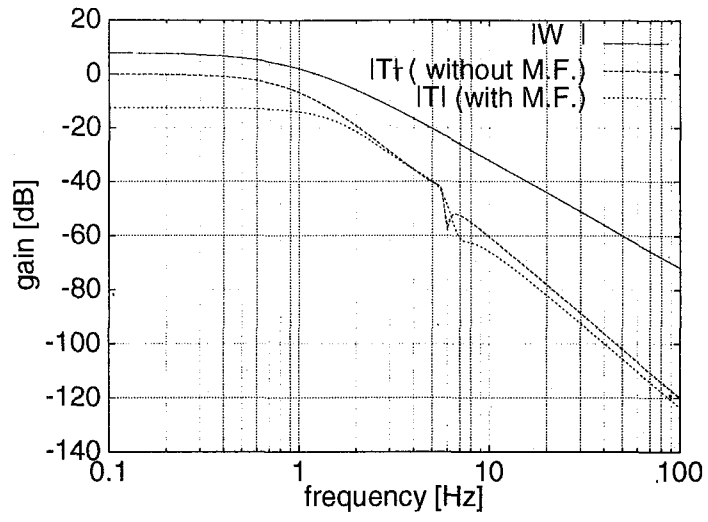
Figure 6.4.7: gain plots of complementary sensitivity function and its weighting function (inverse)
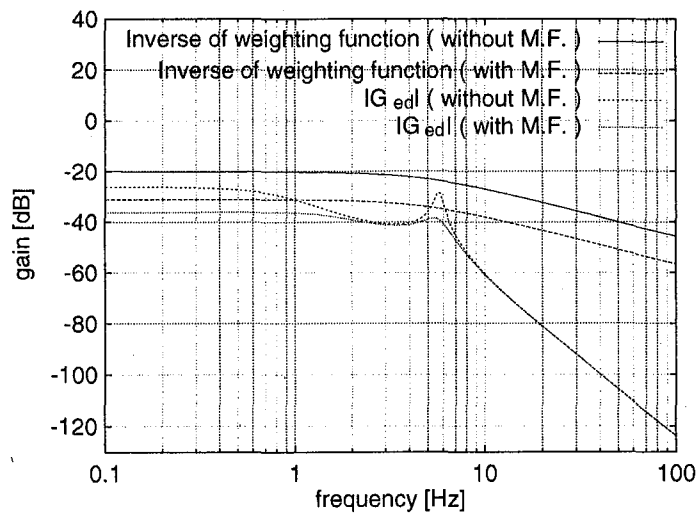
Figure 6.4.8: gain plots of closed-loop transfer function from disturbance to displacement and its weighting function (inverse)
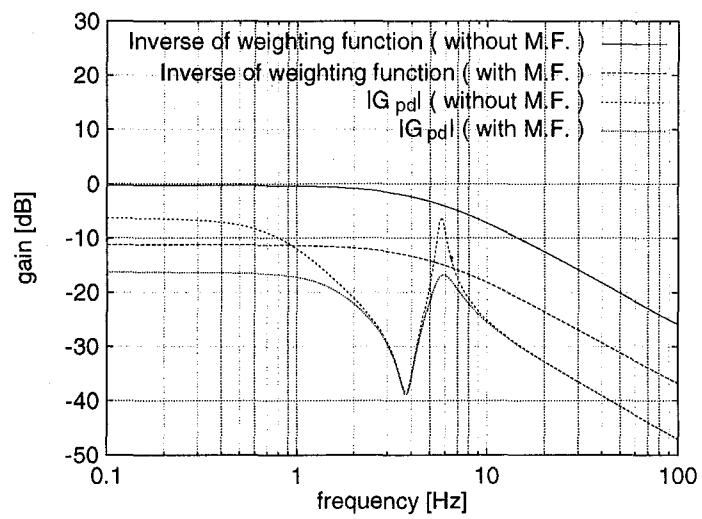
Figure 6.4.9: gain plots of closed-loop transfer function from disturbance to pressure and its weighting function (inverse)

Chapter 7

Conclusion

The finite dimensional linear time invariant (FDLTI) H_∞ control theory establishes one of the most powerful robust control design methods. The uncertainty model used in the H_∞ control is norm bounded, while real modeling error between the real plant and an FDLTI nominal plant is not. Therefore, the determination of the uncertainty model is conservative in particular applications and hence, resulting system performance might be conservative if we apply the H_∞ control to real applications directly. To reduce the conservativeness, FDLTI H_∞ control scheme with minor feedback has been examined in this thesis. The approach used here gains suitability of FDLTI H_∞ control without losing its tractability.

We summarize the main contributions as follows.

- Since minor feedback changes both nominal plant and uncertainty model, we cannot conclude immediately that it improves system performance, even if the magnitude of uncertainty model is reduced. A disturbance attenuation problem was introduced to investigate the effect of the minor feedback. A sufficient condition shows that minor feedback improves the disturbance attenuation level if it reduces the magnitude of nominal plant and that of uncertainty model.

- Experimental results for a pressure control system have shown that a minor feedback reduces the magnitude and the variation of modified modeling error over the frequency domain. From the sufficient condition, we conclude that the minor feedback improves the disturbance attenuation level and this has been confirmed experimentally.

- Feedback linearizing control was reformulated so that the linearized plant is coincident with the linear approximated plant of the original nonlinear plant. According to this reformulation, we can easily conclude that feedback linearization improves system performance if nonlinearity of the real plant occupies dominant part of uncertainty model. In addition, a class of feedback

72

linearizable plants has been derived and linearization control with disturbance rejection has been proposed. These results gain suitability of feedback linearization for pneumatic systems.

- The minor feedback should satisfy an H_∞ norm constraint to improve system performance subject to the real parametric uncertainty. A norm bound test for real parametric perturbed systems has been given based on sign definite condition. Frequency restricted norm (FRN), a generalization of the H_∞ norm, has been proposed and a special class of real parametric perturbed systems has been derived such that their FRNs are bounded by the FRNs of fixed systems. Based on these results, a design method of minor feedback controller against real parametric uncertainty has been given by using parameter space design method.

- For a pneumatic actuator systems with a rubber artificial muscle, it has been verified experimentally that the proposed linearizing control with disturbance rejection improves linearity. In addition, it has been confirmed that minor pressure feedback improves disturbance attenuation level.

We would like to point out some relevant future research topics.

- Performance improvement with minor feedback is guaranteed only for a disturbance attenuation problem. It is necessary to find out improvement conditions in a more general framework.

- For pneumatic control systems, usage of position and velocity loops as minor feedback should be clarified.

Bibliography

[Boyd 1989] S. Boyd, V. Balakrishnan, and P. Kabamba. A bisection method for computing the h_∞ norm of a transfer matrix and related problems. *Math. Contr. Sig. Syst.*, 2:207–219, 1989.

[Bhattacharyya 1991] S. P. Bhattacharyya. *Robust parametric stability: the role of the CB segments.* in Contr. of Uncertain Dyn. Systs. CRC Press, Sept. 1991.

[Bhattacharyya 1992] S. P. Bhattacharyya and L. H. Keel. Robust stability and control of linear and multilinear interval systems. *Contr. and Dyn. Syst.*, 51:31–77, 1992.

[Bouhal 1993] A. Bouhal et. al. Nonlinear adaptive pressure regulation. *Proc. of 6th Bath Internat. Fluid Power Workshop on Modeling and Simulation*, 1993.

[Chapellat 1990] H. Chapellat, M. Dahleh, and S. Bhattacharyya. Robust stability under structured and unstructured perturbations. *IEEE Trans. Automat. Contr.*, 35:1100–1107, 1990.

[Doyle 1982] J.C.Doyle. Analysis of feedback systems with structured uncertainties. *IEE Proc. Pt.D*, page 242/250, 1982.

[Doyle 1992] J.C.Doyle, B.A.Francis, and A.R.Tannenbaum. *Feedback Control Theory.* Macmillan Publishing Co., 1992.

[Fukuda 1994] K.Fukuda. H_∞ control combined with dvdfb for flexible structured systems. Master's thesis, Tokyo Inst. of Tech., 1994.

[Hara 1991] S. Hara, T. Kimura, and R. Kondo R. h_∞ control system design by a parameter space approach. *Proc. of MTNS-91*, 1991.

[Hara 1992] S. Hara, G. Yamamoto, M. Oshima, and R. Kondo. A distributed computing environment for control system analysis and design. *Proc. of Symposium on Computer-Aided Control System Design (CACSD)*, pages 47–54, 1992. California.

[Hollot 1992] C. V. Hollot, R. Tempo, and V. Blondel. h_∞ performance of interval plants and interval feedback systems. *Proc. of the Internat. Workshop on Robust Control (to appear)*, 1992.

[Imura 1994] J.Imura, T.Sugie, and T.Yshikawa. Strict h_∞ control of nonlinear systems based on the hamilton-jacobi inequality. *Proc. of Asian Control Conference(ASCC)*, pages 189–192, 1994.

[Kagawa 1993] T.Kagawa, T.Fujita, and T.Yamanaka. Nonlinear model of artificial muscle. *Tran. of the Society of Instrument and Contr. Engineers(SICE)*, 29(10):1241–1243, 1993. (in Japanese).

[Kawakami 1993] Y.Kawakami. Fast position control with a pneumatic cylinder. *Journal of the Japan Hydraulics & Pneumatics Society*, (7):769/774, 1993.

[Kawashima 1993] K.Kawashima et.al. Measurement method of air flow rate using isothermal changing chamber,. *Proc. of 4th Joint Sympo. on Fluid Contr. and Measur.*, pages 75–80, 1993.

[Keel 1991] L.H.Keel, J.Shaw, and S.P.Bhattacharyya. Robust control of interval systems. *Proc. of MTNS-91*. Kobe. 1991

[Kharitonov 1978] V. L. Kharitonov. Asymptotic stability of an equilibrium position of a family of linear difference equations. *Differential. Uravnen.*, 14:2086–2088, 1978.

[Kimura 1993] T.Kimura et. al. Pressure control problems on a rubber artificial muscle. *Proc. of 4th Joint Sympo. on Fluid Contr. and Measurement*, pages 63–68, 1993.

[Kimura 1994] T.Kimura and S.Hara. Frequency restricted norm bounds for interval systems. *International Journal of Nonlinear and Robust Control*, page 575/593, 1994.

[Matsushita 1993] H.Matsushita, S.Dohta, and T.Noritsugu. Attitude control of a two wheeled vehicle model with pneumatic servo type active suspension. *Proc. of the 2nd Japan Hydraulics and Pneumatics Society Internat. Sympo. on Fluid Power.*, pages 707–712, 1993.

[Miyata 1990] K.Miyata, K.Ishida, and H.Hanafusa. Double structured feedback control with variable gain pressure control system for positioning of pneumatic cylinders. *Tran. of the Society of Instrument and Contr. Engineers(SICE)*, 26(6):787–794, 1990. (in Japanese).

[Mori 1986] T. Mori and Kokame. A geometrical interpretation of kharitonov's theorem. *Tran. of the Society of Instrument and Contr. Engineers(SICE)*, 22(8):817–822, 1986. (in Japanese).

[Osuka 1990] K.Osuka, T.Kimura, and T.Ono. h_∞ control of a certain nonlinear actuator. *Proc. of the 29th IEEE CDC*, pages 370–371, 1990.

[Pu 1993] J.Pu et.al. A study of gain-scheduling method for controlling the motion of pneumatic servos. *Proc. of 6th Bath Internat. Fluid Power Workshop on Modeling and Simulation*, 1993.

[Sampei 1993a] M.Sampei and T.Kobayashi. Application of nonlinear control theory to path tracking control of articulated vehicles with double trailers. *Proc. of 12th World Congress of IFAC*, 7:263–266, 1993.

[Sampei 1993b] M.Sampei. *Optimal Control System Design and Basics, Theories and Applications of Control Methods in Practice.* I.N.G. Publishing, 1993. (in Japanese).

[Siljak 1971] D. D. Šiljak D. D. New algebraic criterion for positive realness. *Journal of the Franklin Institute*, 291:109–120, 1971.

[Su 1982] R. Su. On the linear equivalents of nonlinear systems. *Syst. Contr. Lett.*, 2(1):48–52, 1982.

[Sugie 1993] T.Sugie, K.Shimizu, and J.Imura. h_∞ control with exact linearization and its application to magnetic levitation systems. *Proc. of 12th World Congress of IFAC*, 4:363–366, 1993.

[Takagi 1930] T.Takagi. *Lecture of Algebra.* Kyoritsu Publish, 1930. (in Japanese).

[Takagi 1993] Y.Takagi and et.al. A design of power system stabilizer applying state-space linearization. *Tran. of the Society of Instrument and Contr. Engineers(SICE)*, 29(2):194–200, 1993. (in Japanese).

Appendix A

A.1　The proofs of Claims 1) and 2) of Theorem 4.3.1

[The proofs of Claims 1) and 2)]

We only focus on $a_{2k}(k = 0, 1, 2, \ldots, [n/2])$ here, since the proof associated with $a_{2k+1}(k = 0, 1, 2, \ldots, [n/2])$ can be carried out by the same technique as that associated with a_{2k}. Hence, we fix the values of $a_{2k+1}(k = 0, 1, 2, \ldots, [n/2])$ as $a_{2k+1}^{\star}(k = 0, 1, 2, \ldots, [n/2])$ without loss of generality from now on. Furthermore, we define the following four classes:

$$
\begin{aligned}
\mathcal{G}_R &:= \{G(s) = \overline{q}(s)/a(s) \mid a(s) \in \mathcal{A}_R\} \\
\mathcal{A}_R &:= \{a(s) \mid a_{2i} \in [\underline{a}_{2i}, \overline{a}_{2i}],\ a_{2i+1} = a_{2i+1}^{\star} \ ;\ i = 0, 1, \ldots, [n/2]\} \\
\mathcal{V}_R &:= \{a(s) \mid a_{2i} = \underline{a}_{2i} \ \text{or} \ \overline{a}_{2i},\ a_{2i+1} = a_{2i+1}^{\star} \ ;\ i = 0, 1, \ldots, [n/2]\} \\
\mathcal{K}_R &:= \{k_{R1}(s),\ k_{R2}(s)\}
\end{aligned}
\tag{A.1.1}
$$

where

$$
\begin{aligned}
k_{R1}(s) &:= (\underline{a}_0 + \underline{a}_4 s^4 + \cdots) + (\overline{a}_2 s^2 + \overline{a}_6 s^6 + \cdots) + (a_1^{\star} + a_5^{\star} s^5 + \cdots) + (a_3^{\star} + a_7^{\star} s^7 + \cdots) \\
k_{R2}(s) &:= (\overline{a}_0 + \overline{a}_4 s^4 + \cdots) + (\underline{a}_2 s^2 + \underline{a}_6 s^6 + \cdots) + (a_1^{\star} + a_5^{\star} s^5 + \cdots) + (a_3^{\star} + a_7^{\star} s^7 + \cdots).
\end{aligned}
\tag{A.1.2}
$$

Consequently, we will prove the followings instead of proving Claims 1) and 2):

Claim 1') If there exist $a^{\#}(s) \in \mathcal{A}_R$ and $\omega^{\#} \in (\omega_L, \omega_H)$ such that $|G^{\#}(j\omega^{\#})| \geq \|G(s)\|_{[\omega_L, \omega_H]}$ holds for all $G(s) \in \mathcal{G}_R$, then $a^{\#}(s) \in \mathcal{V}_R$.

Claim 2') If there exist $a^{\#}(s) \in \mathcal{V}_R$ and $\omega^{\#} \in (\omega_L, \omega_H)$ such that $|G^{\#}(j\omega^{\#})| \geq \|G(s)\|_{[\omega_L, \omega_H]}$ holds for all $G(s) \in \mathcal{G}_R$, then $a^{\#}(s) \in \mathcal{K}_R$.

We will give the proof considering the following three cases:

case 1) $R^{\#}(\omega^{\#}) \neq 0$

case 2) $R^{\#}(\omega^{\#}) = 0,\ \phi^{\#}(\omega^{\#}) \neq 0$

case 3) $R^{\#}(\omega^{\#}) = 0$, $\phi^{\#}(\omega^{\#}) = 0$

where

$$a^{\#}(j\omega) \quad =: \quad R^{\#}(\omega) + jI^{\#}(\omega) \tag{A.1.3}$$

$$\phi^{\#}(\omega) \quad := \quad \frac{dI^{\#}(\omega)}{d\omega}(\overline{Q}_0^2 + \overline{Q}_1^2\omega^2) - \overline{Q}_1^2\omega I^{\#}(\omega) \tag{A.1.4}$$

Remark: The proof of the Claim 1') is executed by using contradiction and the proof of the Claim 2') is almost same. The outline of the proof strategy for the Claim 1') is described as follows.

We have already noted that the scripts $^{\#}$ indicate the values associated with the maximum, in the following discussions, we also use the scripts $^{@}$ to indicate the values which will lead to a contradiction.

In the case 1, if $a^{\#}(s) \notin \mathcal{V}_R$, where $a^{\#}(s)$ is the denominator of $G^{\#}(s)$, we can find a coefficient $a_{2k}^{@} := a_{2k}^{\#} + \epsilon$, $\epsilon \neq 0$, $|\epsilon| \ll 1$ so that the resulting system $G^{@}(s)$ satisfies the inequality

$$|G^{@}(j\omega^{\#})| > |G^{\#}(j\omega^{\#})| \tag{A.1.5}$$

where

$$G^{@}(j\omega) := \frac{\overline{Q}_0 + \overline{Q}_1 j\omega}{R^{@}(\omega) + jI^{\#}(\omega)} \tag{A.1.6}$$

and

$$R^{@}(\omega) := a_0^{\#} + a_2^{\#}(j\omega)^2 + \cdots \\ + a_{2(k-1)}^{\#}(j\omega)^{2(k-1)} + a_{2k}^{@}(j\omega)^{2k} + a_{2(k+1)}^{\#}(j\omega)^{2(k+1)} + \cdots + a_{2[n/2]}(j\omega)^{2[n/2]} \tag{A.1.7}$$

This contradicts the maximality of $G^{\#}(s)$ in (4.3.23). Fig. A-1 illustrates the situation.

In the cases 2 and 3, we use the fact that $|G^{\#}(\omega)|$ is partitioned into

$$|G^{\#}(j\omega)|^2 = 1/(U^{\#}(\omega) + V^{\#}(\omega)) \tag{A.1.8}$$

where

$$U^{\#}(\omega) := \frac{R^{\#2}(\omega)}{\overline{Q}_0^2 + \overline{Q}_1^2\omega^2}, \quad V^{\#}(\omega) := \frac{I^{\#2}(\omega)}{\overline{Q}_0^2 + \overline{Q}_1^2\omega^2} \tag{A.1.9}$$

Here we note that $\frac{d}{d\omega}V^{\#}(\omega)$ is represented by

$$\frac{d}{d\omega}V^{\#}(\omega) = \frac{2I^{\#}(\omega)\phi^{\#}(\omega)}{(\overline{Q}_0^2 + \overline{Q}_1^2\omega^2)^2} \tag{A.1.10}$$

where $\phi^{\#}(\omega)$ is defined by (A.1.4).

In the case 2, we can see from (A.1.9) and (A.1.10) that $U^{\#}(\omega)$ is zero at $\omega = \omega^{\#}$ and $dV^{\#}(\omega^{\#})/d\omega \neq 0$. (suppose $dV^{\#}(\omega^{\#})/d\omega > 0$ for example). Let us define $U^{@}(\omega)$ as

$$U^{@}(\omega) := \frac{R^{@}(\omega)}{\overline{Q}_0^2 + \overline{Q}_1^2\omega^2} \tag{A.1.11}$$

where $R^{@}(\omega)$ is defined by (A.1.7). If $a^{\#}(s) \notin \mathcal{V}_R$, then we can find a coefficient $a_{2k}^{@} := a_{2k}^{\#} + \epsilon$ so that the resulting function $U^{@}(\omega)$ has zero at $\omega^{@} := \omega^{\#} - \epsilon_\omega$, $\epsilon_\omega > 0$, $|\epsilon_\omega| \ll 1$ with sufficiently small $\epsilon > 0$. Since $dV^{\#}(\omega^{\#})/d\omega > 0$ and $U^{\#}(\omega^{\#}) = U^{@}(\omega^{@}) = 0$, we have the inequality $U^{\#}(\omega^{\#}) + V^{\#}(\omega^{\#}) > U^{@}(\omega^{@}) + V^{\#}(\omega^{@})$. According to (A.1.8), this contradicts the maximality of $G^{\#}(s)$ in (4.3.23). Fig. A-2 illustrates this situation.

In the case 3, we have $U^{\#}(\omega^{\#}) = 0$ and $dV^{\#}(\omega^{\#})/d\omega = 0$ from (A.1.9) and (A.1.10). Moreover, from Lemma A.1.2 , we see that $\omega^{\#}$ achieves a local maximum of $V^{\#}(\omega)$. Therefore, as in the case 2, we can find a coefficient $a_{2k}^{@} := a_{2k}^{\#} + \epsilon$, $\epsilon \neq 0$, $|\epsilon| \ll 1$ so that $U^{@}(\omega)$ has zero at $\omega^{@} := \omega^{\#} - \epsilon_\omega$, $\epsilon_\omega \neq 0$, $|\epsilon_\omega| \ll 1$. with sufficiently small $\epsilon > 0$. Therefore, since $\omega^{\#}$ is a local maximum of $dV^{\#}(\omega)/d\omega$, we obtain $U^{\#}(\omega^{\#}) + V^{\#}(\omega^{\#}) > U^{@}(\omega^{@}) + V^{\#}(\omega^{@})$. According to (A.1.8), this contradicts the maximality of $G(s)^{\#}$ in (4.3.23). Fig. A-3 illustrates this situation.

Details of the proofs are stated as follows.

We note that we can assume $\overline{Q}_0 + \overline{Q}_1 j\omega^{\#} \neq 0$, since $\overline{Q}_0 + \overline{Q}_1 j\omega^{\#} = 0$ implies $G(s) \equiv 0$. Furthermore, when $\omega^{\#} = 0$, the Theorem 4.3.1 is trivial. Thus, we will investigate the case $\omega^{\#} \neq 0$. In addition, since $G(j\omega)$ is symmetric w.r.t. $\omega \in \mathbf{R}$, we can assume $\omega^{\#} > 0$ from now on.

The proof of Claim 1':

We first suppose that $a^{\#}(s) \notin \mathcal{V}_R$, i.e., there exists an integer k such that $a_{2k}^{\#} \in (\underline{a}_{2k}, \overline{a}_{2k})$.

case 1) $R^{\#}(\omega^{\#}) \neq 0$:

Observing

$$|G^{\#}(j\omega^{\#})|^2 = \frac{\overline{Q}_0^2 + \overline{Q}_1^2 \omega^{\#2}}{R^{\#2}(\omega^{\#}) + I^{\#2}(\omega^{\#})} \tag{A.1.12}$$

yields

$$\frac{\partial}{\partial a_{2k}}|G^{\#}(j\omega^{\#})|^2 = \frac{(-1)^k 2 R^{\#}(\omega^{\#}) w^{\#2k} \left(\overline{Q}_0^2 + \overline{Q}_1^2 w^{\#2}\right)}{\left(R^{\#2}(\omega^{\#}) + I^{\#2}(\omega^{\#})\right)^2} \tag{A.1.13}$$

Since this partial derivative is not equal to zero from the assumptions, if we take $a_{2k}^{@} \in (\underline{a}_{2k}, \overline{a}_{2k})$ as a value in an ϵ-neighborhood of $a_{2k}^{\#}$ such that

$$\begin{cases} a_{2k}^{@} = a_{2k}^{\#} + \epsilon & \text{if } \dfrac{\partial}{\partial a_{2k}}|G^{\#}(j\omega^{\#})|^2 > 0 \\[2mm] a_{2k}^{@} = a_{2k}^{\#} - \epsilon & \text{if } \dfrac{\partial}{\partial a_{2k}}|G^{\#}(j\omega^{\#})|^2 < 0 \end{cases} \tag{A.1.14}$$

then the resulting transfer function $G^{@}(s) \in \mathcal{G}_R$ satisfies

$$|G^{\#}(j\omega^{\#})| < |G^{@}(j\omega^{\#})| \tag{A.1.15}$$

for sufficiently small $\epsilon > 0$, where $G^{@}$ is defined by (A.1.6) with $R^{@}(\omega)$ defined in (A.1.7). This contradicts (4.3.23) and we can conclude that $a_{2k}^{\#} = \underline{a}_{2k}$ or $\overline{a}_{2k}$, i.e., $a^{\#}(s) \in \mathcal{V}_R$.

case 2) $R^{\#}(\omega^{\#}) = 0$ and $\phi^{\#}(\omega^{\#}) \neq 0$:

According to the stability of $a(s)$, we can assume

$$I^{\#}(\omega^{\#}) \neq 0 \tag{A.1.16}$$

and this implies

$$V^{\#}(\omega^{\#}) \neq 0 \tag{A.1.17}$$

and

$$dV^{\#}(\omega^{\#})/d\omega \neq 0 \tag{A.1.18}$$

In addition, we note that

$$dR(\omega^{\#})/d\omega \neq 0 \tag{A.1.19}$$

holds by Lemma A.1.1 in Appendix B. From (A.1.18) and (A.1.19), we first consider the case where the following three conditions hold:

$$dV^{\#}(\omega^{\#})/d\omega > 0, \quad dR^{\#}(\omega^{\#})/d\omega > 0, \quad k \text{ is even.} \tag{A.1.20}$$

Then, from Lemma A.1.3 in Appendix B, if we take $a_{2k}^{@} \in (\underline{a}_{2k}, \overline{a}_{2k})$ as

$$a_{2k}^{@} = a_{2k}^{\#} - \epsilon \tag{A.1.21}$$

then we can obtain $\omega^{@} \in (\omega_L, \omega_H)$, $\omega^{@} = \omega^{\#} - \epsilon_\omega$, $\epsilon_\omega > 0$, $|\epsilon_\omega| \ll 1$ so that

$$R^{@}(\omega^{@}) = 0 \tag{A.1.22}$$

for sufficiently small $\epsilon > 0$, where $R^{@}(\omega)$ is defined by (A.1.7). This implies

$$U^{@}(\omega^{@}) = 0 \tag{A.1.23}$$

where $U^{@}(\omega)$ is defined by (A.1.11).

Since $dV^{\#}(\omega^{\#})/d\omega > 0$, we see that

$$V^{\#}(\omega^{\#}) > V^{\#}(\omega^{@}) , \quad \omega^{@} < \omega^{\#} \tag{A.1.24}$$

and hence we have

$$U^{\#}(\omega^{\#}) + V^{\#}(\omega^{\#}) > U^{@}(\omega^{@}) + V^{\#}(\omega^{@}) \tag{A.1.25}$$

because $U^{\#}(\omega^{\#}) = 0$ and $U^{@}(\omega^{@}) = 0$. In general

$$\begin{array}{lllll}
\text{If} & dV^{\#}(\omega^{\#})/d\omega > 0, & dR^{\#}(\omega^{\#})/d\omega > 0(< 0), & k\text{:even,} & \text{take} \quad a_{2k}^{@} := a_{2k}^{\#} - \epsilon(+\epsilon) \\
\text{If} & \quad ,, & dR^{\#}(\omega^{\#})/d\omega > 0(< 0), & k\text{:odd} & \text{take} \quad a_{2k}^{@} := a_{2k}^{\#} + \epsilon(-\epsilon) \\
\text{If} & dV^{\#}(\omega^{\#})/d\omega < 0, & dR^{\#}(\omega^{\#})/d\omega > 0(< 0), & k\text{:even,} & \text{take} \quad a_{2k}^{@} := a_{2k}^{\#} + \epsilon(-\epsilon) \\
\text{If} & \quad ,, & dR^{\#}(\omega^{\#})/d\omega > 0(< 0), & k\text{:odd} & \text{take} \quad a_{2k}^{@} := a_{2k}^{\#} - \epsilon(+\epsilon)
\end{array} \tag{A.1.26}$$

Then, in the same way, we can find $\omega^{@} \in (\omega_L, \omega_H)$ so that the inequality (A.1.25) holds for sufficiently small $\epsilon > 0$.

The inequality (A.1.25) implies

$$|G^{\#}(j\omega^{\#})| < |G^{@}(j\omega^{@})| \qquad (A.1.27)$$

where $G^{@}(s) \in \mathcal{G}_R$ is defined by (A.1.6) and this contradicts the maximality of $G^{\#}(s)$ in (4.3.23). Hence, we conclude that $a_{2k}^{\#} = \underline{a}_{2k}$ or $\overline{a}_{2k}$, i.e., $a^{\#}(s) \in \mathcal{V}_R$.

case 3) $R^{\#}(\omega^{\#}) = 0, \phi^{\#}(\omega^{\#}) = 0$:

The assumption $\phi^{\#}(\omega^{\#}) = 0$ yields

$$\frac{dV^{\#}(\omega^{\#})}{d\omega} = 0 \qquad (A.1.28)$$

Furthermore, considering the assumption $R^{\#}(\omega^{\#}) = 0$, the Lemma A.1.2 in Appendix B leads to

$$\frac{d^2 V^{\#}(\omega^{\#})}{d\omega^2} < 0 \qquad (A.1.29)$$

Therefore, from (A.1.28) and (A.1.29), we see that $V^{\#}(\omega)$ has a local maximum at $\omega = \omega^{\#}$.

Since the variation of the zeros of $U^{\#}(\omega)$ is continuous with respect to the variation of the coefficient $a_{2k}^{\#}$, taking

$$a_{2k}^{@} := a_{2k}^{\#} + \epsilon \qquad (A.1.30)$$

leads to

$$U^{@}(\omega^{@}) = 0, \quad \omega^{@} \neq \omega^{\#}, \quad |\omega^{@} - \omega^{\#}| \ll 1 \qquad (A.1.31)$$

for sufficiently small ϵ, where $U^{@}(\omega)$ is defined by (A.1.11).

Hence, the selection of $a_{2k}^{@}$ in (A.1.30) yields

$$U^{\#}(\omega^{\#}) + V^{\#}(\omega^{\#}) > U^{@}(\omega^{@}) + V^{\#}(\omega^{@}) \qquad (A.1.32)$$

and this implies

$$|G^{\#}(j\omega^{\#})| < |G^{@}(j\omega^{@})| \qquad (A.1.33)$$

where $G^{@}(s) \in \mathcal{G}_R$ is defined by (A.1.6). This contradicts (4.3.23), and hence, we can conclude that the maximum is not attained in the case 3.

Combining the cases 1), 2) and 3), we conclude Claim 1'. □

Proof of Claim 2':

Let us assume $a^\#(s) \notin \mathcal{K}_R$ but $a^\#(s) \in \mathcal{V}_R$. This implies following four possibilities, namely, there exist integers k and l, $k \neq l$ such that

a) $\quad R^\#(\omega) \;=\; (a_0^\# + a_4^\# \omega^4 + \cdots + \underline{a}_{2k} \omega^{2k} + \cdots + \overline{a}_{2l} \omega^{2l} + \cdots) - (a_2^\# \omega^2 + a_6^\# \omega^6 + \cdots)$

b) $\quad R^\#(\omega) \;=\; (a_0^\# + a_4^\# \omega^4 + \cdots) - (a_2^\# \omega^2 + a_6^\# \omega^6 + \cdots + \underline{a}_{2k} \omega^{2k} + \cdots + \overline{a}_{2l} \omega^{2l} + \cdots)$

c) $\quad R^\#(\omega) \;=\; (a_0^\# + a_4^\# \omega^4 + \cdots + \underline{a}_{2k} \omega^{2k} + \cdots) - (a_2^\# \omega^2 + a_6^\# \omega^6 + \cdots + \underline{a}_{2l} \omega^{2l} + \cdots)$

d) $\quad R^\#(\omega) \;=\; (a_0^\# + a_4^\# \omega^4 + \cdots + \overline{a}_{2k} \omega^{2k} + \cdots) - (a_2^\# \omega^2 + a_6^\# \omega^6 + \cdots + \overline{a}_{2l} \omega^{2l} + \cdots)$

$$(A.1.34)$$

case 1) $R^\#(\omega^\#) \neq 0$:

Let us first consider case a) and suppose $R^\#(\omega^\#) > 0$. Then, taking $a_{2k}^@ \in [\underline{a}_{2k}, \overline{a}_{2k}]$ and $a_{2l}^@ \in [\underline{a}_{2l}, \overline{a}_{2l}]$ as

$$a_{2k}^@ := a_{2k}^\#, \quad a_{2l}^@ := a_{2l}^\# - \epsilon \tag{A.1.35}$$

and defining

$$
\begin{aligned}
R^@(\omega) \;&:=\; a_0^\# + a_2^\# (j\omega)^2 + \cdots + a_{2k}^@ (j\omega)^{2k} + \cdots + a_{2l}^@ (j\omega)^{2l} + \cdots \\
&=\; R^\#(\omega^\#) - \epsilon \omega^{\#2l}
\end{aligned}
\tag{A.1.36}
$$

lead to

$$|R^\#(\omega^\#)| > |R^@(\omega^\#)| \tag{A.1.37}$$

for sufficiently small $\epsilon > 0$.

In general,

for case a):

If $R^\#(\omega^\#) > 0 (< 0)$, take $a_{2k}^@ := a_{2k}^\# \quad, a_{2l}^@ := a_{2l}^\# - \epsilon \ (a_{2k}^@ := a_{2k}^\# + \epsilon, a_{2l}^@ := a_{2l}^\#)$

for case b):

If $R^\#(\omega^\#) > 0 (< 0)$, take $a_{2k}^@ := a_{2k}^\# + \epsilon, a_{2l}^@ := a_{2l}^\# \quad (a_{2k}^@ := a_{2k}^\# \quad, a_{2l}^@ := a_{2l}^\# - \epsilon)$

for case c):

If $R^\#(\omega^\#) > 0 (< 0)$, take $a_{2k}^@ := a_{2k}^\# \quad, a_{2l}^@ := a_{2l}^\# + \epsilon \ (a_{2k}^@ := a_{2k}^\# + \epsilon, a_{2l}^@ := a_{2l}^\#)$

for case d):

If $R^\#(\omega^\#) > 0 (< 0)$, take $a_{2k}^@ := a_{2k}^\# - \epsilon, a_{2l}^@ := a_{2l}^\# \quad (a_{2k}^@ := a_{2k}^\# \quad, a_{2l}^@ := a_{2l}^\# - \epsilon)$

Then, the inequality (A.1.37) holds.

The inequality (A.1.37) yields

$$|G^\#(j\omega^\#)| < |G^@(j\omega^@)| \tag{A.1.38}$$

where $G^@(s)$ is defined by (A.1.6) with $R^@(\omega)$ defined by (A.1.36) of which the coefficients are selected above. This contradicts (4.3.23) and we conclude $a^\#(s) \in \mathcal{K}_R$.

case 2) $R^\#(\omega^\#) = 0, \phi^\#(\omega^\#) \neq 0$:

Again consider the cases a) ~ d). According to lemma A.1.1 in Appendix B, we have $dR^{\#}(\omega^{\#})/d\omega \neq 0$. In the same argument in the case 3 of Claim 1', Lemma A.1.3 in Appendix B leads to the fact that we can select $a_{2k}^{@} \in [\underline{a}_{2k}, \overline{a}_{2k}]$ and $a_{2l}^{@} \in [\underline{a}_{2l}, \overline{a}_{2l}]$ so that

$$U^{\#}(\omega^{\#}) + V^{\#}(\omega^{\#}) > U^{@}(\omega^{@}) + V^{\#}(\omega^{@}) \qquad (A.1.39)$$

holds, where

$$U^{\#}(\omega^{\#}) = U^{@}(\omega^{@}) = 0 \qquad (A.1.40)$$

by the following selection with sufficiently small $\epsilon > 0$:

for case a):

If $\frac{d}{d\omega}V^{\#}(\omega^{\#}) > 0$, $\frac{\partial R^{\#}(\omega^{\#})}{\partial \omega} > 0 (< 0)$, take $a_{2k}^{@} := a_{2k}^{\#}$, $a_{2l}^{@} := a_{2l}^{\#} - \epsilon$ $(a_{2k}^{@} := a_{2k}^{\#} + \epsilon, a_{2l}^{@} := a_{2l}^{\#})$

If $\frac{d}{d\omega}V^{\#}(\omega^{\#}) < 0$, $\frac{\partial R^{\#}(\omega^{\#})}{\partial \omega} > 0 (< 0)$, take $a_{2k}^{@} := a_{2k}^{\#} + \epsilon, a_{2l}^{@} := a_{2l}^{\#}$ $(a_{2k}^{@} := a_{2k}^{\#}, a_{2l}^{@} := a_{2l}^{\#} - \epsilon)$

for case b):

If $\frac{d}{d\omega}V^{\#}(\omega^{\#}) > 0$, $\frac{\partial R^{\#}(\omega^{\#})}{\partial \omega} > 0 (< 0)$, take $a_{2k}^{@} := a_{2k}^{\#} + \epsilon, a_{2l}^{@} := a_{2l}^{\#}$ $(a_{2k}^{@} := a_{2k}^{\#}, a_{2l}^{@} := a_{2l}^{\#} - \epsilon)$

If $\frac{d}{d\omega}V^{\#}(\omega^{\#}) < 0$, $\frac{\partial R^{\#}(\omega^{\#})}{\partial \omega} > 0 (< 0)$, take $a_{2k}^{@} := a_{2k}^{\#}$, $a_{2l}^{@} := a_{2l}^{\#} - \epsilon$ $(a_{2k}^{@} := a_{2k}^{\#} + \epsilon, a_{2l}^{@} := a_{2l}^{\#})$

for case c):

If $\frac{d}{d\omega}V^{\#}(\omega^{\#}) > 0$, $\frac{\partial R^{\#}(\omega^{\#})}{\partial \omega} > 0 (< 0)$, take $a_{2k}^{@} := a_{2k}^{\#}$, $a_{2l}^{@} := a_{2l}^{\#} + \epsilon$ $(a_{2k}^{@} := a_{2k}^{\#} + \epsilon, a_{2l}^{@} := a_{2l}^{\#})$

If $\frac{d}{d\omega}V^{\#}(\omega^{\#}) < 0$, $\frac{\partial R^{\#}(\omega^{\#})}{\partial \omega} > 0 (< 0)$, take $a_{2k}^{@} := a_{2k}^{\#} + \epsilon, a_{2l}^{@} := a_{2l}^{\#}$ $(a_{2k}^{@} := a_{2k}^{\#}, a_{2l}^{@} a_{2l}^{\#} + \epsilon)$

for case d):

If $\frac{d}{d\omega}V^{\#}(\omega^{\#}) > 0$, $\frac{\partial R^{\#}(\omega^{\#})}{\partial \omega} > 0 (< 0)$, take $a_{2k}^{@} := a_{2k}^{\#} - \epsilon, a_{2l}^{@} := a_{2l}^{\#}$ $(a_{2k}^{@} := a_{2k}^{\#}, a_{2l}^{@} := a_{2l}^{\#} - \epsilon)$

If $\frac{d}{d\omega}V^{\#}(\omega^{\#}) < 0$, $\frac{\partial R^{\#}(\omega^{\#})}{\partial \omega} > 0 (< 0)$, take $a_{2k}^{@} := a_{2k}^{\#}$, $a_{2l}^{@} := a_{2l}^{\#} - \epsilon$ $(a_{2k}^{@} := a_{2k}^{\#} - \epsilon, a_{2l}^{@} := a_{2l}^{\#})$

Therefore, (A.1.39) leads to the inequality

$$|G^{\#}(j\omega^{\#})| < |G^{@}(j\omega^{@})| \qquad (A.1.41)$$

and this contradicts (4.3.23). Hence, we conclude $a^{\#}(s) \in \mathcal{K}_R$.

case 3) $R^{\#}(\omega^{\#}) = 0, \phi^{\#}(\omega^{\#}) = 0$:

From the proof in the case 3 of Claim 1', we see that the arbitrary sufficiently small variation of $a_{2k}^{\#}$ yields (A.1.31). Hence, we conclude that the maximum is not attained in the case 3.

Combining the cases 1),2) and 3), we conclude Claim 2'.

$\square$

Lemma A.1.1 *Consider an n-th order stable interval polynomial $a(s)$*

$$a(s) = a_0 + a_1 s + a_2 s + \cdots + a_n s^n \; ; \quad a_k \in [\underline{a}_k, \overline{a}_k] \qquad (A.1.42)$$

and partition $a(j\omega)$ *as*

$$a(j\omega) = R(\omega) + jI(\omega) \tag{A.1.43}$$

where

$$
\begin{aligned}
R(\omega) &= (a_0 + a_4\omega^4 + \cdots + a_{4k}\omega^{4k} + \cdots) - (a_2\omega^2 + a_6\omega^6 + \cdots + a_{4k+2}\omega^{4k+2} + \cdots) \\
I(\omega) &= (a_1\omega + a_5\omega^5 + \cdots + a_{4k}\omega^{4k+1} + \cdots) - (a_3\omega^3 + a_7\omega^7 + \cdots + a_{4k}\omega^{4k+3} + \cdots)
\end{aligned}
\tag{A.1.44}
$$

Then

$$R(\omega^{\#}) = 0 \implies \frac{dR(\omega^{\#})}{d\omega} \neq 0 \tag{A.1.45}$$

Proof) Since $a(s)$ is stable, all roots of $R(\omega) = 0$ must be distinct each other. This leads to (A.1.45).

□

Lemma A.1.2 *If there exists an* $w^{\#} \in \mathbf{R}$ *satisfying*

$$R^{\#}(\omega^{\#}) = 0 \quad and \quad \frac{d}{d\omega}V^{\#}(\omega^{\#}) = \frac{2I^{\#}(\omega^{\#})\phi^{\#}(\omega^{\#})}{(\overline{Q}_0^2 + \overline{Q}_1^2\omega^{\#2})^2} = 0 \tag{A.1.46}$$

then we have

$$\frac{d^2}{d\omega^2}V^{\#}(\omega^{\#}) < 0 \tag{A.1.47}$$

Proof) Suppose the order of $I^{\#}(\omega)$ is m. Then, $\frac{d}{d\omega}V^{\#}(\omega) = 0$ has $2m+1$ roots. According to the stability of $G^{\#}(s)$, we have the following facts:

   1) $I^{\#}(\omega) = 0$ has m distinct real roots, that is, $V^{\#}(\omega) = 0$ has m distinct double real roots.

   2) $I^{\#}(\omega^{\#}) \neq 0$ holds, that is, $V^{\#}(\omega^{\#}) \neq 0$ holds.

Therefore, it is necessary for satisfying 1) and 2) that $\frac{d}{d\omega}V^{\#}(\omega) = 0$ has the following $2m-1$ roots:

$$m \quad \text{real roots so that} \quad V^{\#}(\omega) = 0 \text{ holds.} \tag{A.1.48}$$

$$m-1 \quad \text{real roots so that} \quad V^{\#}(\omega) \neq 0 \text{ and } \frac{d^2}{d\omega^2}V^{\#}(\omega) < 0 \tag{A.1.49}$$

According to the stability of $G^{\#}(s)$, we see that $V^{\#}(\omega) = 0$ implies $R^{\#}(\omega) \neq 0$. Hence, if $\omega^{\#}$ coincides to one of these $2m-1$ roots, we have the lemma. There are two roots left and let them refer as ω_1 and ω_2. If $\omega_1, \omega_2 \in \mathbf{R}$, then $V^{\#}(\omega) = V^{\#}(-\omega)$, $^{\forall}\omega \in \mathbf{R}$ implies $\omega_1 = \omega_2 = 0$ or $\omega_1 = -\omega_2 \neq 0$.

If $\omega_1 = \omega_2 = 0$, we easily obtain $V^{\#}(0) = 0$, that is, $R^{\#}(0) \neq 0$. Furthermore, we see from (A.1.48) and (A.1.49) and the symmetry $V^{\#}(\omega) = V^{\#}(-\omega)$, $^{\forall}\omega \in \mathbf{R}$ that the case $\omega_1 = -\omega_2 \neq 0$ cannot happen. The above whole discussions lead to the lemma. Figure A-5 shows an illustrative image connecting $V(\omega)$ and $R(\omega)$.

□

Lemma A.1.3 *[Lemma 2 in [Mori 1986]] Consider an n-th order stable interval polynomial $a(s)$ defined in (A.1.42). Then, if a variation of a_{2k} preserves Hurwitz-stability of $a(s)$, the variation of a zero ω^0 of $R(\omega^0)$ is monotonic with respect to the variation of a_{2k}, where $R(\omega)$ is the real part of $a(j\omega)$ defined by (A.1.44). More precisely,*

$$\frac{\partial \omega^0}{\partial a_{2k}} \begin{cases} > 0 & if \quad \dfrac{dR(\omega^0)}{d\omega} > 0 \ and \ k \ is \ even \quad or \quad \dfrac{dR(\omega^0)}{d\omega} < 0 \ and \ k \ is \ odd \\ < 0 & if \quad \dfrac{dR(\omega^0)}{d\omega} < 0 \ and \ k \ is \ even \quad or \quad \dfrac{dR(\omega^0)}{d\omega} > 0 \ and \ k \ is \ odd \end{cases} \qquad \text{(A.1.50)}$$

List of Publications

Tetsuya Kimura

Journal Papers

1. T.Kimura, T.Fujita, S.Hara, and T.Kagawa "Control for Systems with Pneumatic Actuator using Feedback Linearization," in Trans. of the Institute of Systems, Control and Information Engineers, Vol. 8, No.2, 10/18 (1995) (in Japanese)

2. T.Kimura and S.Hara "Frequency restricted norm bounds for interval systems," in International Journal of Nonlinear and Robust Control, Vol. 4, 575/593 (1994)

3. T.Kagawa, T.Fujita, K.Yamanaka, T.Kadau, and T.Kimura, "Power Assist Circuit using Artificial Muscle," in Trans. of the Japan Society of Mechanical Engineers, Vol. 59, No.564-C 112/117 (1993) (in Japanese)

Conference Papers (international)

1. T.Kimura, S.Hara, T.Fujita, and T.Kagawa, "Control for Pneumatic Actuator Systems Using Feedback Linearization with Disturbance Rejection," in Proc. of American Control Conference(ACC), 825/829 (1995)

2. T. Kimura and S. Hara, "Robust Control analysis Considering Real Parametric Perturbations based on Sign Definite Conditions," in Proc. of the 12nd IFAC World Congress, Vol.1, 37/40 (1993)

3. T.Kimura and S.Hara, "A Robust Control System Design by a Parameter Space Approach Based on Sign Definite Condition," in Proc. of Korean Automatic Control Conference(KACC), 1533/1538 (1991)

4. S.Hara, T.Kimura and R.Kondo, "H_∞ Control system Design by a Parameter Space Approach," in Proc. of International Symposium on the Mathematical Theory of Networks and Systems(MTNS-91) (1991)

5. K.Osuka, T.Kimura and T.Ono, "H_∞ Control of a Certain Nonlinear Actuator," in Proc. of the 29th IEEE CDC, 370/371 (1990)

Conference Papers (domestic)

1. T.Kimura, T.Tomisaka, and S.Hara "H_∞ Control for Pressure Control Systems," in Proc. of the 39th Annual Conference of the Institute of Systems, Control and Information Engineers, 521/522 (1995)

2. S.Ohno, T.Kimura, T.Fujita, S.Hara, and T.Kagawa, "Feedback Linearization Control for a Pneumatic Servo System," in Proc. of Dynamics and Design Conference (D&D'94), Vol. B, 5/8 (1994) (in Japanese)

3. T.Kimura, S.Ohno, T.Fujita, T.Kagawa, S.Hara, "Pressure Control Problems on a Rubber Artificial Muscle," in Proc. of 4th Joint Symposium on Fluid Control and Measurement of the Society of Instrument and Control Engineers, 63/68 (1993)

4. T.Kimura, S.Ohno, T.Fujita, S.Hara, and T.Kagawa, "Nonlinear Control of a Pneumatic Actuator," in Proc. of JSME Annual Conference on Robotics and Mechatronics (ROBOMEC '93), 1120/1123 (1993) (in Japanese)

5. T.Kimura and S.Hara, "Robust Performance Analysis for Closed-Loop Systems with Interval Plants," in Proc. of the 15th Society of Instrument and Control Engineers(SICE) Symposium on Dynamical System Theory, 75/80 (1992) (in Japanese)

6. T.Kimura and S.Hara, "Robust PI-Control System Design in the Parameter Space," in Proc. of the 13th Society of Instrument and Control Engineers(SICE) Symposium on Dynamical System Theory, 95/100 (1991) (in Japanese)

7. K.Osuka, T.Kimura, and T.Ono, "H_∞ control of rubbatuator," in Proc. of the 19th Society of Instrument and Control Engineers(SICE) Symposium on Control Theory, 167/172 (1990) (in Japanese)